

Institut National de la Recherche Scientifique  
Centre Armand-Frappier Santé Biotechnologie

**OPTIMIZATION OF A 3D CELL CO-CULTURE MODEL AND A BI-LAYERED CELL CO-CULTURE MODEL AS BIOLOGICALLY REPRESENTATIVE ALTERNATIVES FOR MAMMARY GLAND STUDIES.**

Par  
Melany Nicole Juárez Velázquez

Mémoire présentée pour l'obtention du grade de  
Maître ès Sciences (M.Sc.)  
en sciences expérimentales de la santé.

Ce mémoire intitulé

**OPTIMIZATION OF A 3D CELL CO-CULTURE MODEL AND A BI-LAYERED CELL CO-CULTURE MODEL AS BIOLOGICALLY REPRESENTATIVE ALTERNATIVES FOR MAMMARY GLAND STUDIES.**

et présenté par  
Melany Nicole Juárez Velázquez

a été évalué par un jury composé de:

**Jury d'évaluation**

Président du jury et  
examinatrice interne

Dre Geraldine Delbes  
INRS-AFSB

Examineur externe

Dr Vincent C. Chen  
Département du chimie  
Brandon University

Directeur de recherche

Dre Isabelle Plante  
INRS-AFSB

## ACKNOWLEDGMENTS

---

In the accomplishment of this thesis I want to thank firstly my supervisor, Profesor Isabelle Plante. Thank you for welcoming into your lab at my 21 years old for my exciting summer internship. Your guidance and passion for science, inspired me to come back 2 years later to follow my master's thesis. The time invested in me, my project, forming and teaching me are priceless. More than my supervisor, you have guided my path and at the same time gave me enough freedom to decide where I want to go. You have trusted me when I stop trusting in myself, we have enjoyed my victories together and you have boost me through my failures.

This master would have not been the same without my family in the laboratory: Bélinda Crobeddu, Rita Gouesse and Alexandre Petit. You adopted me since the first day and taught me everything you know and more. I have admired you and learned from you in a professional and personal way. Thank you for being my big supports and pushing me to be the very best version of myself. Your time invested to train me, correct my work, discuss results and share knowledge were essential for my formation. *Je vous aime beaucoup.*

Alec Mcdermott, my little *stagère*, your amazing mind and friendship helped me unlock problems faced during my master's project, thanks to your hard work, we were able to get this project to the end.

Miguel, MAJU, you have been a crucial piece for me to come all this way. You taught me to fight for what I wanted and always stand for what I believe. Never stay quiet. Your advices, the laughs we had and you being my number one fan have kept me from not quitting and being truthful to myself. Thank you.

Being away from home was especially hard for me, the work in the laboratory and away from it would have not been possible without the unconditional support of Eric. Your time to repeat my presentations at midnight, your patience when I got stressed, your love and the incredible support you offer me in every project I take, have been crucial for me finishing this dream. You trust that I am capable of achieving absolutely everything I get into my mind and this have kept me running when I felt like I could not do it anymore. You are the biggest blessing I could have asked for. Your family, Alma and René, thank you for accepting me as part of your family and watching over me. I will never be able to return the love and care you have offered me, and which helped me in this project of life.

Roger Avendaño, my life would have not been the same without you. You have watch me grow and taught me to always search excellence. You pushed me hard to kept dreaming about a better future. You have always trusted I could do and be more. When I said I wanted a challenge, you pushed me to go for a bigger one. You have love me as a daughter and raised me the best you knew. Thanks for believing and helping me all the way through.

Mom, Maria de los Angeles, I will never get tired of telling you that this one and every single one of my achievements are for you and thanks to you. You have fought for me since day one. You are my inspiration and my guiding light. No one knows better than you, everything I went through in order to get here. *Incluso en la distancia, eres my más grande fuerza. Tú, Jeziel, Elian, Zusa y Pau. Ustedes me hacen despertarme todos los días y disfrutar el sueño. Gracias a ti, logré eso que soñábamos y creíamos inalcanzable. Gracias a tus sacrificios y tu amor. Espero algún día ser como tú.*





## RÉSUMÉ

---

L'unité fonctionnelle de la glande mammaire est l'acinus bicouche, composé d'une couche interne de cellules épithéliales lumineales polarisées et d'une couche externe de cellules myoépithéliales. Notre projet vise à développer un modèle *in vitro* représentatif des interactions entre les cellules lumineales et myoépithéliales de la glande mammaire. Ceci est réalisé en établissant un modèle de co-culture bicouche 3D et un modèle de co-culture en couches utilisant les deux types de cellules. Nos résultats montrent que des cellules humaines MCF-12A lumineales co-cultivées avec des cellules myoépithéliales Myo1089 dans du Matrigel forment des acini bicouches. Ces modèles 3D miment de près la structure des acini bicouches observés *in vivo*. Dans le modèle en couche, les cellules MCF-12A et Myo1089 ont été co-cultivées chacune sur un côté différent de la membrane poreuse d'inserts pour créer un système de culture en couches. Nos résultats ont démontré que les cellulesensemencées de chaque côté de la membrane peuvent communiquer via des jonctions lacunaires, comme le montrent les tests de transfert de colorant utilisant la calcéine et le DiI. L'analyse par immunofluorescence suggère que des jonctions se forment entre les cellules lumineales et myoépithéliales à l'intérieur des pores de la membrane. Les expériences futures viseront à évaluer l'impact de la communication bidirectionnelle sur la signalisation cellulaire dans chaque type de cellules. Nous espérons que nos modèles *in vitro* innovants fourniront des options plus pertinentes sur le plan biologique pour les études toxicologiques en imitant la structure, la communication et la composition de la glande mammaire.

Mots clés: glande mammaire; co-culture; Matrigel; MCF-12A; Myo1089; acinus bicouche; culture cellulaire 3D, Vitrogel, jonctions

## ABSTRACT

---

The functional unit of the mammary gland is the bilayered acinus, composed of an inner layer of polarized luminal epithelial cells and an outer layer of myoepithelial cells. Our project aims to develop a representative *in vitro* model of the interactions between luminal and myoepithelial cells of the mammary gland. This is achieved by establishing a 3D bilayered co-culture model and a layered co-culture model using both types of cells. Our results showed that luminal MCF-12A and myoepithelial-like Myo1089 human cells co-cultured in Matrigel form bilayered acini. This 3D models closely mimic the structure of the bilayered acini observed *in vivo*.

In the second model, MCF-12A and Myo1089 cells were co-cultured on each side of the porous membranes of inserts to create a layered cultured system. Our results have demonstrated that cells seeded on each side of the membrane can communicate via gap junctions, as demonstrated by dye transfer assays using calcein and DiI. Immunofluorescence analysis suggested that junctions are formed between luminal and myoepithelial cells within the pores of the membrane. Future experiments will aim to evaluate the impact of bidirectional crosstalk on cell signaling in each cell type. We expect that our innovative *in vitro* models will provide a more biologically relevant options for toxicological studies by mimicking the structure, the communication and the composition of the mammary gland.

Key words: mammary gland, co-culture, Matrigel, MCF-12A, Myo1089, bilayered acinus, 3D cell culture, VitroGel, gap junctions

## SOMMAIRE RÉCAPITULATIF

---

**Since this thesis is written in English, this section presents a French résumé of the main sections, as required by the program. The figures cited in this section can be found in the main document.**

### **Introduction**

#### **La glande mammaire**

La glande mammaire est un organe spécifique aux mammifères dont la fonction principale est la synthèse et la sécrétion du lait. Elle est composée d'un épithélium dynamique qui subit des cycles de prolifération, de différenciation et d'apoptose en réponse aux signaux endocriniens, et d'un stroma complexe qui subit un remodelage de sa composition tout au long du cycle de développement, de la grossesse et de lactation (Campbell *et al.*, 2017). La glande mammaire adulte est composée de plusieurs types de cellules: cellules épithéliales, adipeuses, fibroblastes, immunitaires, lymphatiques et vasculaires. Elles contribuent toutes au développement et au bon fonctionnement de la glande (figure 1) (Inman *et al.*, 2015).

#### **Structure et composition**

La glande mammaire est composée d'un épithélium glandulaire et de tissu adipeux (stroma). Le tissu sécrétoire est drainé par un système canalaire qui stocke et transporte le lait vers le mamelon pendant la lactation. Ce système canalaire-lobulaire ramifié est formé de lobules organisés en lobes qui sont drainés par les canaux collecteurs convergeant au niveau du mamelon. Chaque lobule est composé d'acini (également appelés alvéoles). Les acini sont reconnus comme étant l'unité sécrétoire fonctionnelle de la glande mammaire (figures 1, 2) (Hassiotou & Geddes, 2012). Les acini et les canaux ont une lumière centrale et sont bordés de deux couches cellulaires, une couche interne de cellules épithéliales luminales polarisées et une couche externe de cellules basales (principalement des cellules myoépithéliales) qui sécrètent des composants de la membrane basale (Gudjonsson *et al.*, 2005). Ces deux couches de cellules sont entourées d'une membrane basale qui sépare l'épithélium du stroma (Osborne MP, 2000).

## **Rôle des cellules myoépithéliales dans la polarisation**

L'épithélium de la glande mammaire comprend des cellules épithéliales polarisées. Cette polarité divise la membrane plasmique en domaines apicale, latérale et basale et permet à des molécules distinctes d'être insérées dans des zones spécifiques de la membrane plasmique. Par conséquent, grâce à ce processus, les composantes de la membrane basale, tels que la laminine et le collagène IV, sont sécrétées dans le domaine de la membrane basale par les cellules myoépithéliales, tandis que d'autres protéines, telles que les protéines du lait, sont sécrétées à la surface apicale dans la lumière, par les cellules luminales (Inman *et al.*, 2015). Une orientation correcte de la polarité est donc essentielle pour la fonction tissulaire et est requise pour les modèles 3D mammaires *in vitro*. De plus, il est reconnu que la laminine 1 est l'un des principaux médiateurs de cette polarité (Sogaard *et al.*, 2019).

Dans la glande mammaire, la polarité de la couche interne des cellules luminales est induite par les cellules myoépithéliales de la couche externe de l'épithélium (Gudjonsson *et al.*, 2002). Il a également été démontré que les interactions cellule-matrice extracellulaire sont importantes pour l'orientation de la polarité apico-basale (Rodriguez-Boulan & Macara, 2014).

## **Membrane basale**

La membrane basale est une couche continue de matrice extracellulaire directement en contact avec la couche myoépithéliale de cellules de la glande mammaire, ancrant l'épithélium mammaire au stroma. Elle contient principalement du collagène de type IV et des laminines (Nerger & Nelson, 2019). Cette matrice aide à maintenir la polarité épithéliale, permettant la sécrétion et l'éjection du lait.

## **Cellules luminales**

Les cellules épithéliales luminales sont des cellules glandulaires polarisées exprimant les cytokératines 8 et 18 avec des domaines membranaires apicaux et basolatéraux spécialisés (Ronnov-Jessen *et al.*, 1996). Elles forment la couche interne de l'épithélium bicouche de la glande mammaire, et peuvent être divisées en cellules luminales canalaire, qui tapissent la couche interne des canaux, et en cellules luminales alvéolaires, qui sécrètent le lait dans la lumière de l'acinus pendant la lactation (Macias & Hinck, 2012). La surface apicale des cellules luminales délimite la lumière tandis que la surface basale est en contact avec les cellules myoépithéliales ou la

membrane basale. Le côté apical est chargé de protéines mucines, telles que la mucine 1 et la sialomucine, empêchant l'adhésion, tandis qu'au contraire, la surface basale exprime des molécules d'adhésion (Adriance *et al.*, 2005). La composition de la structure polarisée des cellules luminales est fortement régulée par des jonctions serrées et adhérentes (Anderson *et al.*, 2007).

### **Cellules myoépithéliales**

La couche externe de l'épithélium de la glande mammaire, bordant la membrane basale qui sépare la couche épithéliale du stroma, est composée de cellules myoépithéliales ainsi que de certains types de cellules souches et progénitrices (Inman *et al.*, 2015). Les cellules myoépithéliales ont une forme et une distribution différentes selon leur emplacement sur l'épithélium de la glande mammaire. Au niveau des canaux, elles sont en forme de fuseau et orientées de manière à former une couche continue autour des cellules luminales. Lors de la contraction, elles diminuent la longueur et augmentent le diamètre des canaux pour éjecter le lait. Au niveau des acini, elles sont plutôt de forme étoilée, formant un maillage en forme de filet discontinu autour des cellules luminales. La contraction de ce myoépithélium en forme de maille éjecte le lait des alvéoles sécrétoires dans les canaux, vers le mamelon et hors du corps (Cagnet *et al.*, 2017).

### **Les jonctions lacunaires**

Les jonctions lacunaires sont des canaux intercellulaires qui connectent directement le cytoplasme des cellules adjacentes pour permettre le transfert intercellulaire d'ions et de petites molécules hydrophiles (Goldberg *et al.*, 2002). La jonction est composée de plusieurs canaux qui sont eux-mêmes formés par l'amarrage tête-à-tête d'hexamères de protéines appelées connexines (abrégiées Cx, suivies de leur masse moléculaire en kilodaltons) (Goldberg *et al.*, 2002; Goodenough *et al.*, 1996; Goodenough & Paul, 2009).

### **Les jonctions serrées**

Les jonctions serrées jouent un rôle crucial dans l'établissement et le maintien de la polarité cellulaire dans les tissus. Dans la glande mammaire, elles sont essentielles pour séparer les domaines apical et basolatéral (Goldberg *et al.*, 2002). Les jonctions serrées créent une barrière semi-perméable contrôlant la circulation paracellulaire des molécules à travers les feuilles épithéliales, maintenant ainsi l'homéostasie tissulaire. Ce sont des complexes macromoléculaires

composés de plusieurs types de protéines membranaires, de protéines cytosquelettiques et de molécules de signalisation (Markov *et al.*, 2017).

### **Les jonctions adhérentes**

Une fonction majeure des jonctions adhérentes est de maintenir l'association physique entre les cellules; leur perturbation provoque le relâchement du contact cellule-cellule, entraînant une désorganisation de l'architecture tissulaire. Elles sont composées d'une famille de protéines transmembranaires, les cadhérines, et d'une famille de protéines cytoplasmiques, les caténines (Nakanishi & Takai, 2004).

### **Modèles de culture cellulaire *in vitro* actuellement disponibles**

Depuis de nombreuses années, les scientifiques se sont appuyés sur des modèles *in vivo* comme outils de recherche importants pour étudier et comprendre le développement de maladies et les effets des composés toxiques et des médicaments. L'utilisation de modèles *in vivo* est une étape essentielle entre les systèmes *in vitro* et les études cliniques. Dans les modèles *in vivo*, les cellules sont maintenues dans un environnement réactif avec un apport constant de nutriments et l'élimination des déchets via le système circulatoire, fournissant ainsi un modèle complexe mieux adapté pour observer les effets globaux d'une expérience sur un sujet vivant (Antoni *et al.*, 2015).

De manière similaire, pour étudier la glande mammaire, les modèles animaux ont été la référence pendant plusieurs années, car ils présentent un système intégral (vascularité, système immunitaire et système endocrinien) (Knight & Przyborski, 2015). Même si l'utilisation animale a considérablement progressé au cours des 20 à 30 dernières années, l'utilisation d'animaux dans la recherche, l'enseignement et les tests se pose de plus en plus comme un problème éthique important (Knight & Przyborski, 2015). De plus, les modèles animaux augmentent considérablement le coût des projets expérimentaux, les études impliquant des modèles *in vivo* sont longues à compléter et nécessitent des installations et personnel spécialisé, ainsi que l'approbation préalable d'un comité d'éthique (Antoni *et al.*, 2015). Ces préoccupations avaient déjà été établies dans "The Principles of Humane Experimental Technique" (Les principes d'une technique expérimentale plus humaine) publié par William Russell et Rex Burch en 1959. Il y avait été proposé que bien que les animaux soient nécessaires à l'expérimentation, tous les efforts devraient être faits pour les remplacer par des alternatives, pour réduire à un minimum le nombre

d'animaux utilisés et d'affiner les expériences afin qu'ils causent le minimum de douleur et de détresse (figure 7).

### **Modèles de culture cellulaire 2D**

Les tests cellulaires utilisent typiquement des cellules cultivées en monocouches bidimensionnelles (2D) sur une surface plane et rigide (Edmondson *et al.*, 2014). Ces cellules peuvent être obtenues à partir de lignées cellulaires standardisées avec un phénotype connu ou peuvent être isolées de tissus. Cependant, de nombreuses études ont démontré que les cellules sur des surfaces 2D ne conservent pas la même différenciation ou expression génétique observée *in vivo* (Nerger & Nelson, 2019). De plus, bien que la culture cellulaire 2D se soit révélée être une méthode précieuse pour les études mécanistiques, elle présente certaines limites en raison du fait qu'elle ne prend pas suffisamment en compte l'environnement 3D naturel des cellules. Par conséquent, parfois, la culture cellulaire 2D fournit des données trompeuses pour les réponses *in vivo* (Knight & Przyborski, 2015). La culture cellulaire a été une plate-forme importante en science fondamentale, fournissant un outil simple, rapide et rentable pour réduire les tests sur les animaux. De nombreux composés toxiques et des produits pharmaceutiques ont été testés sur culture cellulaire 2D lors de leur développement, mais ont quand même démontré une toxicité ou se sont avérés inefficaces lors d'études subséquentes avec des animaux (Edmondson *et al.*, 2014). ***Pour réduire les coûts associés à la recherche et l'utilisation animale, il est nécessaire d'identifier les médicaments et les composés toxiques inefficaces ou inacceptables le plus tôt possible, avant même les tests sur les animaux. Il est donc nécessaire d'améliorer les techniques in vitro utilisées de nos jours afin d'obtenir des résultats plus prévisibles. En outre, il existe également un besoin de modèles biologiquement représentatifs et malléables pour l'étude du développement et de la fonction de la glande mammaire.***

### **Modèles de culture cellulaire 3D**

Des modèles de culture 3D se sont développés dans les dernières années en tant que systèmes pour étudier des voies de signalisation spécifiques et la structure de la glande mammaire. Ce type de modèles *in vitro* consiste à cultiver des cellules en trois dimensions (3D) afin de récapituler la structure de la glande mammaire. Ils ont été développés soit à l'aide d'un échafaudage généré à partir de matériaux naturels ou synthétiques, soit dans un environnement sans échafaudage (Knight

& Przyborski, 2015). Ces systèmes sont conçus pour récapituler les principales caractéristiques biophysiques et biochimiques d'un tissu et de son microenvironnement. L'utilisation de modèles tridimensionnels simplifiés offre plusieurs avantages dans l'analyse des organes en laboratoire (Nerger & Nelson, 2019). Pour améliorer le développement de médicaments et le dépistage toxicologique à l'aide de modèles 3D, l'unité fonctionnelle des tissus doit être récapitulée en son entièreté, plutôt qu'étudiée sous forme de cellules individuelles. Dans le cas de la glande mammaire, l'unité fonctionnelle comprend les cellules luminales et myoépithéliales et leurs interactions cellule-cellule spécialisées (Breslin & O'Driscoll, 2013). ***Il existe donc un réel besoin pour un modèle d'acini bicouche qui récapitule la structure 3D de la glande mammaire.***

### **Modèles alternatifs pour l'analyse de la communication intercellulaire**

Compte tenu des limites établies précédemment pour l'utilisation des modèles traditionnels *in vitro* et *in vivo*, différents modèles alternatifs ont commencé à apparaître. Par exemple, des modèles de culture cellulaire utilisant des inserts à membranes poreuses ont été utilisés dans l'analyse de la barrière hémato-encéphalique. Dans ce modèle, les astrocytes sont cultivés dans des conditions sans contact au fond d'un puits, bien séparés des cellules endothéliales cérébrales qui sont cultivées sur une membrane poreuse (Deli *et al.*, 2005). Ce type de modèles permet la communication de différents types cellulaires par des facteurs solubles dans les milieux (Coisne *et al.*, 2005)(figure 7). Pour mieux ressembler aux interactions des cellules et à la structure anatomique de la barrière hémato-encéphalique *in vivo*, des modèles plus avancés ont été développés en cultivant des cellules dans des conditions de contact direct, de chaque côté de la membrane (Gaillard *et al.*, 2001).

### **Les avantages et les inconvénients de la culture cellulaire en 2D par rapport à la culture cellulaire en 3D**

La culture cellulaire en monocouche ou 2D a été un outil important pour la recherche biologique, mais la croissance de cellules en monocouches plates sur des surfaces en plastique ne reproduit pas avec précision les conditions d'organisation et les interactions cellulaires observées *in vivo*. Par rapport à la 2D, la culture cellulaire 3D permet aux cellules de croître et d'interagir avec leur environnement dans les trois dimensions. Les cellules cultivées dans des modèles 3D sont plus pertinentes physiologiquement et ont montré des améliorations dans les mécanismes biologiques comme la viabilité cellulaire, la morphologie, la prolifération, la différenciation, la réponse aux



stimuli, la migration, l'invasion, le métabolisme des médicaments, l'expression des gènes et la synthèse des protéines (Knight & Przyborski, 2015; Simian & Bissell, 2017).

### **État de l'art dans les modèles 3D**

Le développement de modèles de culture cellulaire 3D a commencé au début des années 1900 et n'a cessé d'évoluer parallèlement aux avancées technologiques en matière de matériaux, de biologie cellulaire et de conception pour l'ECM (figure 10). Ainsi, de nombreuses techniques ont été développées pour produire des modèles 3D, y compris des explants d'organes, des organoïdes, des mammosphères, des tumosphères, des sphéroïdes, la bio-impression 3D, des systèmes en suspension et de flottement forcé, entre autres. Divers substrats synthétiques et naturels ont également été développés pour soutenir la croissance 3D des cellules. Dans la plupart des cas, y compris les modèles représentant les glandes mammaires et la tumorigenèse, les deux substrats les plus couramment utilisés sont la matrice extracellulaire riche en membrane basale isolée des sarcomes de souris Engelbreth-Holm-Swarm (par exemple Matrigel) et le collagène extrait des queues de rats (Bruno *et al.*, 2019).

### **Problématique**

Dans la glande mammaire, l'unité fonctionnelle est l'acinus bicouche composé de cellules luminales et myoépithéliales. Bien que de bons modèles alternatifs 3D aient été développés pour l'étude de la glande mammaire, ils comportent encore des limitations. En effet, la majorité des modèles sont composés soit de cellules luminales uniquement, soit de cellules luminales et myoépithéliales issues de la culture primaire. D'un côté, ces modèles sont moins représentatifs de la structure *in vivo* car ils manquent les cellules myoépithéliales. D'un autre côté, même s'ils représentent physiologiquement l'acinus de la glande mammaire, les modèles constitués de cellules primaires sont plus difficiles à manipuler et sont moins reproductibles. En conséquence, les modèles qui sont physiologiquement pertinents tout en étant malléables, reproductibles et peu coûteux font toujours défaut. Par conséquent, les objectifs de mon projet de maîtrise étaient le développement de deux modèles différents:

1. Développement d'un modèle de culture cellulaire d'acinus bicouche 3D
2. Développement d'un système de culture cellulaire en couches

## **Matériaux et méthodes**

### **Les cellules**

Les cellules MCF-12A et MCF-10A ont été achetées chez ATCC. Les cellules Myo1089 ont été généreusement données par la Dre Louise J. Jones du Barts Cancer Institute, Université de Londres. Chaque type de cellule a été maintenu dans leurs milieux de culture cellulaire respectifs à 37°C avec 5% de CO<sub>2</sub>.

### **Western Blot pour la caractérisation cellulaire**

Les protéines ont été extraites de monocouches cellulaires à 90% de confluence. Des échantillons de protéines ont été migrés sur des gels d'acrylamide « stain-free » (Bio-Rad) et transférés sur des membranes de fluorure de polyvinylidène. Les membranes ont été bloquées et incubées pendant une nuit à 4°C ou 2h à température ambiante avec un anticorps primaire. L'anticorps primaire a été détecté à l'aide d'anticorps secondaires conjugués à la HRP, suivi d'une visualisation à l'aide du système Bio-Rad ChemiDoc MP.

### **Culture cellulaire 3D intégrée dans une matrice extracellulaire**

Deux matrices extracellulaires ont été utilisées: le Vitrogel®-RGD et le Matrigel. Dans le Matrigel, les cellules ont étéensemencées à une densité de 35 000 à 50 000 cellules/100 µl de Matrigel 75% (v/v) dilué avec un milieu de croissance froid. Lorsque le Vitrogel®-RGD a été utilisé, les cellules ont étéensemencées à une densité de 200 000 cellules/100-250 µl de Vitrogel dilué avec du PBS stérile. Le mélange d'ECM et de cellules a étéensemencé sur un pétri MatTek 35 mm et conservé dans l'incubateur pendant 10 à 14 jours; le milieu de culture cellulaire a été changé tous les 2 à 3 jours. La mise en place d'un modèle d'acinus bi-couches 3D a consisté en un processus d'optimisation constant: plusieurs paramètres ont été testés et donc ajustés afin d'obtenir la version la plus efficace du modèle. Le tableau 1 résume les principaux paramètres testés et les conditions optimales choisies pour chacun de ces paramètres. Il est à noter que bien que les résultats ont été analysés par microscopie confocale et d'autres méthodes pour chaque condition, seuls les résultats obtenus avec les conditions optimales sont présentés dans la thèse.

### **Immunofluorescence de la culture 3D**

Le milieu de culture a été aspiré et les cultures 3D ont été rincées deux fois avec du PBS 1x. Les cellules ont été fixées et perméabilisées, puis elles ont été incubées dans une solution de blocage pendant 1h. Les anticorps primaires ont été dilués dans la solution de blocage et les cellules ont été incubées avec l'anticorps primaire sur une table à bascule pendant 120 minutes à température ambiante ou pendant une nuit à 4°C. Les cellules ont ensuite été incubées avec les anticorps secondaires appropriés pendant 60 minutes à température ambiante. Les noyaux ont été colorés en utilisant une solution de DAPI. Les images d'immunofluorescence ont été obtenues avec un microscope confocal Nikon A1R + (Nikon) et analysées à l'aide du logiciel NIS-elements (Nikon).

### **Développement d'un modèle de co-culture en couches de la glande mammaire**

Des inserts de culture cellulaire avec une membrane poreuse de 3,0 µm ont été utilisés dans le développement de ce modèle. Les cellules Myo1089 ont étéensemencées sur un insert inversé à une densité cellulaire de 750 000 cellules dans 500 µl de milieu pour les inserts de plaques à 6 puits ou 300 000 cellules dans 200 µl de milieu pour les inserts de plaques à 12 puits (figure 1). Les inserts ont été maintenus à 37°C et 5% de CO<sub>2</sub> pendant 6 heures pour permettre l'adhésion cellulaire. Afin de maintenir la stérilité pendant cette période d'adhésion cellulaire, les inserts ont été maintenus dans une plaque inversée (figure 2: les inserts inversés ont été placés sur le dessus du couvercle d'une plaque à 6 puits, puis le bas de la plaque a été placé comme couvercle, ce qui maintenait le milieu en place grâce à la tension de surface et évitait que les cellules ne sèchent. Après 6h, les inserts et la plaque ont été retournés en position normale, et les cellules MCF-12A ont étéensemencées à la même densité cellulaire que les cellules Myo1089 sur la face supérieure de la membrane poreuse. Le milieu utilisé pour les MCF-12A a été ajouté pour couvrir entièrement les deux couches de cellules. Le système a été maintenu à 37°C et 5% de CO<sub>2</sub> pendant 16h-18h avant que les analyses ne soient effectuées.

### **Marquage cellulaire pour l'analyse par transfert de colorant**

Pour analyser la communication entre les cellules dans le modèle en couche, de nombreuses études utilisent des colorants fluorescents. La GJIC peut être analysée et quantifiée en utilisant la calcéine-AM et le Dil (Goldberg, Lampe et Nicholson, 1999). La calcéine-AM est un colorant fluorescent

vert perméable qui est largement utilisé pour étudier la viabilité cellulaire dans les cellules eucaryotes. Dans les cellules vivantes, la calcéine-AM non fluorescente est convertie en calcéine fluorescente (verte). Le colorant pénètre dans la cellule à travers la membrane, mais suite à l'hydrolyse de l'ester acétoxyméthylrique (AM) par les estérases intracellulaires, il est ensuite piégé à l'intérieur des cellules. Après ce processus, le colorant ne peut quitter la cellule que par des jonctions lacunaires (Mariappan *et al.*, 1999). Le Dil est un colorant membranaire lipophile qui se diffuse pour colorer la membrane cellulaire dans sa totalité. Il se colore d'une fluorescence rouge orangé après avoir été incorporé dans la membrane et ne se transfère pas aux cellules adjacentes. Il est donc utilisé comme contrôle négatif pour le test de GJIC. Pour analyser la GJIC dans le modèle de culture en couche, les cellules MCF-12 ont été marquées avec la calcéine-AM et Dil. Pour ce faire, les cellules ont été incubées dans du milieu contenant un mélange des deux colorants à une concentration de 0,072  $\mu\text{M}$  Dil et 5  $\mu\text{M}$  Cal. Les cellules ont ensuite étéensemencées sur l'insert pré-ensemencé avec les cellules Myo1089. La coculture a été maintenue pendant 16 à 18h et analysée soit par cytométrie en flux, soit par microscopie confocale.

### **Cytométrie en flux**

Après 16 à 18h d'incubation, les cellules ont été récupérées à partir d'inserts contenant des cellules MCF-12A marquées calcéine-DiL (donneuses) et des cellules Myo1089 (receveuses) de chaque côté de la membrane. Les cellules ont été analysées en utilisant un appareil BD LSRFortessa. Notez que pour s'assurer que les colorants passent par une interaction directe entre les deux couches de cellules et ne fuient pas dans le milieu, les cellules MCF-12A (non marquées) ont également étéensemencées au fond du puits et analysées par cytométrie en flux. Les cellules receveuses étaient positives pour la calcéine, tandis que les cellules donneuses étaient positives pour la calcéine et le Dil.

### **Cryosection des co-cultures sur insert**

Après 16-18h de maintien du système dans l'incubateur, les membranes poreuses contenant les MCF-12A (marquées ou non avec la calcéine et DiL) et les cellules Myo1089 de chaque côté, ont été coupées avec un scalpel jetable et placées dans de la cryomatrix FSC 22 sur un récipient métallique refroidi à l'aide de glace carbonique. L'installation a été maintenue à  $-80^{\circ}\text{C}$  pendant au

moins 48h pour permettre une solidification complète. Des coupes de 10  $\mu\text{m}$  ont été réalisées en utilisant le cryostat Microm HM 525 réglé à  $-20^{\circ}\text{C}$ .

### **Immunofluorescence des cryosections**

Les cryosections ont été fixées et bloquées. Les anticorps primaires ont été dilués dans une solution de blocage et les sections ont été incubées pendant 2 heures à température ambiante. Après lavages, les cryosections ont été incubées avec l'anticorps secondaire et les noyaux ont été colorés avec du DAPI. Les images d'immunofluorescence ont été obtenues avec un microscope confocal Nikon A1R + (Nikon) et analysées à l'aide du logiciel NIS-elements (Nikon).

### **Microscopie confocale de membranes entières**

Des analyses d'immunofluorescence ont également été réalisées sur toute la membrane. Les cellules ont été co-cultivées en utilisant le système en couches, comme décrit précédemment. Après 16h, les cellules ont été fixées en utilisant du formaldéhyde à 4%. Le blocage et l'incubation des anticorps ont été effectués comme décrit dans la section précédente directement sur la membrane. Les noyaux ont été colorés avec une solution de DAPI. Après la procédure, la membrane a été coupée avec un scalpel propre pour être montée à l'aide de Fluoromount-G (SouthernBiotech) entre deux lamelles de microscope.

## **Résultats**

### **Caractérisation cellulaire**

Pour le développement des modèles *in vitro*, les lignées cellulaires proposées ont d'abord été caractérisées afin de confirmer l'expression de marqueurs spécifiques des types cellulaires appropriés et de protéines jonctionnelles. Les résultats ont montré que les cellules MCF-12A et MCF-10A expriment la plupart des marqueurs luminaux testés (PRa, PRb et k18 pour les deux lignées cellulaires et ER $\alpha$  pour MCF-12A), mais seulement quelques marqueurs des cellules myoépithéliales (k5, k14 pour les deux lignées cellulaires et Caldesmon 1 pour MCF-12A) (tableaux 2 et 3). En revanche, les cellules Myo1089 expriment la plupart des marqueurs myoépithéliaux testés (Caldesmon 1, Calponin 1 et k14), et seulement quelques marqueurs luminaux (ER  $\alpha$ ). De plus, les trois lignées cellulaires expriment la E-cadhérine, la  $\beta$ -caténine,

Cx43, Cx32. Ensemble, ces résultats suggèrent que ces lignées cellulaires ont un phénotype près de ce qui est attendu et expriment des protéines jonctionnelles cruciales. Elles sont donc appropriées pour nos études.

### **Les cellules luminales MCF-12A et MCF-10A forment des acini dans le Matrigel, mais pas dans le Vitrogel.**

Nous avons d'abord voulu évaluer séparément le comportement des cellules luminales et myoépithéliales en 3D. Pour ce faire, les cellules MCF-12A, MCF-10A et Myo1089 ont d'abord été cultivées dans le Matrigel et conservées dans l'incubateur pendant 10-12 jours. Alors que les cellules luminales MCF-12A et MCF-10A formaient des structures de type acinus lorsqu'elles étaient ensemencées dans le Matrigel (figures 15a et b), les cellules Myo1089 formaient des amas de cellules sans structure spécifique (figure 15c). Fait intéressant, pour tous les types de cellules, le marquage pour la E-cadhérine a été localisé au niveau des membranes cellulaires, formant probablement une jonction d'adhérence entre les cellules adjacentes (figure 15). Néanmoins, ces résultats ont confirmé que les cellules MCF-12A et MCF-10A, mais pas les cellules Myo1089, sont capables de former des structures de type acini dans Matrigel. Les cellules Luminales MCF-12A, MCF-10A et myoépithéliales Myo1089 ont ensuite été ensemencées en monoculture dans du Vitrogel et conservées dans l'incubateur pendant 12 à 14 jours. Dans le Vitrogel, les cellules luminales MCF-12A et MCF10A ont formé des structures sphériques composées d'un maximum de dix cellules à la fois (figures 16a et 16b). Les cellules Myo1089 ont formé des structures en forme de maille, comportant une seule couche de cellules (figure 16c). Ces résultats suggèrent qu'aucune des lignées cellulaires testées n'est capable de former des acini lorsqu'elles sont seules cultivées dans du Vitrogel.

### **Les cellules luminales MCF-12A forment des acini bicouches lorsqu'elles sont co-cultivées avec les cellules Myo1089 dans du Matrigel**

Dans une deuxième série d'expériences, les cellules luminales et myoépithéliales ont été co-cultivées afin de déterminer si elles pouvaient former des acini bicouches. Tout d'abord, les cellules MCF-10A ont été ensemencées avec les cellules Myo1089 dans Matrigel. Après 12 à 14 jours de culture, les cellules MCF-10A ont formé des structures de type acini, tandis que les cellules Myo1089 ont formé des groupes de cellules sans structure spécifique, comme précédemment

démontré (figure 15). Cependant, les cellules luminales et myoépithéliales sont restées séparées dans différents plans de profondeur et n'ont pas interagi, ce qui suggère que les cellules MCF-10A et Myo1089 ne forment pas d'acini bi-couche lorsqu'ils sont co-cultivés dans du Matrigel (figure 17). Dans une deuxième série d'expériences, les cellules luminales MCF-12A et myoépithéliales Myo1089 ont été co-cultivées dans du Matrigel. Dans ce cas, des structures similaires aux acini bicouches de la glande mammaire ont été observées. Les cellules luminales forment un acinus polarisé avec les cellules myoépithéliales qui les entourent à la manière d'un maillage (figure 18). Enfin, les cellules les luminales MCF-12A et MCF10A ont été co-cultivées avec les cellules Myo1089 dans du VitroGel. Même si de nombreuses conditions ont été testées, aucune structure de type acini n'a pu être observée dans ces co-cultures (figure 19). Fait intéressant, cependant, les structures formées par les cellules luminales ont montré une différence importante lorsqu'elles ont été co-cultivées avec des cellules myoépithéliales dans le VitroGel. En effet, bien que les deux types de cellules n'interagissent pas directement, les cellules luminales formaient des structures plus organisées que lorsqu'elles étaient cultivées seules (figure 16). Ces résultats suggèrent que l'interaction indirecte contribue au bon positionnement des cellules luminales dans la glande mammaire. L'ensemble de ces résultats a démontré que les cellules MCF-12A et Myo1089 peuvent former des acini bicouches lorsqu'elles sont co-cultivées dans du Matrigel, mais pas dans du VitroGel. Ces acini bicouches sont polarisés et imitent fidèlement la structure de l'épithélium de la glande mammaire *in vivo*

### **Les cellules luminales MCF-12A et Myo1089 peuvent être co-cultivées dans un système de culture en couches**

Les cellules luminales MCF-12A et les cellules myoépithéliales Myo1089 ont été co-cultivées de chaque côté d'une membrane poreuse de 3  $\mu\text{m}$  sur un insert de culture cellulaire. Dans un premier temps, nous avons confirmé que les deux couches de cellules étaient correctement fixées à la membrane (figure 20). En utilisant la coloration par immunofluorescence, nous avons démontré que la  $\beta$ -caténine était localisée à la membrane cellulaire dans les cellules luminales et myoépithéliales, suggérant que les cellules des deux couches de cellules formaient des jonctions adhérentes (figure 20). Fait intéressant, un marquage pour  $\beta$ -caténine a également été observé dans les pores de la membrane, suggérant la présence de projections cellulaires dans les pores de la membrane (figures 18-19) et d'interactions entre les deux couches de cellules. De même, lorsque

les cellules ont été colorées avec la protéine jonctionnelle Cx43 par immunofluorescence, un signal en pointillé typique de Cx43 a pu être observé à la fois dans les cellules luminales MCF-12A et myoépithéliales Myo1089 (figure 19b), mais également à l'intérieur des pores de la membrane. Nos résultats suggèrent que ce système de co-culture permet non seulement l'interaction des cellules à travers la membrane, mais également une communication directe (figure 19).

### **Les cellules luminales MCF-12A et Myo1089 communiquent par jonction d'espace dans un système de culture en couches**

Comme la présence de marquage pour  $\beta$ -caténine et Cx43 dans les pores suggèraient que les cellules luminales et myoépithéliales interagissent, nous avons ensuite voulu déterminer si les cellules communiquent via des jonctions lacunaires en utilisant un test de transfert de colorants. Pour ce faire, les cellules luminales MCF-12A ont été préchargées avec du DiL et de la calcéine (figure 20a), puisensemencées sur un insert sur lequel des cellules Myo1089 étaient déjà fixées de l'autre côté de la membrane. La présence de calcéine et de DiL a pu être observée à travers les pores de la membrane peu de temps après l'ensemencement des cellules MCF-12A (figure 20b), mais pas sur la face inférieure de la membrane (figure 21). A noter que la taille des pores (3  $\mu$ m) a été choisie pour permettre une interaction directe entre les deux faces de la membrane poreuse tout en évitant la migration des cellules. Après 12h d'interaction, le transfert de la calcéine, mais pas du DiL, des cellules luminales aux cellules myoépithéliales a pu être observé (figure 18), confirmant la communication intercellulaire communicationnelle (GJIC) entre les deux types de cellules.

Pour confirmer et quantifier davantage la GJIC, les cellules de chaque côté de la membrane ont été récoltées séparément après 16h de coculture et le nombre de cellules fluorescentes a été mesuré en utilisant la cytométrie en flux. Pour cet essai, une couche de cellules luminales MCF-12A a également étéensemencée au fond du puits pour s'assurer que la calcéine était transférée par les interactions directes plutôt que d'être transférée par le milieu. Tout d'abord, nous avons confirmé que les cellules luminales MCF-12A du côté supérieur de la membrane étaient colorées efficacement puisque 70% et 97% des cellules étaient positives pour le DiL et la calcéine, respectivement (figure 22b). Les cellules MCF-12A ont transféré la calcéine, mais pas le DiL, vers les cellules Myo1089 de l'autre côté de la membrane, car 16% des cellules myoépithéliales étaient positives pour la calcéine, tandis que seulement 2% étaient colorées avec du DiL (figure



22b). Seul un nombre négligeable des cellules lumineales ensemencées au fond du puits ont été colorées à la calcéine et le DiL ( $\leq 0,01\%$  des cellules), confirmant que la calcéine passait bien des cellules lumineales aux cellules myoépithéliales par GJIC (figure 22). L'ensemble de nos résultats confirme que les cellules lumineales et myoépithéliales interagissent et communiquent par jonction lacunaire lorsqu'elles sont co-cultivées dans un système de culture en couches.

## **Discussion**

### **Les MCF-12A, MCF-10A et Myo1089 sont des lignées cellulaires appropriées pour le développement de modèles *in vitro* plus complexes**

Les cellules lumineales MCF-12A, MCF-10A et myoépithéliales Myo1089 ont été caractérisées en utilisant des techniques d'immunobuvardage Western ou d'immunofluorescence. Ce processus a permis de vérifier si les cellules étaient des candidats appropriés pour les modèles. Après la caractérisation, il a été déterminé que les lignées cellulaires lumineales MCF-12A et MCF-10A exprimaient majoritairement des marqueurs de type luminal (tableau 5), alors que les cellules Myo1089 exprimaient surtout des marqueurs myoépithéliaux (tableau 5). Il est à noter que quelques marqueurs épithéliaux étaient également exprimés par les cellules Myo1089, et vice-versa. Ces résultats n'étaient pas surprenants puisqu'il est bien reconnu que la mise en culture de cellules modifie généralement l'expression de certains gènes, et mène à une certaine dédifférenciation. Néanmoins, ces lignées semblaient être de bons candidats pour nos modèles.

L'utilisation de lignées cellulaires a été d'une grande pertinence dans la construction de nos modèles. Nous sommes confrontés à une décision cruciale quant à l'utilisation d'une culture cellulaire primaire ou de lignées cellulaires. Les lignées cellulaires ont été préférées à la culture primaire afin de générer une version standardisée des deux modèles. L'objectif était donc d'obtenir des modèles de culture cellulaire représentatifs réduisant la variation que l'utilisation de la culture cellulaire primaire entraînerait. En effet, jusqu'à présent, la plupart des modèles *in vitro* développés par d'autres chercheurs étaient soit constitués uniquement de cellules lumineales, donc non représentatifs de l'épithélium mammaire bicouche (Froehlich *et al.*, 2016), soit étaient des acini bicouches fabriqués à partir de cellules primaires isolées de tissus, donc moins reproductibles et plus difficiles à manipuler génétiquement (Sokol *et al.*, 2016). Notre but était de maximiser la

reproductibilité de nos modèles et de pouvoir facilement modifier les cellules afin de déterminer les impacts de ces modifications au niveau mécanistiques.

### **Les cellules MCF-12A et Myo1089 forment des acini bicouches dans le Matrigel, mais pas dans le Vitrogel**

Nos résultats démontrent que les cellules MCF-12A et Myo1089 peuvent former des acini bicouches dans le Matrigel, mais pas dans le Vitrogel. Même si plusieurs paramètres ont été ajustés et des interactions constantes ont été maintenues avec le fournisseur tout au long du développement de ce modèle, nous n'avons pas été en mesure de produire des acini ou des acini bicouches en utilisant le Vitrogel. Cette différence notable entre les cultures cellulaires avec le Matrigel par rapport aux cultures cellulaires utilisant le Vitrogel, a renforcé la nécessité d'un environnement riche en laminine pour la formation d'acini polarisé en 3D.

Les cellules luminales MCF-12A et MCF-10A ont formé des structures de type acini lorsqu'elles étaient ensemencées seules dans Matrigel, montrant que la laminine présente dans l'ECM était suffisante pour qu'elles forment des structures polarisées. Dans nos études précédentes, nous avons pu former des acini bicouches dans du Matrigel, par contre, un grand nombre d'acini « monocouche » étaient également présents, puisque la laminine est présente dans le Matrigel (Weber-Ouellette *et al.*, 2018). Ainsi, notre hypothèse pour utiliser le Vitrogel reposait sur le fait que les cellules myoépithéliales pourraient sécréter de la laminine et du collagène IV, tel qu'elles le font *in vivo*, afin de favoriser la formation d'acini bicouche. Même si Matrigel a continué à fournir de meilleurs résultats, le Vitrogel pourrait rester une alternative viable, puisque quelques conditions restent à tester. Ainsi, afin d'augmenter le pourcentage d'acinus bicouche formé par rapport à l'acinus monocouche dans les deux ECM, les conditions de croissance doivent être modifiées. Plus d'expériences seraient nécessaires pour découvrir les paramètres exacts par lesquels la construction de l'acinus bicouche est favorisée. Malgré tout, ce modèle demeure un outil qui pourra servir dans les études toxicologiques ou fondamentales de notre laboratoire.

### **Les cellules luminales et myoépithéliales communiquent via des jonctions lacunaires**

Nous avons montré que la calcéine, mais pas le DiL, était passé entre les cellules, confirmant ainsi une GJIC. Par contre, 2% des cellules myoépithéliales étaient tout de même positives pour le DiL après 16h d'interaction avec les cellules luminales. Le DiL a été utilisé comme contrôle pour

s'assurer que les cellules luminales colorées ne migraient pas de l'autre côté de la membrane. Des études antérieures ont utilisé du DiD, un colorant de la même famille de colorants fluorescents lipophiles, pour marquer les membranes et d'autres structures hydrophobes (Yumoto *et al.*, 2014). Dans ces études, un pourcentage similaire de cellules receveuses étaient positive pour le DiD après avoir été co-cultivé avec des cellules donneuses; ce pourcentage a été considéré comme négligeable par les auteurs (Yumoto *et al.*, 2014). Comme le DiL est incorporé dans la membrane des cellules, on peut postuler que de petites portions de membrane sont échangées entre les cellules luminales et myoépithéliales, soit par le biais d'exosomes ou de connexosomes de jonctions lacunaires (Laird, 2006).

### **Perspectives**

Les modèles développés dans le cadre de cette thèse nous ont permis de construire une base pour des modèles de culture cellulaire plus représentatifs de la glande mammaire *in vitro*. À long terme, deux avenues de développement sont envisagées. Tout d'abord, nos modèles *in vitro* doivent être comparés aux modèles *in vitro* et *in vivo* actuellement disponibles, ainsi qu'aux données humaines si possible, afin de confirmer sa pertinence. Pour se faire, il faudrait idéalement comparer un modèle typique de culture cellulaire *in vitro* en monocouche, nos nouveaux modèles de co-culture 3D et en couches et un modèle animal *in vivo* à la glande mammaire humaine. Cette comparaison devrait d'abord être effectuée en utilisant un composé aux effets mesurables bien connus. Bien qu'il soit impossible de le faire en peu de temps, plus nous utiliserons ces modèles alternatifs, plus ils seront caractérisés et utilisés pour remplacer des modèles animaux.

Deuxièmement, idéalement, nous créerons un modèle encore plus complexe en incorporant d'autres cellules de la glande mammaire, telles que les fibroblastes et les adipocytes présents dans le stroma. Bien que l'acinus de la glande mammaire puisse être une unité fonctionnelle représentative de la glande mammaire, cet organe est également défini par un stroma complexe. Il a été montré précédemment que lors de la culture de cellules mammaires luminales et myoépithéliales dans une ECM, l'ajout d'adipocytes favorise la formation de structures acineuses polarisées (Nash *et al.*, 2015). Il est bien connu que les interactions entre l'épithélium de la glande mammaire et le stroma environnant sont cruciales pour son bon développement. Ainsi, un modèle idéal devrait inclure toutes ces composantes. Ce modèle multicellulaire complexe représenterait de façon encore plus précise la glande mammaire humaine.

Bien que nous ayons réussi à former des acini bicouches *in vitro*, des acini et des acini bicouches étaient présents dans chaque puits. Pour pouvoir utiliser ce modèle pour des études médicamenteuses, toxicologiques ou mécanistiques, nous devons augmenter le ratio d'acini bicouche. Dans une perspective à court terme, l'augmentation du nombre de cellules myoépithéliales dans le processus d'ensemencement cellulaire pourrait améliorer le rapport acini bicouches/monocouches formés. De plus, la compagnie synthétisant le Vitrogel vient de lancer de nouveaux produits, soit du Vitrogel-RGD plus concentré, mais également du Vitrogel contenant des peptides mimant différents types de ECM, dont de la laminine. Ces deux options seront testées dans les prochains mois. Pour les perspectives à long terme, nous pouvons évaluer les avantages d'inclure des techniques de bio-impression 3D pour la création de notre modèle.

Pour le modèle de co-culture en couches, nos résultats ont montré que les cellules luminales et myoépithéliales communiquent via la GJIC. La prochaine étape logique avec ce modèle consiste à analyser l'impact de cette interaction sur la signalisation cellulaire au sein de chaque type de cellule. Les prochaines expériences à réaliser pour ce modèle devraient donc être la caractérisation des cellules avant et après interaction pour déterminer les mécanismes activés lorsque différentes populations cellulaires sont co-cultivées ensemble.

## **Conclusion**

Deux modèles ont été développés pendant projet; le modèle d'acini bicouche 3D et le système de co-culture en couches. Les deux nous permettent d'avoir un modèle alternatif pour l'étude de la structure de la glande mammaire. Le premier est un modèle de culture cellulaire plus représentatif de la structure *in vivo*, grâce à la présence d'une structure 3D et des deux principaux types de cellules composant l'épithélium de la glande mammaire. Le deuxième modèle a donné des informations importantes sur la communication entre les cellules luminales et myoépithéliales. Ce système de culture en couches est le premier modèle, à notre connaissance, à montrer une GJIC fonctionnelle entre les cellules luminales et myoépithéliales de la glande mammaire humaine. La présence de cette communication *in vivo* restait à être confirmée, mais a déjà été suggérée par plusieurs études.

En bref, nos nouveaux modèles pourront être utilisés dans les plateformes de dépistage, offrant un cadre préclinique plus rentable et précis pour les dépistages de découverte de

médicaments ou de toxicologie, mais également servir à une meilleure compréhension du développement et de la fonction des glandes mammaires.



# TABLE OF CONTENTS

---

<b>ACKNOWLEDGMENTS</b> .....	<b>III</b>
<b>RÉSUMÉ</b> .....	<b>V</b>
<b>ABSTRACT</b> .....	<b>VI</b>
<b>SOMMAIRE RÉCAPITULATIF</b> .....	<b>VII</b>
<b>TABLE OF CONTENTS</b> .....	<b>XXVII</b>
<b>FIGURE LIST</b> .....	<b>XXIX</b>
<b>LIST OF TABLES</b> .....	<b>XXXI</b>
<b>LIST OF ABBREVIATIONS</b> .....	<b>I</b>
<b>1 LITERATURE REVIEW</b> .....	<b>1</b>
1.1 THE MAMMARY GLAND.....	1
1.1.1 <i>Structure and composition</i> .....	2
1.1.1 <i>Development of the mammary gland</i> .....	3
1.2 INTERCELLULAR JUNCTIONS WITHIN THE MAMMARY GLAND .....	9
1.2.1 <i>Gap junctions</i> .....	9
1.2.2 <i>Tight junctions</i> .....	11
1.2.3 <i>Adherens junctions</i> .....	12
1.3 <i>IN VIVO</i> MODELS CURRENTLY AVAILABLE .....	14
1.4 <i>IN VITRO</i> CELL CULTURE MODELS .....	16
1.4.1 <i>2D cell culture models</i> .....	16
1.4.2 <i>3D cell culture models</i> .....	17
1.4.3 <i>Alternative models for communication analysis</i> .....	18
1.5 THE ADVANTAGES AND DISADVANTAGES OF 2D VS 3D.....	19
1.6 STATE OF ART IN 3D MODELS .....	21
1.6.1 <i>Extracellular Matrix</i> .....	21
1.6.2 <i>Organ explants</i> .....	23
1.6.3 <i>Organoids</i> .....	24
1.6.4 <i>Mammospheres, Spheroids and Tumorspheres</i> .....	25
1.6.5 <i>3D bioprinting</i> .....	26
1.6.6 <i>Hanging drop</i> .....	28
1.6.7 <i>Forced-floating systems</i> .....	29
<b>2 PROBLEM</b> .....	<b>30</b>
<b>3 MATERIALS AND METHODS</b> .....	<b>33</b>
3.1 DEVELOPING A 3D MODEL <i>IN VITRO</i> OF THE MAMMARY GLAND.....	33
3.1.1 <i>Cell culture</i> .....	33
3.1.2 <i>Western Blot for cell characterization</i> .....	33

3.1.3	<i>3D Cell culture embedded in extracellular matrix</i> .....	34
3.1.4	<i>Immunofluorescence of 3D embedded culture in VitroGel</i> .....	37
3.1.5	<i>Immunofluorescence of 3D embedded culture in Matrigel</i> .....	37
3.2	DEVELOPING A LAYERED CO-CULTURE MODEL OF THE MAMMARY GLAND .....	38
3.2.1	<i>Cell lines</i> .....	38
3.2.2	<i>Porous membrane co-culture system</i> .....	39
3.2.3	<i>Cell labeling for dye transfer analysis</i> .....	39
3.2.4	<i>Flow cytometry</i> .....	40
3.2.5	<i>Cryosection of transwell membranes</i> .....	41
3.2.6	<i>Immunofluorescence of cryosections</i> .....	41
3.2.7	<i>Confocal imaging of whole membranes</i> .....	42
<b>4</b>	<b>RESULTS</b> .....	<b>43</b>
4.1	CELL CHARACTERIZATION .....	43
4.2	3D BI-LAYERED ACINUS MODEL.....	45
4.2.1	<i>Luminal MCF-12A and MCF-10A cells form acini in Matrigel, but not in VitroGel</i> .....	45
4.2.2	<i>Luminal MCF-12A cells form bilayered acini when co-cultured with Myo1089 cells in Matrigel</i> .47	
4.3	LAYERED CO-CULTURE MODEL .....	49
4.3.1	<i>Luminal MCF-12A and Myo1089 cells can be co-cultured in a layered culture system</i> .....	49
4.3.2	<i>Luminal MCF-12A and Myo1089 cells communicate by gap junction in a layered culture system</i> 51	
<b>5</b>	<b>DISCUSSION</b> .....	<b>55</b>
5.1	MCF-12A, MCF-10A AND MYO1089 ARE APPROPRIATE CELL LINES FOR THE DEVELOPMENT OF MORE COMPLEX <i>IN VITRO</i> MODELS.....	55
5.2	MCF-12A AND MYO1089 CELLS FORM BILAYERED ACINI IN MATRIGEL, BUT NOT IN VITROGEL .....	57
5.3	BEATING THE GRAVITY: THE COMPLEX ESTABLISHMENT OF THE LAYERED CO-CULTURE MODEL .....	59
5.4	LUMINAL AND MYOEPITHELIAL CELLS ARE COMMUNICATING THROUGH GAP JUNCTIONS.....	61
<b>6</b>	<b>PERSPECTIVES</b> .....	<b>63</b>
6.1	3D BILAYERED MODEL: CHARACTERIZATION AND BIOPRINTING .....	63
6.2	THE LAYERED CO-CULTURE MODEL: UNRAVELLING THE ROLE OF THE BIDIRECTIONAL CROSSTALK ON SIGNALING IN EACH CELL TYPE.....	64
<b>7</b>	<b>CONCLUSION</b> .....	<b>65</b>
<b>8</b>	<b>BIBLIOGRAPHY</b> .....	<b>66</b>



## FIGURE LIST

---

FIGURE 1: THE STRUCTURE OF THE ADULT HUMAN MAMMARY GLAND.....	2
FIGURE 2: REPRESENTATION OF A CROSS-SECTION OF THE BILAYERED ACINUS. ....	3
FIGURE 3: THE MAMMARY DEVELOPMENT. ....	4
FIGURE 4: ACINUS IN A LACTATING MAMMARY GLAND.....	9
FIGURE 5: MOLECULAR ORGANIZATION OF A GAP-JUNCTIONAL PLAQUE. ....	11
FIGURE 6: SCHEMATIC REPRESENTATION OF THE ADHERENS AND TIGHT JUNCTIONS. ....	14
FIGURE 7: THE PRINCIPLES OF HUMANE EXPERIMENTAL TECHNIQUE.....	16
FIGURE 8: INDIRECT AND DIRECT COMMUNICATION MODELS USING TRANSWELL INSERTS.....	19
FIGURE 9: COMPARISON BETWEEN 2D CELL CULTURE AND 3D CELL CULTURE. ....	21
FIGURE 10: TIMELINE OF TECHNIQUES AND EXPERIMENTS LEADING TO THE CURRENT 3D CELL CULTURE MODELS FIELD. (SIMIAN & BISSELL, 2017) .....	22
FIGURE 11: MAJOR COMPONENTS FOR BIOPRINTING. ....	27
FIGURE 12: SCHEMATIC REPRESENTATION OF THE HANGING DROP FORMATION PROCESS.....	29
FIGURE 13: BILAYERED CO-CULTURE METHODOLOGY. ....	38
FIGURE 14: BILAYERED CO-CULTURE SYSTEM. ....	39
FIGURE 15: CHARACTERIZATION OF LUMINAL MCF-12A, MCF-10A AND MYOEPITHELIAL MYO1089 CELLS THROUGH WESTERN BLOT. ....	45
FIGURE 16: CELLS SEEDED IN MONOCULTURE IN MATRIGEL.....	46
FIGURE 17: CELLS SEEDED IN MONOCULTURE IN VITROGEL. ....	46
FIGURE 18: MCF-10A AND MYO1089 CELLS SEEDED IN MIXTURE IN MATRIGEL AND CO-CULTURED FOR 12-14 DAYS. ....	47
FIGURE 19: MCF-12A AND MYO1089 CELLS WHEN CO-CULTURED IN MATRIGEL FORM STRUCTURES THAT REPRESENT THE BILAYERED ACINI OF THE MAMMARY GLAND. ....	48
FIGURE 20: MCF-12A AND MYO1089 CELLS SEEDED IN CO-CULTURE IN VITROGEL.....	49
FIGURE 21: IMMUNOFLUORESCENCE OF THE LAYERED CO-CULTURE SYSTEM CRYOSECTIONS.....	50
FIGURE 22: JUNCTIONS WERE FORMED BETWEEN LUMINAL MCF-12A AND MYOEPITHELIAL MYO1089 CELLS IN THE LAYERED CO-CULTURE SYSTEM.....	50
FIGURE 23: MCF-12A CELLS DO NOT MIGRATE TO THE OTHER SIDE OF THE MEMBRANE.....	51
FIGURE 24: MCF-12A CELLS CO-CULTIVATED WITH MYO1089 CELLS, SEPARATED BY A POROUS MEMBRANE.....	52
FIGURE 25: LUMINAL AND MYOEPITHELIAL CELLS COMMUNICATE THROUGH GAP JUNCTIONS. ....	53
FIGURE 26: CELL CO-CULTURE MODEL OF THE BRAIN BLOOD BARRIER.....	60
FIGURE 27: FIRST ADAPTATION OF NIEGO AND MEDCALF MODEL MEDCALF MODEL FOR CO-CULTURE OF CELLS ON INSERTS.....	61



## LIST OF TABLES

---

TABLE 1: ADVANTAGES AND DISADVANTAGES OF 3D CELL CULTURE MODELS. ....	20
TABLE 2: OPTIMIZATION PARAMETERS FOR 3D BI-LAYERED ACINUS MODEL.....	36
TABLE 3: CHARACTERIZATION OF LUMINAL MCF-12A, MCF-10A AND MYOEPITHELIAL MYO1089 CELLS BY IMMUNOFLUORESCENCE. ....	44
TABLE 4: COMPARISON BETWEEN PRIMARY CELL CULTURE AND CELL LINES. ....	56
TABLE 5: LUMINAL MCF-12A, MCF-10A AND MYOEPITHELIAL MYO1089 CELLS. EITHER PERFORMED BY IMMUNOFLUORESCENCE OR WESTERN BLOT. ....	56

## LIST OF ABBREVIATIONS

---

**ADP** Adenosine diphosphate  
**ATP** Adenosine triphosphate  
**AJs** Adherens junctions  
**AT** N-terminus  
**BBB** Blood-brain barrier  
**BCA** Vicinichoninic acid  
**BECs** Brain endothelial cells  
**BM** basement membrane  
**BSA** Bovine Serum albumin  
**CAD** Computer aided design  
**Calcein** 1,1'-dioctadecyl-3,3,3',3'-tetramethylindocarbocyanine perchlorate  
**Cxs** Connexins  
**CL** Cytoplasmic loop  
**CT** C- terminus  
**DAPI** 4',6-diamidino-2-phenylindole  
**DBB** Droplet-based bioprinting  
**DiL** 1,1'-dioctadecyl-3,3,3',3' tetramethylindodicarbocyanine perchlorate  
**EBB** Extrusion-based bioprinting  
**EC** Extra cellular  
**ECM** Extra cellular matrix  
**EGF** Epidermal Growth Factor  
**EHS** Engelbreth-Holm-Swarm  
**EL** Extracellular loops  
**ER** Estrogen Receptor  
**FACS** Fluorescence-Activated Cell Sorting  
**GJIC** Gap-junctional intercellular communication  
**hEGF** Epidermal Growth Factor  
**Ig-like** Immunoglobulin-like  
**K** cytokeratin  
**LBB** Laser-based bioprinting  
**MaSCs** Mammary gland stem cells  
**MECs** myoepithelial cells  
**MLC** Myosin light chains  
**MMPs** Matrix metalloproteinases  
**PBS** Phosphate-buffered saline  
**PET** Polyethylene terephthalate  
**PLC** Pregnancy lactation cycle  
**poly-HEMA** poly-2-hydroxyethyl methacrylate  
**PR** Progesterone receptor  
**PVDF** Polyvinylidene fluoride  
**rBM** Reconstituted basement membrane  
**RNA** Ribonucleic acid  
**SMA** Smooth muscle actin  
**TEBs** Terminal end buds

**TJs** Tight junction  
**ZO** Zona occludens  
**2D** Two dimensions  
**3D** Three dimensions

---

# 1 LITERATURE REVIEW

---

## 1.1 The mammary gland

The mammary gland is an organ specific to mammals whose main function is the synthesis and secretion of milk. It is composed by a dynamic epithelium that undergoes cycles of proliferation, differentiation and apoptosis in response to endocrine signals, and a complex stroma which undergoes composition remodeling throughout the development and pregnancy lactation cycle (PLC) (Campbell *et al.*, 2017). The adult mammary gland is composed of multiple types of cells: epithelial, adipose, fibroblast, immune, lymphatic and vascular cells. They all work together to construct and keep a functional gland (Figure 1)(Inman *et al.*, 2015).

This organ has a unique developmental process, being highly responsive to hormones and achieving its fully mature developmental stage at PLC (Hassiotou & Geddes, 2012). At birth, the mammary gland is present as a rudimentary ductal structure. At puberty, the branching morphogenesis initiates, causing the ductal tree to elongate into the fat pad. Upon pregnancy, alveoli are generated under the combine action of progesterone and prolactin, in order to secrete milk during lactation. At weaning, in response to the lack of demand of milk, the process of involution takes place in which the mammary gland is remodeled back into its pre-pregnancy state (Macias & Hinck, 2012).

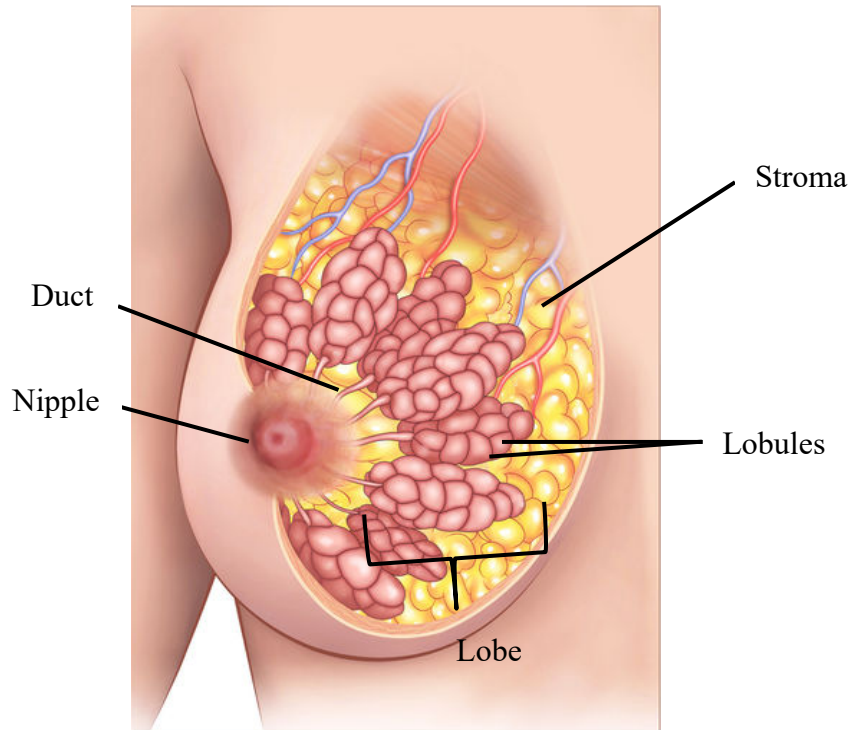


**Figure 1: The structure of the adult human mammary gland.**

*The structure of the adult human mammary gland including its ramified bilayered epithelial structure and the stroma. The stroma is composed of several different cells (adipocytes, fibroblast, endothelial cells, nervous cells and immune cells) and acellular components of the extracellular matrix (Silberstein, 2001). In this structure, milk is produced in the lobules at the lobes which are connected by the milk ducts. These ducts converge on the nipple. Rights obtained from Shutterstock.com*

### **1.1.1 Structure and composition**

The mammary gland at its mature stage is composed by a glandular epithelium and adipose tissue (in the stroma) supported by a loose framework of fibrous connective tissue called Cooper's ligaments. The secretory tissue is drained by a ductal system that stores and transports milk to the nipple during lactation. This branched ductal-lobular system is formed by lobules organized into 15-20 lobes which are drained by the collecting ducts converging at the nipple. Each lobule is made up of 10-100 acini (also called alveoli) which are approximately 0.12 mm in diameter. The acini are recognized as the functional secretory unit of the mammary gland (Figures 1, 2) (Hassiotou & Geddes, 2012). The acini and ducts have a central lumen and are lined by two cell layers, an inner layer of polarized luminal epithelial cells and an outer layer of basal cells which secrete basement membrane components (Gudjonsson *et al.*, 2005). Myoepithelial cells, the main cell type found in the basal layer, express phenotypic markers of cell from smooth muscle cells

(Deugnier *et al.*, 2002). The external layer of basal cells also includes populations of breast stem cells (MaSCs) and progenitor cells, required for generation and maintenance of the structure during the PLC (Vafaizadeh *et al.*, 2010).

These two layers of cells are surrounded by a basement membrane (BM) which separates the epithelium from the stroma. The latter is composed of adipocytes, fibroblast, endothelial cells, nervous cells, immune cells, blood vessels, connective tissue, and lymphatics (Figure 2) (Osborne MP, 2000).

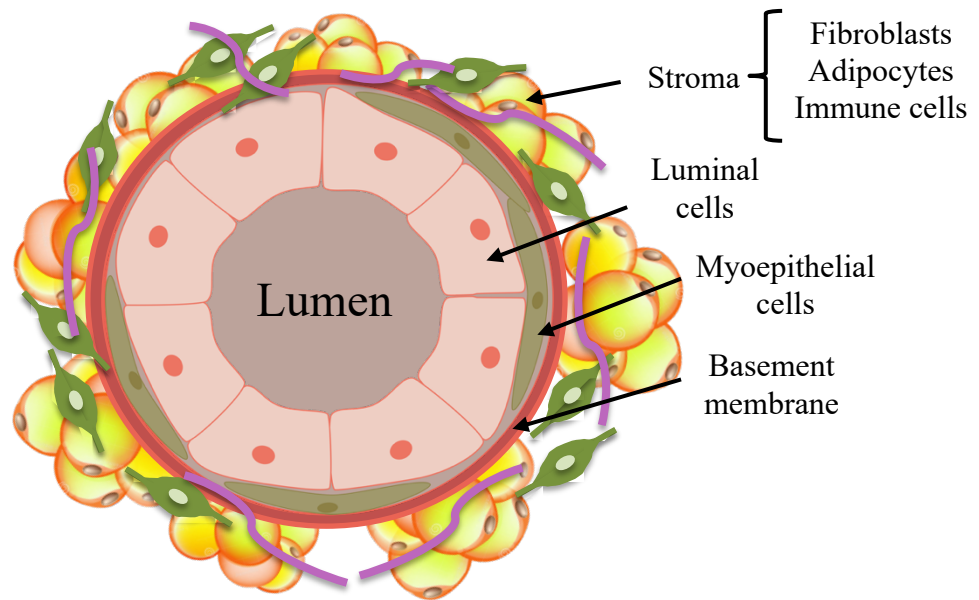


**Figure 2: Representation of a cross-section of the bilayered acinus.**

*The bilayered acinus is the functional unit of the mammary gland. The acinus is formed by an internal layer of luminal cells which secrete milk into the lumen surrounded by a layer mainly composed of myoepithelial cells. The epithelium is separated from the stroma by the basal membrane (Image adapted from Mélanie Bysby (unpublished)).*

### 1.1.1 Development of the mammary gland

The mammary gland is composed as a rudimentary duct at birth and remains relatively quiescent until puberty, growing only in an isometric rate with the body (Figure 3). In response to hormones at puberty, the epithelial ductal cells expand into the mammary fat pad, led by highly proliferative multilayered terminal end buds (TEBs) (Inman *et al.*, 2015). In the TEB of the developing mammary epithelium, an outer layer of cap cells surrounds a multi-layered population of body cells (Figure 3). The cap cells appear to be a population of mammary stem cells that differentiate into the myoepithelium, whereas the body cells give rise to luminal epithelial cells (Hennighausen



& Robinson, 2005). After the first important phase of proliferation and differentiation, the mammary gland at the adult virgin stage is filled with epithelial branching structures (Figure 3). The ducts of this structure contain an outer layer of myoepithelial cells and an inner layer of luminal epithelial cells. During pregnancy, the mammary epithelium undergoes an additional phase of remodeling, the alveologensis, as the luminal epithelium proliferates and differentiates into structures known as alveoli, which produce and secrete milk (Figure 3). During pregnancy, hormonal changes trigger a large expansion of alveolar cells which mature into milk-secreting acini during lactation. Upon weaning, involution is characterized by massive cell death and extra cellular matrix (ECM) remodeling, returning the mammary gland to a state that resembles the resting adult mammary gland (Figure 3) (Inman *et al.*, 2015). During involution, the stroma surrounding the mammary gland is also remodeled as a result of the secretion of matrix metalloproteinases (MMPs) (Watson, 2006). Once involution is complete, the mammary epithelium re-enters a period of relative quiescence. Indeed, the mammary gland is never totally quiescent as cycles of proliferation-differentiation-apoptosis are taking place during the entire reproductive life of the women (or the female) with every menstrual cycle (of estrus).

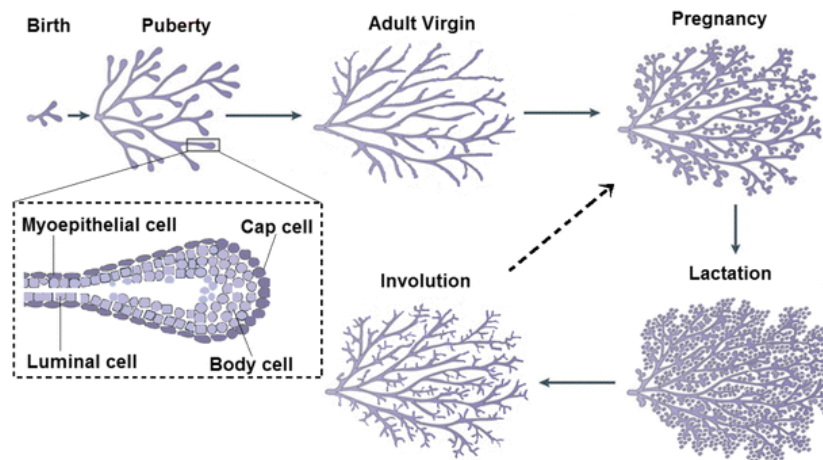


**Figure 3: The Mammary Development.**

*At birth the gland is constructed as a rudimentary duct which remains relatively quiescent until the onset of puberty, when TEBs are formed to be proceeded by ductal elongation. During pregnancy, alveolar budding and differentiation take place to give rise to the functional unit called the acinus were milk is produced and store. (Paine & Lewis, 2017)*

#### 1.1.1.1 Role of myoepithelial cells in polarization

The mammary gland epithelium encompasses polarized epithelial cells. This polarity divides the plasma membrane into apical, lateral and basal membrane domains, and allows distinct molecules to be inserted to specific areas of the plasma membrane. Therefore, thanks to this process, the components of the basal membrane, such as laminin and collagen IV, are secreted to the basal membrane domain by the myoepithelial cells, whereas other proteins, such as milk proteins, are secreted to the apical surface into the lumen by the luminal cells (Inman *et al.*, 2015). Correct orientation of polarity is therefore essential for tissue function and thus is a clear requirement for *in vitro* mammary 3D models (Sogaard *et al.*, 2019).

In the mammary gland, the polarity of the internal layer of luminal cells is induced by the myoepithelial cells from the external layer of the epithelium (Gudjonsson *et al.*, 2002). It has been shown that when primary luminal cells are cultured in laminin-rich ECM in 3D, they form polarized acini-like spheroids, even in absence of myoepithelial cells (Petersen *et al.*, 1992). However, when they were culture in a collagen 1 matrix (without laminin), they formed structures with an altered expression of integrins, inverse polarity and an absence of central lumen (Gudjonsson *et al.*, 2002). This phenomenon was reversed when these primary luminal cells were co-cultured with primary myoepithelial human cells in laminin; acinus polarity was restored, confirming the important role of laminin, which is secreted by myoepithelial cells *in vivo* (Gudjonsson *et al.*, 2002). It has also been shown that cell-ECM interactions are important for the orientation of apico-basal polarity and that ECM receptors, such as integrins, play important roles during polarization (Rodriguez-Boulán & Macara, 2014).

Laminin 1 is composed as a heterotrimer and is a major component of the basal membrane. Among the laminins present in the human breast basal membrane (laminin 1, 5, 10 and 11), laminin 1 has been shown to be unique in its ability to substitute for myoepithelial cells for polarization (Ekblom *et al.*, 2003). Polarization is crucial for the proper development and function of the mammary gland epithelium. As a result, one characteristic of breast tumor histology is the loss of epithelial polarity (Campbell *et al.*, 2017) and a reduction or absence of basement membrane (Kodama *et al.*, 2005), which was further supported by evidence that breast carcinoma cells exhibit a down-regulation in the laminin-binding integrin subunits (Koukoulis *et al.*, 1991).

#### 1.1.1.2 Basal Membrane

The basal membrane is a continuous layer of ECM directly in contact with the myoepithelial layer of cells in the mammary gland, anchoring the mammary epithelium to the surrounding stroma. It primarily contains type IV collagen and laminins (Nerger & Nelson, 2019). This ECM aids to maintain epithelial polarity, allowing secretion and ejection of milk. For the mammary gland, the basal membrane is involved in important signalization; the expression of milk protein genes such as  $\beta$ -casein,  $\beta$ -lactoglobulin and whey acidic protein are tightly dependent of cell interactions with basement membrane, more specifically integrin ligands presented to the laminin component of ECM (Streuli *et al.*, 1991). From a structural perspective, the protein components, including laminins, fibronectin and collagens, provide resistance to tensile forces while the carbohydrates chelate water and provide resistance to compressive forces (Sokol *et al.*, 2016). Normal myoepithelial and luminal cells deposit basement membrane, particularly the  $\alpha$ 3 and  $\alpha$ 5 chains of laminin 1, but only myoepithelial cells deposit  $\alpha$ 1 laminin chains (Campbell *et al.*, 2017). It has been shown that alteration in ECM organization or composition as well as excessive ECM deposition is related to diseases such as fibrosis and cancer (Naba *et al.*, 2017).

#### 1.1.1.3 Stroma

In the human mammary gland, the interstitial stroma accounts for >80% of the breast volume in non-pregnant women. However, the volume of the stroma changes up to 20% during the menstrual cycle as the epithelium proliferates, getting ready for a potential pregnancy (Ronnov-Jessen *et al.*, 1996). The stroma is more than just a passive supporting structure; it contains many cell types including fibroblasts, adipocytes and immune cells that can influence the epithelium by releasing growth factors and cytokines or directly modulating the ECM in which the cells reside (Haslam & Woodward, 2003). Studies have demonstrated the importance and influence of the stroma over epithelium in many ways. By instance, when the mammary gland epithelium was cultured within salivary gland stroma, the resulting epithelial tissue morphology closely resembled branching patterns typical of salivary gland rather than mammary gland (Sakakura *et al.*, 1976).

Mammary gland adipose tissue was previously seen as a relatively inert energy storage network. However, in the last decade, some research groups have highlighted its endocrine and paracrine activity. Signaling factors released from adipocytes can modulate tissue metabolism and

homeostasis, in addition to ECM, through MMPs deposition and release (Ahima & Flier, 2000). Furthermore, these adipokines can influence both the development of the branching network, but also tumor invasion through increased cell motility, migration and angiogenesis (Poltavets *et al.*, 2018). Adipocyte-secreted factors can affect tumorigenesis by increasing the stabilization of pro-oncogenic factors as a result of a reduction in the gene expression of their inhibitors (Iyengar *et al.*, 2003). Type VI collagen, a soluble extracellular matrix protein abundantly expressed in adipocytes, is further upregulated in adipocytes during tumorigenesis. It promotes GSK3beta phosphorylation, beta-catenin stabilization, and increased beta-catenin activity in breast cancer cells and may critically contribute towards tumorigenesis when not counterbalanced by other factors (Iyengar *et al.*, 2003).

#### 1.1.1.4 Luminal cells

The luminal epithelial cells are polarized glandular cells expressing cytokeratins 8 and 18 with specialized apical and basolateral membrane domains (Ronnov-Jessen *et al.*, 1996). They form the internal layer of the mammary gland bilayered epithelium. They can be divided into the ductal luminal cells, which line the inner layer of the canals, and the alveolar luminal cells, which secrete milk into the lumen of the acinus during lactation (Macias & Hinck, 2012). The apical surface of the luminal cells delimits the lumen while the basal surface is in contact with the myoepithelial cells or the basal membrane. The apical side is charged with mucine proteins, such as the mucine 1 and the sialomucin, preventing adhesion, while on the contrary, the basal surface express adhesion molecules (Adriance *et al.*, 2005). The composition of the polarized structure of luminal cells is highly regulated by tight and adherens junctions (Anderson *et al.*, 2007).

#### 1.1.1.5 Myoepithelial cells

The outer layer of the mammary gland epithelium is composed of myoepithelial cells as well as some putative stem and progenitor cell types, bordering the basal membrane which separates the epithelial layer from the stroma. They express basal-type cytokeratins 5, 14 and 17, P-cadherin and high levels of  $\Delta$ Np63, as well as smooth muscle actin which mediates their contractile function (Inman *et al.*, 2015). Myoepithelial cells have a different shape and distribution depending on their location on the mammary gland's epithelium; ductal myoepithelial cells are spindle shaped and

oriented such that they form a continuous layer around luminal cells. Upon contraction, the myoepithelial cells decrease the length and increase the diameter of the ducts to eject the milk. In the contrary, myoepithelial cells located in the acini are stellate shaped, forming a discontinuous basket-like mesh around the luminal cells. During pregnancy and lactation, the myoepithelial cell body and processes extend to fully encompass the expanded alveolar epithelial cells (Figure 4) (Adriance *et al.*, 2005). The contraction of this mesh-like myoepithelium eject the milk from the secretory alveoli into the ducts, towards the nipple and out of the body (Cagnet *et al.*, 2017).

The contraction of the myoepithelial cells takes place during lactation in response to oxytocin, a neuropeptide produced by the pituitary gland. Their contraction, like that of smooth muscle, is induced by the phosphorylation of myosin light chains (MLC) by MLC kinase. The subsequent dephosphorylation of MLC by a specific phosphatase leads to relaxation (Cagnet *et al.*, 2017). Although the induction of the contraction of myoepithelial cells results from oxytocin stimulation, there are also others, still unknown, autocrine mechanisms which participate in the regulation of this process. Contraction for milk ejection is not the only work of myoepithelial cells, they are also involved in mammary gland morphogenesis in all developmental stages, modulating proliferation and differentiation of luminal cells. They also take part in the formation of extracellular matrix by synthesizing its components and secreting proteinases and their inhibitors. As a result, myoepithelial cells are being considered as natural cancer suppressors, stabilizing the normal structure of the mammary gland, but also secreting suppressor proteins limiting the cancer growth, its invasiveness, and angiogenesis (Sopel, 2010). A number of myoepithelial-specific proteins have shown to inhibit epithelial tumor formation (Sun *et al.*, 1999), including  $\alpha$ -smooth muscle actin (Okamoto-Inoue *et al.*, 1999), keratin 5 (Zajchowski *et al.*, 1990),  $\alpha 6$  integrin (Sager *et al.*, 1993), caveolin-1 (Lee *et al.*, 1998), and connexin 43 (Hirschi *et al.*, 1996; Plante *et al.*, 2011), among others.

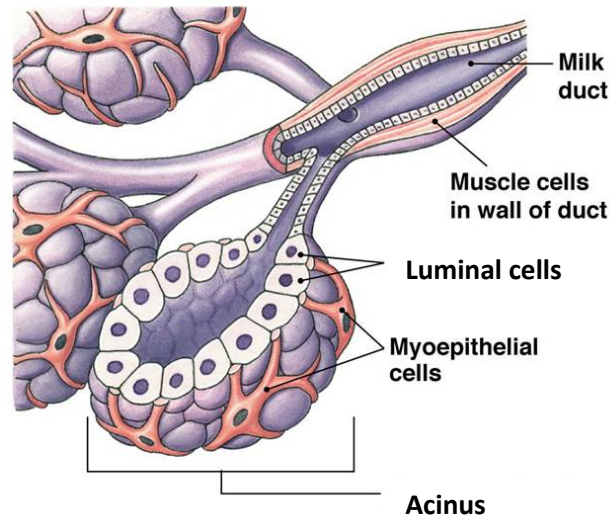


**Figure 4: Acinus in a lactating mammary gland.**

*The Myoepithelial cells surround in a mesh-like structure the luminal cells which secrete milk into the lumen. (Quora.com)*

## **1.2 Intercellular junctions within the mammary gland**

### **1.2.1 Gap junctions**

Gap junctions are clusters of intercellular channels that directly connect the cytoplasm of adjacent cells to allow intercellular transfer of ions and small hydrophilic molecules. They are composed by gap-junctional channels which are complexes formed by head-to-head docking of hexamers (connexons) of proteins called connexins (commonly abbreviated by Cx, followed by their molecular mass in kilodaltons). Gap junctional communication is essential for proper development and health in animals and humans. In humans, connexins form a family of 21 proteins (Goldberg *et al.*, 2002; Goodenough *et al.*, 1996; Goodenough & Paul, 2009). The function of gap junctions in cell and tissue biology is of highest importance as gap-junctional intercellular communication (GJIC) exists in nearly every mammalian cell type (Goodenough *et al.*, 1996). While the channels assembled from connexin family members serve a common purpose of allowing the intercellular exchange of small metabolites, second messengers and electrical signals, the diversity of function is attributed to the subset of connexins that are expressed in any one cell type. While not all channels are the same, they share the property of excluding molecules that exceed 1 kDa in size (Alexander *et al.*, 2004). Important transjunctional molecules include cAMP, InsP<sub>3</sub>, adenosine,

ADP and ATP, to name only a few (Goldberg *et al.*, 2004). Many tissues and cell types express two or more members of the connexin family. The most ubiquitously expressed connexin in mammals is Cx43. It is well known that Cx43 is endogenously expressed in at least 35 distinct tissues encompassing over 35 cell types that include cardiomyocytes, keratinocytes, astrocytes, endothelial cells and smooth-muscle cells, among many others.

Connexins are polytopic integral membrane proteins where the polypeptide backbone goes through the membrane four times, yielding two extracellular loops (EL-1 and EL-2), a cytoplasmic loop (CL) with both the N-terminus (AT) and the C-terminus (CT) exposed to the cytoplasm (Figure 5). The four transmembrane domains and the two extracellular loops are highly conserved between each connexins and between species. The highest degree of diversity among connexins is in the sequence and size of the CL region and both the size and posttranslational modified status of the CT domain. The adjacent connexons are connected by intramolecular disulphide bonds located within the EL domains, as all connexins have three conserved cysteine residues in each EL (Laird, 2006).

Three different types of gap junctions have been reported and classified depending on their molecular composition: homomeric/homotypic, heteromeric and heterotypic. Homotypic or heterotypic gap junctions comprise two identical or two different types of hemichannel, respectively. Homomeric or heteromeric hemichannels are composed of one or more type of connexin, respectively (Figure 5a) (Sohl *et al.*, 2005).

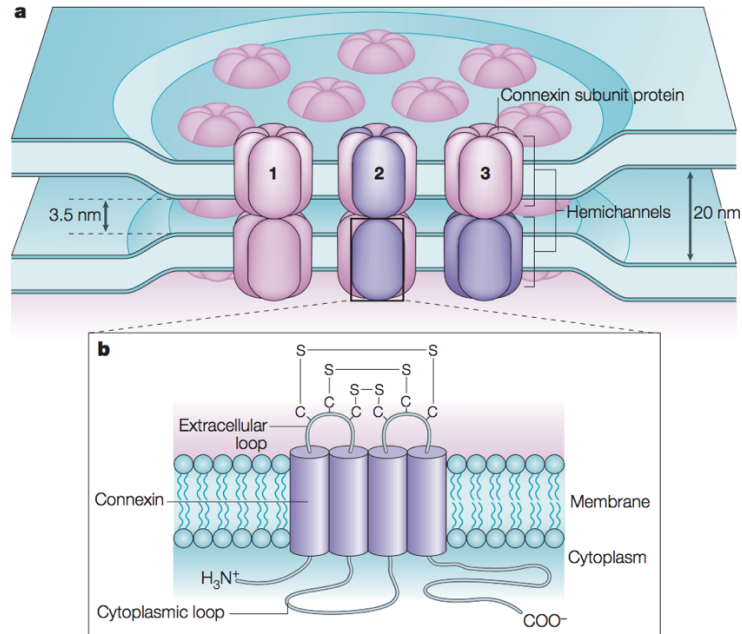


**Figure 5: Molecular organization of a gap-junctional plaque.**

A) Connexons from neighboring cells can dock to each other and form a gap junction channel. Gap junctions can be 1) homomeric/homotypic, 2) heteromeric or 3) heterotypic. B) Connexin protein subunits are tetra-spanning membrane proteins that share three conserved extracellular cysteine residues, which are crucial for docking. The subunits vary mainly in their cytoplasmic loop and carboxy-terminal region. S-S represents conserved disulphide bonds in the extracellular domains of connexins. (Sohl *et al.*, 2005)

### 1.2.2 Tight junctions

Tight junctions (TJs), play a crucial role in the establishment and maintenance of cell polarity within tissues. In the mammary gland, they are crucial for separating apical and basolateral domains. TJs also create the regulator barrier paracellular movement of molecules through epithelial sheets, thereby maintaining tissue homeostasis. They are macromolecular complexes composed of several types of membrane proteins, cytoskeletal proteins, and signaling molecules. The TJs are made up of two major transmembrane spanning structural proteins, called occludin and claudins, linked intracellularly to the actin cytoskeleton via scaffolding proteins, such as the zona occludens (ZO) (Stelwagen & Singh, 2013). Generally, TJs exhibit four major functions: 1) a gate function, defining transepithelial permeability properties; 2) a fence function, determining epithelial cell polarity; 3) a signaling function in regulatory pathways; and 4) a stabilizing function, maintaining the integrity of the epithelium (Markov *et al.*, 2017).



The mammary epithelium synthesizes and secretes milk components apically into an alveolar lumen. The existence and maintenance of a small transepithelial potential difference, in the order of 30 to 35mV, between basolateral (blood side) and the apical side (milk side) of the mammary epithelial cells is a requisite for the secretory process to take place (Stelwagen & Singh, 2013). In the mammary gland, TJs between adjacent secretory epithelial cells are formed during lactogenesis and are instrumental in establishing and maintaining milk synthesis and secretion (Kobayashi *et al.*, 2013). Loss of TJs integrity during established lactation, experimentally induced or caused by mammary inflammation, has been linked to reduced milk secretion and mammary function and increased paracellular transport of blood components into the milk and vice versa (Brennan *et al.*, 2010). Increasingly, the importance of TJ integrity is recognized in the prevention and progression of mammary cancer (Stelwagen & Singh, 2013). Many of these components are regulated during mammary gland development and pregnancy cycles, and several have received much attention as possible tumor suppressors during progression to breast cancer (Itoh & Bissell, 2003) (Dianati *et al.*, 2016)

### **1.2.3 Adherens junctions**

A major function of adherens junctions (AJs) is to maintain the physical association between cells; their disruption causes loosening of cell-cell contact, resulting in a disorganization of tissue architecture. The AJs contain two subcomplexes: the nectin-based adhesions, which form the first attachment of cells to their neighbors and the cadherin-based adhesions which mediate strong cell-cell adhesion (Campbell *et al.*, 2017). These junctions provide a calcium independent cell-cell adhesion performed by the nectins and a calcium-dependent cell-cell adhesion performed by the cadherin complexes (Nakanishi & Takai, 2004).

Adherent junctions are composed of a family of transmembranal proteins, the cadherines; within the group, the classic cadherins are the best studied. They include the neural cadherin (N-cadherin, the epithelial cadherin (E-cadherin), the placental cadherin (P-cadherin) and the retinal cadherin (R-cadherin). Although the classic cadherins were originally named from the tissue in which they were firstly found, it is now known that their distributions are not limited to these tissues (Meng & Takeichi, 2009). Their extracellular (EC) domain is divided into five repetitive subdomains, called cadherin repeats or EC domains, and each subdomain contains calcium-binding sequences (Overduin *et al.*, 1995). The interaction of calcium ions with these sequences

controls the conformation of the extracellular domain, therefore providing its adhesive function an on/off system. This extracellular domain of cadherins undergoes homophilic interaction with the domain present on the adjacent cell (Meng & Takeichi, 2009).

The cytoplasmic domains are highly conserved among classic cadherin, and they interact with cytoplasmic proteins, including the  $\alpha$ -,  $\beta$ -,  $\gamma$ -catenins (also known as plakoglobin) and the catenin p120 (Knudsen & Wheelock, 2005). These catenins associate then with a variety of molecules, such as cytoskeletal proteins and their regulators. These cytoplasmic components of AJs affect the adhesive action of the extracellular domain of cadherins in various ways, leading to alterations in the strength and stability of cell–cell contacts.

The nectins, a family of immunoglobulin-like (Ig-like) transmembrane proteins, contains four members each with several splice variants (Takai *et al.*, 2003). The nectin extracellular domain contains three Ig-like loops, followed by a single pass transmembrane domain and a cytoplasmic tail. The cytoplasmic tails of nectins are involved in protein-protein interactions, and at the C-terminus they bind to afadin, which is an actin binding protein that anchors nectins to the actin cytoskeleton (Takahashi *et al.*, 1999). In addition to afadin, nectins interact with cell polarity proteins, ensuring the correct establishment of apico-basolateral polarity.

Both, cadherins and nectins mediate cell-cell adhesion and facilitate the establishment of apical-basolateral polarity but nectin dimers are unable to support strong cell-cell adhesion, therefore cadherins remain as the major cell-cell adhesion (Takekuni *et al.*, 2003).

Even though the tight and adherens junctions have been studied independently, it has been shown that the formation of tight junctions is dependent on the cadherin- and nectin-complexes formation. In addition, mutated tight junction proteins delay the maturation of adherens junctions (Campbell *et al.*, 2017).

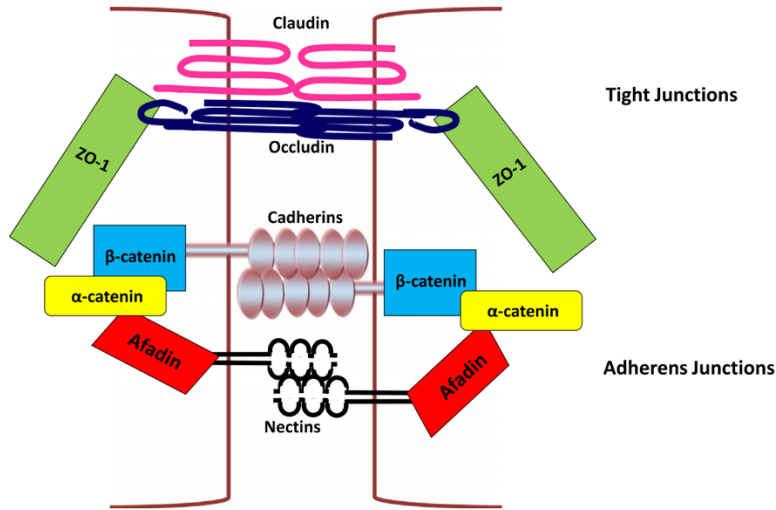


**Figure 6: Schematic representation of the adherens and tight junctions.**

The adherens junctions are composed of the nectin-based adhesions and the cadherin-based adhesions. The extracellular domains of nectins dimerize with nectins on neighboring cells and the cytoplasmic tail recruits afadin. Similarly, cadherins bind to cadherins on adjacent cells. The cadherin cytoplasmic tail recruits  $\beta$ -catenin which in turn binds  $\alpha$ -catenin. More apical to the adherens junction are the tight junctions. The main constituents of the tight junctions are two transmembrane spanning proteins, occludin and claudin. Occludin recruits ZO-1, an actin binding protein, that can during the formation of cell-cell junctions bind to the adherens junction protein,  $\alpha$ -catenin. The brown lines indicate the plasma membranes of two adjacent cells (Campbell *et al.*, 2017).

### 1.3 *In vivo* models currently available

For a long period, scientist have relied on *in vivo* models as an important research tools to study and understand the initiation of diseases, and the effects of toxic compounds and drugs. Using *in vivo* models is an essential step between *in vitro* systems and clinical studies. A large number of different models are currently available, reflecting different types and stages of several diseases; choosing which one to use depends on the specific research hypothesis to be analyzed (Holen *et al.*, 2017). In the *in vivo* state, cells are maintained in a responsive environment with a constant supply of nutrients and removal of waste products via the circulatory system, therefore providing a complex model better suited for observing the overall effects of an experiment on a living subject (Antoni *et al.*, 2015). Consistently, to study the mammary gland, animal models have been the reference, since they present an integral system (vascularity, immune system and endocrine system) (Knight & Przyborski, 2015). There are also many rodent models genetically engineered to spontaneously develop human-like tumors in response to experimental modification of gene expression for breast cancer research. However, testing on this models still fail regularly to be

translated into new therapies on human diseases (Hait, 2010). In addition, there are some forms of deadly cancer that currently lack qualified animal models (Steele & Lubet, 2010).

The difficulties faced when extrapolating from the laboratory to human are still determined by species differences, making this transition hard to manage (Perlman, 2016 #4165}). The process of validating an animal model therefore includes two types of variables, the ones that can be identified and the ones that are untraceable (Pound & Ritskes-Hoitinga, 2018). The first group includes problems such as the laboratory animal populations being rather homogenous samples which do not extrapolate to the heterogenous human populations (Henderson *et al.*, 2015). Moreover, this type of variables includes the stage of life, existing pre-conditions and in general the lack of complexity between animal models and the human being (Pound & Ritskes-Hoitinga, 2018). When talking about mammary gland, the most common animal model are rodents. They are chosen due to their short reproductive cycle, the fact that their mammary gland is remodeled through lifecycle such as in the human and the great genetic homology between rodents and humans as well as biochemical and physiological similarities (Borowsky, 2003).

The second group of difficulties to face are due to the fact that we assume that gene functions and systems are conserved between species and through the evolutionary process (Borowsky, 2011). Moreover, we fail to assume that even if two systems appear to be homologous, they are not necessarily going to function identically. In further detail, even two molecular pathways which appear identical between rodents and humans, may have differences in specific receptors or enzymes, which could cause them to behave very differently (Mestas & Hughes, 2004). Considering all the difficulties when extrapolating a result from an animal model to the human reality, the decision of which *in vivo* model to use should rely on the experiment question (Preuss, 2006).

Even though, this field has progressed considerably in the last 20-30 years, the use of animals in research, teaching and testing is increasingly arising as an important ethical and political issue, since many of the experiments can cause pain or reduce their quality of life (Knight & Przyborski, 2015). In addition, animal models increase considerably the cost for experimental projects, the studies involving *in vivo* models are long to complete and require specialized personal and adequate installations, as well as previous approval from an ethical committee (Antoni *et al.*, 2015). As a result, “The Principles of Humane Experimental Technique” was published by William Russell and Rex Burch in 1959. They proposed that if animals were required to be used

in experiments, every effort should be made to Replace them with alternatives, to Reduce to a minimum the number of animals used and to Refine experiments so that they caused the minimum pain and distress (Figure 7). Initially these 3R's of animal research were given little attention, but gradually they have become essential considerations when animals are used in research and they have become formally incorporated into some animal procedures such as in United Kingdom (Flecknell, 2002). For mammary gland studies, while many efforts were made to create suitable *in vitro* models, there is still a need for an appropriate model to understand the epithelium formation and function.

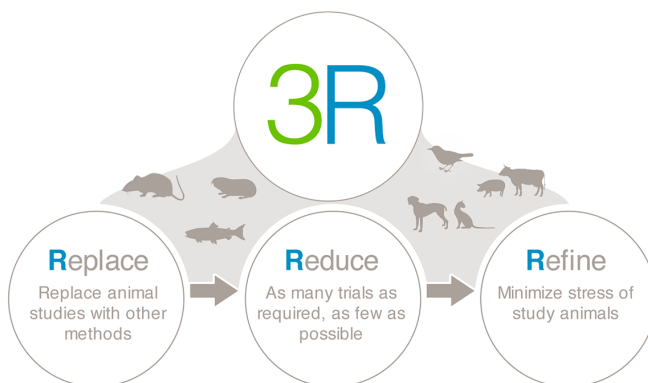


**Figure 7: The principles of Humane Experimental Technique.**

*Published in 1959, these principles state to Replace, Reduce and Refine animal models (Bayer.com)*

## **1.4 *In vitro* cell culture models**

### **1.4.1 2D cell culture models**

Cell-based assays use traditional two-dimensional (2D) monolayer cells cultured on a flat and rigid surface (Edmondson *et al.*, 2014). Cells can be obtained from standardized cell lines with a known phenotype or can be extracted from tissues and grown in culture. The immortalized cells, therefore, provide some advantages, considering that they remain relatively stable and they are easily accessible to scientist worldwide, thus, facilitating the replicability of the experiments. Cells obtained from primary culture, give more accurate regarding the diversity among individuals, since they come from different beings. However, primary cultured cells are only kept in culture for short periods and imply a higher cost than regular immortalized cells (Honegger, 2001).

However, many studies have been reviewed and showed that cells on 2D surfaces do not maintain the same differentiation or gene expression observed *in vivo* (Nerger & Nelson, 2019). In addition, while 2D cell culture has proven to be a valuable method for mechanistic studies, it has some limitations due to the fact that it does not adequately take into account the natural 3D environment of cells. Therefore sometimes, 2D cell culture provides misleading data for *in vivo* responses (Knight & Przyborski, 2015). Cell culture has been an important platform in fundamental science, providing a simple, fast and cost-effective tool to reduce large-scale and cost-intensive animal testing. Toxic compounds and developing pharmaceuticals have been tested on 2D cell culture on a regular basis (Edmondson *et al.*, 2014).

The standard procedure for screening compounds still starts with the 2D cell culture tests, followed by animal model tests and clinical trials in the case of drug testing. However, only about 10% of the compounds progress successfully through clinical development, the majority of them fail during clinical trials, largely due to the lack of the expected effect or unacceptable toxicity (Hopkins, 2008; Kola, 2008). An important portion of these failures is attributed to data collected from the 2D cell culture experiments in which cellular response might be altered due to the lack of natural microenvironment (Edmondson *et al.*, 2014).

***There is a need to identify ineffective or unacceptable drugs and toxic compounds as early as possible, even before animal tests. Therefore, it is required to evolve and improve the *in vitro* techniques used nowadays in order to get more predictable results. Moreover, there is also a need for biologically representative and malleable models for the study of development and function of the mammary gland.***

#### **1.4.2 3D cell culture models**

3D culture models are being developed as systems to study specific signaling pathways and structure of the mammary gland. This type of *in vitro* models consists of cells being cultured with the finality of making them form spheroids that recapitulate the structure of the mammary gland. They have been developed either using a scaffold generated from natural or synthetic materials, or in a scaffold-free environment (Knight & Przyborski, 2015). These systems are engineered to gather key biophysical and biochemical characteristics of a tissue and its microenvironment. Primary components of a branched organ, such as the mammary gland, include the epithelium, basement membrane, ECM, muscle, vasculature, connective tissue and nerves. Being able to engineer a

culture system that simultaneously incorporates all these elements has not been achieved up to date. However, the use of simplified tridimensional models already provide several advantages in analyzing organs in the laboratory (Nerger & Nelson, 2019). To improve drug development and toxicology screening using 3D models, the functional unit of tissues must be considered rather than single cells. In the case of the mammary gland, it comprises luminal and myoepithelial cells epithelial cells with specialized cell-cell interactions (Breslin & O'Driscoll, 2013). In current 3D models, epithelial cells are grown in gels that model the ECM and stroma or as cell aggregates floating in media. Normal mammary epithelial cells are usually cultured in or on gels. This monolayered epithelium has been used extensively to study the role of oncogenes in cancer initiation. However, it still fails to recapitulate the collective processes that occur during mammary gland development and, most importantly, is not representative of the bilayered epithelium of the mammary gland. Although bilayered epithelium have been created *in vitro* from cells isolated from mouse or human mammary gland epithelium or with whole-gland explants as starting material, these models are not ideal for mechanistic studies as they are hard to genetically manipulate (Florian *et al.*, 2019).

In our laboratory, a 3D cell culture model of the mammary gland has already been developed. Bilayered acini was successfully achieved using luminal MCF-12A cells and myoepithelial Hs578Bst cells (Weber-Ouellette *et al.*, 2018). This structure represented, to the best of our knowledge, the first model to use luminal and myoepithelial cell lines in a 3D cell culture model. Even though the bilayered acini formed represented 50% of the total structures, while the rest were composed of luminal cells only, this model represented a step forward towards a biologically-relevant *in vitro* model of the human mammary gland that needed to be further optimized to be used routinely in the lab.

***There is thus, still a need for a representative, reproducible, malleable and efficient bilayered acini model that recapitulates the 3D structure of the human mammary gland.***

### **1.4.3 Alternative models for communication analysis**

Taking into account the limitations established previously for the usage of traditional *in vitro* and *in vivo* models, different alternative models have started to arise. By example, cell culture models using inserts with porous membranes have been used in the analysis of the blood-brain barrier (BBB). In this model, astrocytes are grown in non-contact conditions in the bottom of a well

separated from brain endothelial cells (BECs) which are cultured on a porous membrane (Deli *et al.*, 2005). This type of models allows the communication of different cell types through soluble factors in the media (Coisne *et al.*, 2005) (Figure 7). To better resemble the interactions of the cells and the anatomical structure of the BBB *in vivo*, more advanced models have been developed by cultured astrocytes and BECs in direct contact conditions, maintaining them on opposite sides of the membrane (Gaillard *et al.*, 2001). Using this type of models, it has been established that for true contact to occur, the pores of the membrane should be  $\geq 1\mu\text{m}$  in diameter (Figure 8) (Coisne *et al.*, 2005). Seeding cells in direct contact in each side of the porous membrane cause its own challenges; a protocol was proposed in 2013 for this purpose. In this system, cells were seeded on the abluminal side of the insert kept from leaking by using plastic tubing, creating a chamber to hold the cell culture media and cells for them to adhere. After the cells were adhered, the plastic tubing was disassembled and the inserts were turned, in order to seed cells on the luminal side of the insert (Figure 25) (Niego & Medcalf, 2013).

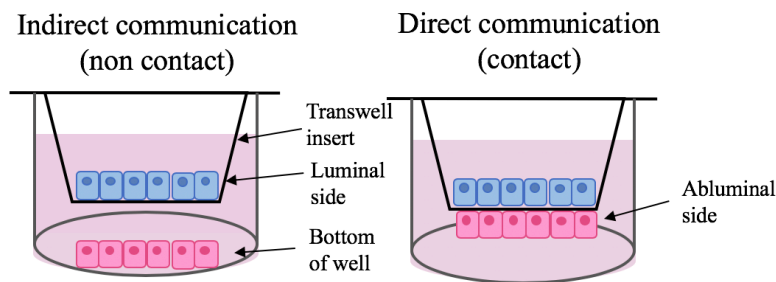


Figure 8: Indirect and Direct communication models using transwell inserts.

### 1.5 The advantages and disadvantages of 2D vs 3D

Cell culture in monolayer or 2D has been an important tool for biological research, but growing cells in flat monolayers on plastic surfaces does not accurately mimic the conditions for organization and cellular interactions observed *in vivo*. As compare to the 2D, the 3D cell culture allows cells to grow and interact with their surroundings in all three dimensions. Different cell types grown in 3D models have proven to be more physiologically relevant and reflect better the *in vivo* biological mechanisms like cell viability, morphology, proliferation, differentiation, response to stimuli, migration, invasion, drug metabolism, gene expression, protein and synthesis (Knight & Przyborski, 2015) (Simian & Bissell, 2017). Cells in 2D monolayers are routinely used as initial model systems for fundamental studies, for evaluating the effectiveness of therapeutic



drugs and to evaluate the safety of molecules. This initial testing precedes *in vivo* studies and further advancing into human clinical trials, when required (Weaver *et al.*, 2002). 2D cell culture results generally determine the crucial decisions into moving forward or stopping a research project. Nevertheless, outcomes from 2D models are not always reproducible *in vivo*. Therefore, growing cells as 3D models, being more analogous to their human representation *in vivo*, might give more relevant results (Breslin & O'Driscoll, 2013).

3D model development has itself difficulties to overcome, including the engineering of the extracellular matrices and the changes of conditions for cell culture. Some of the advantages and disadvantages of using 3D cell culture models have been included in table 1.

**Table 1: Advantages and disadvantages of 3D cell culture models.**

Advantages	Disadvantages
More accurate representation of: Morphology Proliferation Differentiation Response to stimuli Cell-cell communication Migration and invasion (for cancerous cells) Cell polarization Drug metabolism Gene expression Protein synthesis General cell function Physiological genotype relevance Physiological phenotype relevance	Reproducibility between batches of biomimetic scaffold Engineering of 3D matrices Capacity to scale up or down a single 3D format Handling of post culturing processing Imaging depending on the scaffold size, material transparency and microscope Optimization of 3D cell culturing assays used to determine the cellular response to drug interaction (dose dependent cell viability, cell-cell/cell-ECM interaction) Control of culture condition (temperature, pH, etc)

Hela cells have been bioprinted to form 3D structures in a bioink composed of 10% gelatin, 1% sodium alginate and 2% fibrinogen to create an *in vitro* cervical cancer model; the cells showed higher proliferation rate, greater tendency to form spheroids, increased matrix metalloproteinase expression and higher chemoresistance than cells in 2D culture (Zhao *et al.*, 2014). This outcomes suggest that 3D models may better predict drug efficacy than conventional 2D cell culture or animal models (Swaminathan *et al.*, 2019). 3D human cancer model biomanufacturing would enable advance study of healthy and disease cells and provide a powerful platform for drug screening (Charbe *et al.*, 2017; Jackson & Thomas, 2017).

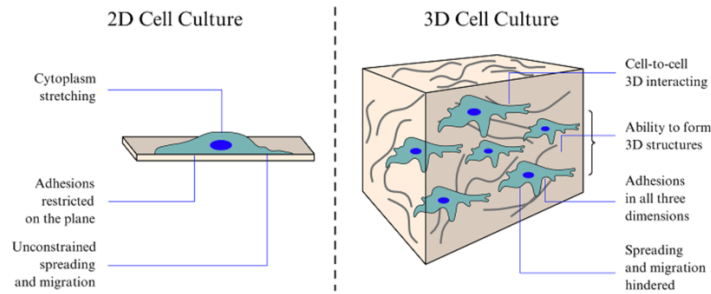


**Figure 9: Comparison between 2D cell culture and 3D cell culture.**

The main differences between cell behavior and the constraints when cultivated on 2D are shown (Ustyugov *et al.*, 2018).

## 1.6 State of art in 3D models

The development of 3D cell culture models started in the early 1900's and have been constantly evolving in parallel to the technological advances in materials, cell biology and design for ECM (Figure 10). The first use of the words three-dimensional culture models can be tracked down to some assays developed back in 1989 and in 1992 (Barcellos-Hoff *et al.*, 1989; Petersen *et al.*, 1992). Since then, many techniques have been developed to produce 3D models.

### 1.6.1 Extracellular Matrix

Various synthetic and naturally occurring substrates have been developed that support 3D growth of cells. In most fields, including mammary gland biology and tumorigenesis, the two most common substrates used are the basement membrane rich extracellular matrix (ECM) isolated from Engelbreth-Holm-Swarm (EHS) mouse sarcomas (e.g. Matrigel) and collagen extracted from rat-tails (Bruno *et al.*, 2019).

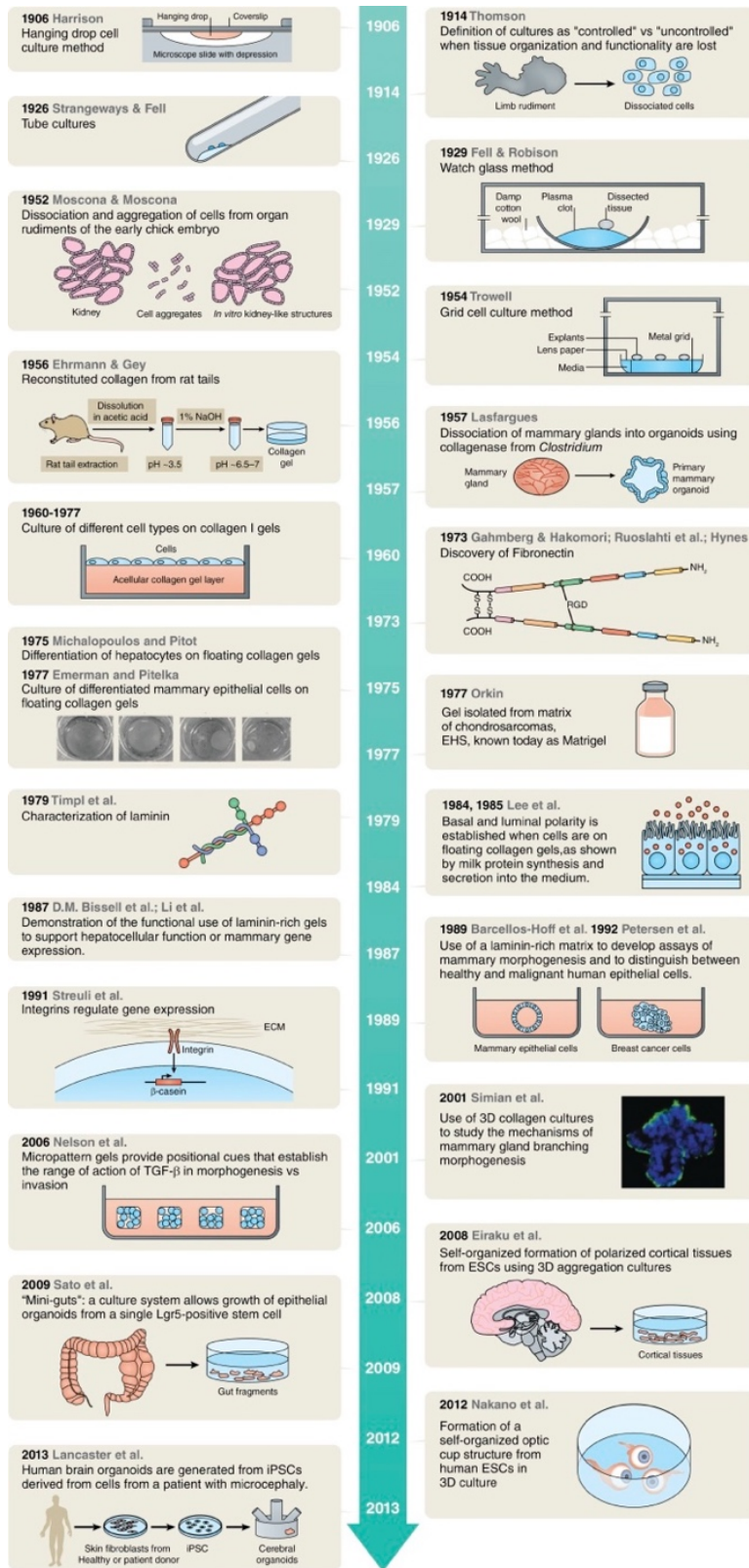


Figure 10: Timeline of techniques and experiments leading to the current 3D cell culture models field. (Simian & Bissell, 2017)

### 1.6.2 Organ explants

This methodology consists on maintaining *ex vivo* whole organs or a piece of them. Explants can remain viable for several days in culture, allowing to directly observe changes in tissue architecture and cellular composition. In addition to epithelial tissue, explants often include additional component from the ECM, and therefore they might be processed to isolate specific regions of the tissue. An advantage of using this technique, is that cells or molecules which are normally not accessible in *in vivo* models can be labeled and tracked during the culture of the organ (Shamir & Ewald, 2014). The organ explants can be culture in a variety of microenvironments, using only cell culture media or embedding them in ECM such as collagen I or Matrigel. The mammary gland has been studied using whole-organ explants, for example, by recovering mice glands and exposing them to hormone-supplemented media to analyze the lobuloalveolar growth *in vitro* (Ichinose & Nandi, 1964). Whole-organs explants of the mouse mammary gland have been used to study mammary stem cells, which drive branching morphogenesis, showing that the TEB is comprised of lineage-committed MaSCs (stem cells) that contribute to ductal elongation on short-term and growth of the mammary gland as long-term function (Scheele *et al.*, 2017).

There are limitations to be considered when working with organ explants. Above all, explants cannot be cultured indefinitely, limiting the timescales for experimentation. Explants are typically cultured over several days but there have been studies keeping mouse mammary gland explants for more than 30 days (Harbell *et al.*, 1977). There might also be differences on the development of explants cultured *ex vivo* and the organs being developed *in vivo*. For instance, mammary gland explants that have been cultured in collagen I gels fail to form normal TEBs unless they are cultured in direct contact with adipocytes (Daniel *et al.*, 1984). Another constrain to be taken into account, is that to obtain sufficient results for statistical significance, it is required to isolate several explants for every condition tested, which is time-consuming, raises the cost of the experiment and poses ethical concerns. Finally, it is also challenging to analyze specific individual cells within whole-organ explants due to its thickness and what it causes for light scattering and imaging (Nerger & Nelson, 2019).

### 1.6.3 Organoids

The term organoid has experienced a change in meaning throughout the years. In the 1950s and 1960s, papers using the term organoids often referred to the intracellular structures (now, known as organelles). However, between 1980 and 2005, the word organoid was used as an extension of 3D cell cultures. Nowadays there are slightly different definitions found in research when referring to organoids:

- 1) Fragment of tissue from the organ or interest grown in a matrix in order to reproduce an organ-like structure (Simian & Bissell, 2017).
- 2) Organ specific cell-types developed either from stem cells or primary cell culture, which are capable of recreating some organ specific function. These structures are therefore, able to self-organize through cell sorting and spatially restricted cell-type growth in a similar manner to *in vivo* (Lancaster & Knoblich, 2014) (Clevers, 2016) (Fatehullah *et al.*, 2016).

Therefore, in the development of the present work, organoids were considered as a cluster of self-organized cells coming from stem cells. Making a differentiation between organoids and organ explants.

Many scientists have contributed to the technological development of systems allowing the culture of organoids from practically any mouse or human organ. This methodology replicates tissue architecture and biological signaling observed *in vivo* and most importantly, organoids comprised of human cells can be used to research characteristics of morphogenesis that still remain inaccessible for its study *in vivo*, due to technical limitations and ethical considerations. Organoids generally involve being decoupled from the adjacent ECM, being useful to modulate and therefore determine the role of the physical and chemical properties of the ECM on morphogenesis and functionality of each organ.

Mammary gland organoids have been created from mouse mammary epithelial cells obtained from the thoracic or inguinal mammary glands (at the developmental stage of interest) (Mroue & Bissell, 2013). Followed by a treatment with collagenase, cells were isolated to be embedded in an ECM and submerged in cell culture media. The resulting mammary organoids can be cultured for days or weeks, after which epithelial polarity and functional differentiation may be lost (Nerger & Nelson, 2019).

Organoids have been obtained by mixing fibroblast recovered from a mammaplasty reduction and the human mammary epithelial cell line MCF-10A embedded either on collagen I or a mixture

of collagen-Matrigel and kept in culture for 6 weeks; these organoids were able to form ductal and alveolar structures (Sokol *et al.*, 2016). Stromal cells proved to be either necessary or accelerators for the formation of epithelial structures (Krause *et al.*, 2008). There has also been experiments including mice mammary cells. When they were grown in collagen I gels, they produced branching structures resembling to the mammary gland of virgin mice (Simian *et al.*, 2001), and undergo alveologenesis when seeded in laminin-rich gels (Fata *et al.*, 2007). This methodology has also been used to investigate mammary stem cells, and the branching process. Researchers have achieved to get whole breast organoids consisting of both basal and luminal cells, derived from a single mammary gland stem cell (Zhang *et al.*, 2017). There have also been mammary organoids generated using single basal mammary epithelial cells that successfully represented the bilayered structure of the mammary gland observed *in vivo* (Jamieson *et al.*, 2017).

Even though, mammary gland organoids represent a robust culture model for investigating mammary gland morphogenesis, they still possess limitations. The timescales and morphologies of branches observed in organoids are not completely consistent with the branching morphologies found *in vivo* (Nguyen-Ngoc *et al.*, 2015). Mammary organoids can have a range of morphologies and cellular composition resembling, but still noticeably different from the mammary gland *in vivo* (Darcy *et al.*, 1991). For example, mammary buds can be incompletely covered by myoepithelial cells in mammary organoids cultured in Matrigel, a topology that is only observed in side branches of the mammary epithelium *in vivo* (Brunelle *et al.*, 2015). It represents a challenge to obtain consistent results from organoid formation due to the variability of the isolated cells; for example, the mammary epithelial branching morphogenesis is tightly related to the mouse strain from which the cells were recovered, the initial size of the organoid and the type of growth factors present (Nguyen-Ngoc *et al.*, 2015). Additionally, the efficiency for organoid formation is low, meaning that this methodology is not yet standardized for high-throughput pharmacology or toxicology screening, not for the study of mammary gland development or function (Nguyen-Ngoc *et al.*, 2015).

#### **1.6.4 Mammospheres, Spheroids and Tumorspheres**

There has been research on the understanding of a small population of tumor cells named cancer stem-like cells (CSCs), so called because they possess self-renewal characteristics and are responsible for tumor initiation and development (Ponti *et al.*, 2005). The neurosphere was

developed in 1992 in order to create an *in vitro* model to analyze this stem cell activity (Reynolds & Weiss, 1992). The assay was later modified for the use for either normal or cancerous mammary gland cells, forming mammospheres, for the study of the stem cell population (Dontu *et al.*, 2003). Mammospheres were subsequently used to quantify both stem cell/early progenitor activity and stem cell self-renewal in normal mammary tissue, ductal carcinoma *in situ* and invasive ductal carcinoma (Harrison *et al.*, 2010). Strictly speaking, mammospheres are considered as spheres cultured from breast stem cells, while tumospheres are cultured from primary tumor cells and cancer cell lines from multiple tissues; spheroids would be considered structures formed from normal cell lines. Nevertheless, in the literature, discrepancies in the use of these terms are commonly found (Smart *et al.*, 2013). These scaffold-based systems have particular advantages when studying early events of tumor initiation and cell-ECM biophysical interactions (Chandler *et al.*, 2011). Finally, non-tumorigenic MCF-10A cells have form 3D acini-like structures, which are generated either by embedding cells inside or on top of Matrigel (Djomehri *et al.*, 2019).

### **1.6.5 3D bioprinting**

A methodology proposing greater accuracy for tissue morphology is 3D bioprinting. It has its roots in polymer printing which began with the invention of stereolithography in 1986 by Charles Hull (Leberfingher *et al.*, 2019). In 1988, Klebe used cytoscribing (the use of either a computer-controlled ink jet printer or a graphics plotter to deposit cell adhesion proteins) technology for 2D micro-positioning of proteins. By late 1990s, scientist began to develop 2D bioprinting techniques with living cells using such micro-positioning techniques. By 2000, Thomas Boland modified an inkjet printer to bioprint cells into a petri dish, giving rise to the first bioprinter (Xu *et al.*, 2005). In 2009 the first commercial bioprinter was Novogen MMX developed by Organovo. Since then, various different bioprinters and extracellular matrix (bioink) have been developed to bioprint a wide range of tissues from cartilage and bone to muscle and liver (Florian *et al.*, 2019).

There exist a variety of bioinks either natural or synthetic hydrogels, including Matrigel, fibrin, collagen, polyethylene glycol, alginate and gelatin-methacrylate and mixtures among them (Kaemmerer *et al.*, 2014; Liu *et al.*, 2012; Pedron & Harley, 2013; Raeber *et al.*, 2005). The main components to choose and modify for a better outcome are the bioink, the bioprinter construction and the bioprinting modality (extrusion, droplet, and laser-based bioprinting), alone or in combination (Figure 8) (Leberfingher *et al.*, 2019). Extrusion-based bioprinting (EBB) deposits

bioink from a syringe-based system into a platform, based on a CAD design of the structure to be printed. Based on the CAD design, the software is able to determine the locations on the platform to extrude the bioink (Ozbolat & Hospodiuk, 2016). Droplet-based bioprinting (DBB) uses bioink stored in a cartridge which forms droplets by gravity and fluid mechanics which can be controlled by surface tension and viscosity (Gudapati *et al.*, 2016), it originates from traditional paper printing (Klebe, 1988). Finally, laser-based bioprinting (LBB) uses a laser pulse directed through mirrors onto a bioink layer above the substrate. The heat and high-pressure then causes the ink to drip in a layer-wise fashion (Koch *et al.*, 2013). Bioprinting allows tight spatial control over initial cell and growth factor location, promoting formation of the appropriate tissue architecture (Florian *et al.*, 2019). Currently, bioink composed of cells encapsulated within a matrix material is printed layer-by-layer in a specific pattern which guides the cells towards self-organization into the desired 3D architecture. Nevertheless, there have also been protocols mixing techniques and developing a system to print pre-formed 3D spheroids in alginate-based bioink to create a model tissue that can be used almost immediately. Bioprinting process aids in the construction models in monoculture and in co-culture (Swaminathan *et al.*, 2019).

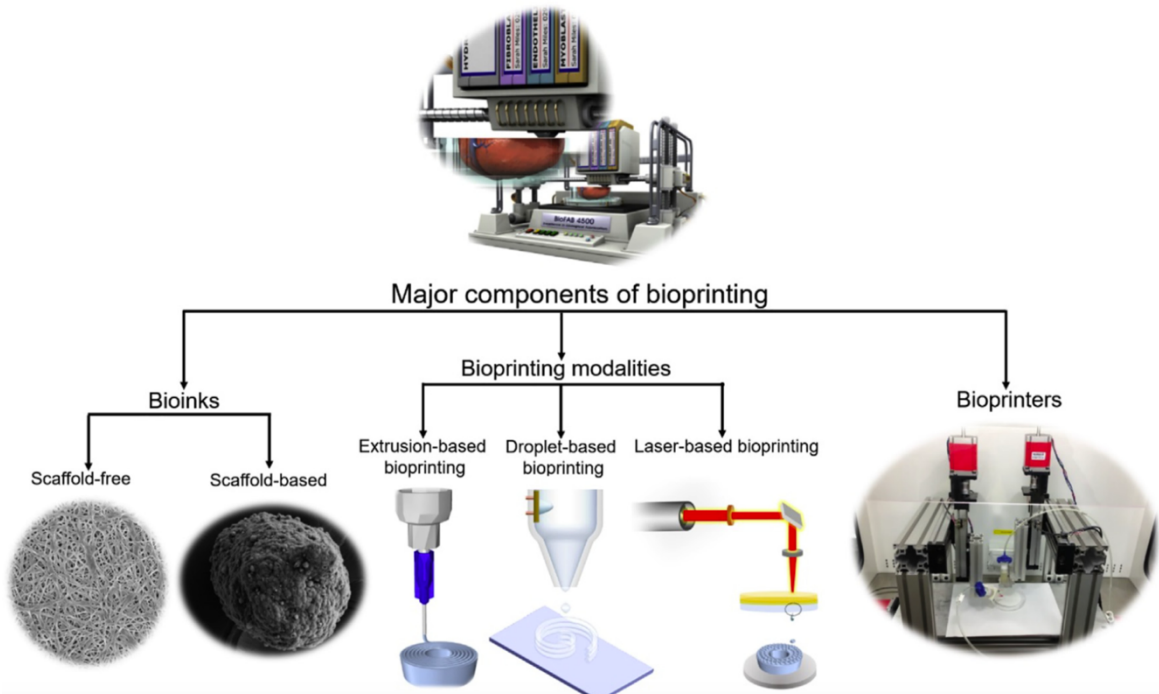


**Figure 11: Major components for bioprinting.**

*Bioink, bioprinting modalities and bioprinters should be chosen and adjusted based on the organ of interest for the research (Leberfinger et al., 2019).*



### 1.6.6 Hanging drop

This technique was the first to generate 3D structures, by culturing suspended droplets of the desired cell lines to force aggregation. As early as in 1880s, Robert Koch and his team invented the hanging-drop methodology to grow anthrax bacilli in a suspended drop of fluid in a special concave microscope slide (Alhaque *et al.*, 2018). Some years later, this method was adopted by Harrison to monitor nerve outgrowth (Harrison *et al.*, 1907). This method experienced another adaptation by Kelm *et al.* to become the model commonly found in literature (Kelm *et al.*, 2003)

The hanging drop uses a small aliquot (around 20  $\mu$ l) of a cell suspension which is pipetted into a Microwell. Following cell seeding, the plate is inverted, and the drops of cell suspension turn into hanging drops that are kept in place due to surface tension. Cells accumulate at the tip of the drop and proliferate; moisture must be kept, and cells can be incubated as per standard cell culture procedures. Nowadays there are high-throughput culture methods that use 384-hanging-drop arrays (Figure 12) (Tung *et al.*, 2011).

This methodology is relatively simple and has been reported to have a high percentage of reproducibility for producing one spheroid per drop using hepatic cell line HepG2 and cancerogenic mammary gland cell line MCF-7 (Kelm *et al.*, 2003). This method is based on cells' natural tendency to adhere to each other as opposed to relying on matrices or scaffolds. Therefore, providing the advantage of using these spheres in the screening of drugs or toxic compounds without the concerns of the effects or interactions that the compounds to be tested might have with the chosen scaffolds. A potential drawback of the hanging drop is the limitation of the volume of the liquid drop containing cells. It can typically accommodate a volume of up to 50 $\mu$ l maximum, including the drug or toxic compound to test, as the surface tension that keeps liquids attached to the culture surface does not support larger volumes (Kurosawa, 2007). Another difficulty is to maintain the spheres in culture for a long period since cell culture media is difficult to change without disturbing the 3D structure (Breslin & O'Driscoll, 2013).

This methodology has been optimized by several protocols and companies as well. A 384-well hanging drop plate was developed by 3D Biomatrix. This version allows large numbers of 3D spheroids to be produced using one plate. This plate incorporates a bottom tray and the hanging drop plate sits into the tray with access holes for cell suspension to be placed to form hanging drops. The bottom tray incorporates liquid, therefore, prevents drying-out. While this platform does not solve the issue of having to use only small volumes, its design allows for changes of cell

culture media, by removing 5 $\mu$ l of media and adding 7 $\mu$ l of media to replace the volume (Tung *et al.*, 2011).

Another system allowing the media exchange but including a trap plate was designed by InSphero. This system allows to harvest the cultures formed in the drops. The trap plate is placed under the cell culture plate. When surplus media is added to the hanging drops, they will get too heavy to remain attached to the culture surface, therefore dropping into their respective wells on the plate underneath. The trap plate has a non-adherence coating to ensure that the spheres remain in suspension (Breslin & O'Driscoll, 2013). This hanging drop plate makes cell spheroid production and handling easier than using an inverted plate and enables 3D cultures produced to be tested in a high-throughput manner. There have been some models modifying the cell culture media to achieve spheres from human non-cancerous mammary gland cells, MCF-10A, in which with 1.5% Matrigel and 10% FBS have achieved to conform self-organized mammary gland-like organoid structures capable of exhibiting multiple lineage phenotypes (Djomehri *et al.*, 2019). Even though this system has allowed the development of several different protocols there are still challenges to overcome in the slow or inefficient aggregation capacity of different cells in a liquid-based setting (Nerger & Nelson, 2019).

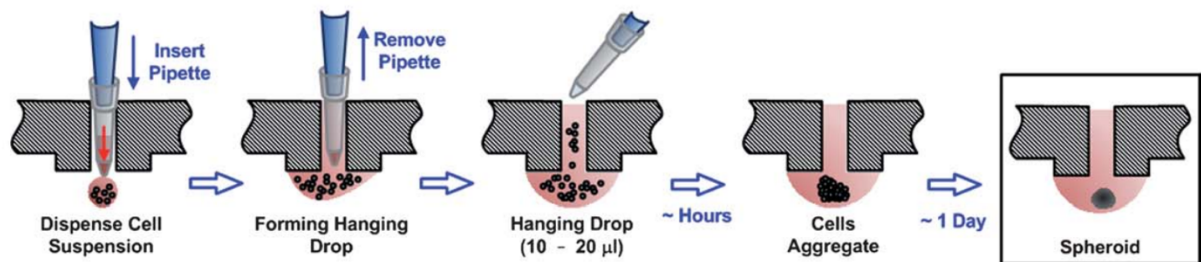


**Figure 12: Schematic representation of the hanging drop formation process.**

*The pipette tip is first inserted through the access hole to the bottom. Cell suspension start forming a hanging drip where individual cells start to aggregate and eventually for a spheroid.(Tung *et al.*, 2011)*

### 1.6.7 Forced-floating systems

A relatively simple methodology for 3D spheroids is to prevent their attachment to the surface by modifying it, resulting in forced-floating cells. This technique promotes cell-to-cell contact which promotes multi-cellular sphere formation (Breslin & O'Driscoll, 2013). Using this approach, 3D spheroids have been formed in round bottomed 96-well plates coated with 0.5% poly-2-hydroxyethyl methacrylate (poly-HEMA) and dried for three days before the addition of cells. The

poly-HEMA prevents cells from attaching to the surface of the wells. With this coating, cell suspension was added into each well followed by centrifugation to promote co-localization and thus adhesion of cells. A panel of eight breast cancer cell lines was used (MCF7, T-47D, MDA-MB-435, MCF7-ADR, MDA-MB-231, MDA-MB-468, SKBR3, MDA-MB-361). While some cell lines (MCF7, T47D, MDA-MB-435, MCF7-ADR) formed spheroids with this method, others (MDA-MB-231, MDA-MB-468, SKBR3, MDA-MB-361) produced cell aggregates only, which means that cells accumulated closely together but did not form packed spheroids. However, when 2.5% liquid reconstituted basement membrane (rBM; BD Biosciences, Bedford, MA) was added to the cell suspensions, these cell lines were then enabled to generate compact 3D spheroids (Ivascu & Kubbies, 2006).

Using forced-floating methodology for spheroid formation has many benefits since it is simple and generally reproducible, nevertheless it is hard to maintain equal number of spheres and sizes. As these 3D spheroids can be generated in 96-well plates, this methodology is compatible with high-throughput drug testing (Ivascu & Kubbies, 2006). This is ideal for investigations comparing efficacy and toxicity of drugs, gene expression in spheroids and other cellular and biochemical assays (Breslin & O'Driscoll, 2013).

A drawback in this methodology is the time and additional steps required to pre-coat the plates before seeding the cells. Nevertheless, precoated low adhesion plates could be purchased, however, it must be considered that the purchase of precoated plates increases overall costs compared with in-house precoating. Examples of commercially available precoated plates include the PrimeSurface low adhesion culture plate from Sumitomo Bakelite (Oda *et al.*, 2010) and Lipidure-coated plates (Morizane *et al.*, 2011).

## **2 Problem**

---

The ultimate unit of function in any organ is clearly the organ itself. In the breast, an important component of this functional unit is the double-layered acinus composed of luminal and myoepithelial cells. While this is not strictly equivalent to the breast gland, it nevertheless captures an essential component of the functional entity of the breast. Although good 3D alternative models have been developed for the study of the mammary gland, there are still some limitations. Indeed, the majority of models are composed either of luminal cells only (Froehlich *et al.*, 2016), or of

luminal and myoepithelial cells obtained from primary culture (Sokol *et al.*, 2016). On one hand, the models created only with luminal cells are less representative of the *in vivo* structure as they lack the interaction with myoepithelial cells. On the other hand, whenever 3D models are obtained from luminal and myoepithelial cells from primary culture, even if they physiologically represent the mammary gland acinus, they are harder to manipulate and are less reproducible. As a result, models which are physiologically relevant while being malleable, reproducible and cost efficient are still lacking.

Therefore, the objectives for my master's thesis project was the development of two different models:

1. Development of a 3D bilayered acinus cell culture model
2. Development of a layered cell culture system



### 3 Materials and Methods

---

#### 3.1 Developing a 3D model *in vitro* of the mammary gland

##### 3.1.1 Cell culture

MCF-12A cells (ATCC<sup>®</sup> CRL-10782<sup>™</sup>), MCF-10A cells (ATCC<sup>®</sup> CRL-10317<sup>™</sup>) were purchased at ATCC (ATCC, Manassas, VA, USA). They are both human epithelial non-tumorigenic mammary gland cell lines. They were derived from adherent cells in the population. Myo1089 cells were received as a donation from Dr. Louise J. Jones from the Barts Cancer Institute, Queen Mary, University of London. They were derived from a human breast reduction mammoplasty tissue and transduced with SV40 large T antigen.

MCF-12A and MCF-10A cells were maintained in phenol red-free Dulbecco's modified Eagle's media Ham's F12 (DMEM/F12; 21041025, Thermo Fisher Scientific, Rockford, Illinois, USA) supplemented with 5% (v/v) horse serum (16050-122, Thermo Fisher Scientific), 20ng/ml human recombinant Epidermal Growth Factor (hEGF) (E9644, Sigma-Aldrich, Oakville, Ontario, Canada), 10 µg/ml Bovine Insulin (I6634, Sigma-Aldrich), 500ng/ml Hydrocortisone (7904, STEMCELL technologies, Cambridge, Massachusetts, USA), 100ng/ml Cholera Toxin (C8052, Sigma-Aldrich) and propagated according to ATCC guidelines. Myo1089 cells were maintained in Ham's F12 culture media (11765054, Thermo Fisher Scientific) supplemented with 10% FBS (12484-028, Thermo Fisher Scientific), 1 µg/ml Hydrocortisone (7904, STEMCELL technologies), 5 µg/ml Bovine Insulin (I6634, Sigma-Aldrich) and 10ng/ml hEGF (E9644, Sigma-Aldrich) and propagated following the same protocol as MCF-12A cells. Cells were all incubated at 37°C with 5% CO<sub>2</sub>. For the characterization using immunofluorescence, cells were cultured on sterile microscope cover glass (12-545-80, Thermo Fisher Scientific) placed on the bottom of P24 plates. The cover glass was then recovered at 90% confluency in order to perform immunofluorescence following the protocol on section 3.2.6.

##### 3.1.2 Western Blot for cell characterization

Cell monolayers at 90% confluency were washed twice with PBS 1x before the addition of lysis buffer (50mM Tris, 150mM NaCl, 0.02% sodium azide, 0.1% SDS, 1% Nonidet P40, 0.5% sodium

deoxycholate, pH: 8) supplemented with NaF 1.25 M, NaVO<sub>3</sub> 1M and a cocktail of inhibitors 1x (Halt Protease and phosphatase cocktail inhibitor, Fisher Scientific Canada). Cells were scraped, collected and incubated on ice for 5 min. Cell lysates were centrifuged for 10 min at 2500 rpm at 4°C. The supernatants were aliquoted and stored at -80 °C until further processing. Lysate protein concentrations were measured using a bicinchoninic acid (BCA) protein assay reagent kit (Thermo Scientific #23227). Protein samples (in a standard curve loading form: 10ng, 20ng, 30ng, 40ng, 50ng and 60ng) were resolved on stain-free acrylamide gels (TGX Stain-Free FastCast Acrylamide kit, 10%, Bio-Rad, Mississauga, On) and transferred onto polyvinylidene fluoride (PVDF) membranes. Membranes were blocked with TBS-Tween 20 (0.1%) containing 3% bovine serum albumin (BSA) or 5% dry milk, according to manufacturer instructions for each antibody, for 1 h and incubated overnight at 4°C or 2h at room temperature with the following primary antibodies: E-cadherin (#3195; Cell Signaling Technology, Danvers, MA), k18 (#ab52948; Abcam, Cambridge, MA), k14 (#MS-115-P1ABX; Thermo Scientific, Cheshire, UK), anti- $\alpha$ -Smooth muscle actin (#M0851; Dako, Glostrup, Denmark),  $\beta$ -catenin (#2677; Cell Signaling Technology), Progesterone receptor A/B (#8757; Cell Signaling Technology), Estrogen receptor  $\alpha$  (#8644; Cell Signaling Technology), Estrogen receptor  $\beta$  (#310B, Thermo Scientific), Cx30 (#712200, Life Technologies), Cx32 (#C3470, Sigma-Aldrich), Cx43 (#C219, Sigma-Aldrich), Calponin-1 (#17819, Cell Signaling Technology), Caldesmon-1 (#12503, Cell Signaling Technology), k5 (#25807, Cell Signaling Technology). All primary antibodies were used at the concentration recommended by the manufacturer. Bound primary antibody was detected using HRP-conjugated secondary antibodies (goat-anti-rabbit (#7074) or horse-anti-mouse (#7076); Cell Signaling Technology) followed by visualization using Bio-Rad ChemiDoc MP System (Bio-Rad Laboratories, Mississauga, On). Chemiluminescent signals were detected using Clarity western ECL substrate (Bio-Rad Laboratories) and analyzed using Image Lab software (Bio-Rad Laboratories).

### **3.1.3 3D Cell culture embedded in extracellular matrix**

Two extracellular matrices were used; Vitrogel<sup>®</sup> – RGD (xeno-free hydrogel – RGD modified) (TWG002, The Well Bioscience, North Brunswick Township, New Jersey, USA) and Matrigel (Corning<sup>®</sup> Growth Factor Reduced (GFR) Basement Membrane Matrix obtained from EHS mouse sarcoma) (CB40230C, Corning, New York, USA).

3D cell culture was performed in 35mm glass bottom poly-D-lysine coated dishes, 14mm microwell (P35GC-0-14-C, MatTek Corporation, Ashland, Massachusetts, USA). Only for Matrigel usage, a pre-coating was performed with 10 $\mu$ l of 100% Matrigel evenly spread and left in the incubator at 37°C and 5% CO<sub>2</sub> for 15-30 minutes to achieve solidification. Cells cultured in a flask were recovered at approximately 90% confluence by using trypsin-EDTA 0.25% (252000-072, Thermo Fisher Scientific). Cells were counted using TC10 Automated Cell counter (Bio-Rad Laboratories) and the proper number of a mixture of luminal and myoepithelial cells (1:0, 1:1, 1:2, 1:3, 1:4, 1:5, 1:9; Table 2) were mixed in the same tube and then centrifuged at 125 x g for 7 minutes at room temperature. In Matrigel, cells were seeded at a density of 35,000 up to 50,000 cells/100 $\mu$ l of Matrigel 75% (v/v) diluted with cold growth media. The supernatant was then removed, and the cells were resuspended in media. The Matrigel was added in order to get 100 $\mu$ l of 75% Matrigel solution containing the mixture of cells. This mixture was distributed rapidly into the MatTek 35mm pre-coated with Matrigel. Dishes were incubated for another 30 minutes at 37°C and 5% CO<sub>2</sub> to allow Matrigel to solidify, before the addition of 1.5ml cell culture media. The culture media was changed every 2-3 days for 10-14 days. Several tests were performed using either the cell culture media for MCF-12A, the media for Myo1089 or a mixture 1:1 of both cell culture media (Table 2).

When VitroGel<sup>®</sup> – RGD was used, cells were seeded at a density of 200,000 cells / 100-250 $\mu$ l of diluted VitroGel. Optimization process was required to determine dilution factors for VitroGel in PBS (1:0, 1:1, 1:2, 1:3, 1:4 and 1:5; table 2), as well as for the proper ratio of diluted VitroGel and cell culture media (4:1, 3:1, 2:1 and 1:1; table 2). PBS-VitroGel-cells mixture was seeded onto a MatTek 35mm and kept at room temperature for one hour, before the addition of 0.5ml of media. The culture media was changed every 2-3 days for 12-14 days. Several tests were performed using either the cell media for MCF-12A, the media for Myo1089 or a mixture 1:1 of both cell culture media (Table 2).

Establishing a 3D bi-layered acinus model was constituted by a constant optimization process, several parameters were tested and therefore adjusted in order to obtain the most efficient version of the model. Table 1 summarizes the main parameters that were tested, and the optimal conditions chosen from each. Noted that while results were analyzed by confocal microscopy and other methods for each condition, only results obtained with the optimal conditions are presented.



**Table 2: Optimization parameters for 3D bi-layered acinus model.**

<b>Characteristic</b>	<b>Parameters</b>
Cell culture media	Three different options were tested: <ol style="list-style-type: none"> <li>1. Ham's F12</li> <li>2. DMEM</li> <li>3. Ham's F12 and DMEM mixed in equal parts</li> </ol>
ECM concentration	Vitrogen was diluted with 0.5x PBS at different concentrations (1:0, 1:1, 1:2, 1:3, 1:4 and 1:5) and further diluted with cell culture media (4:1, 3:1, 2:1 and 1:1). The best results were obtained when Vitrogen was diluted 1:3 with 0.5x PBS, and then 4:1 with cell culture media.  Matrigel diluted at 75% showed optimal results in previous studies (Weber-Ouellette <i>et al.</i> , 2018).
Cell density	For Vitrogen several cell densities were tested: <ol style="list-style-type: none"> <li>1. 100,000</li> <li>2. 150,000</li> <li>3. 200,000</li> <li>4. 500,000</li> </ol> 200,000 cells gave the best results.  For Matrigel several cell densities were tested: <ol style="list-style-type: none"> <li>1. 30,000</li> <li>2. 40,000</li> <li>3. 50,000</li> <li>4. 70,000</li> <li>5. 75,000</li> </ol> 50,000 gave the best results.
Luminal:Myoepithelial cells ratio	The ratio of luminal and myoepithelial cells tested included: 1:0, 1:1, 1:2, 1:3, 1:4, 1:5 and 1:9. The best combination was 1 part of luminal cells per 4 parts of myoepithelial cells for both Matrigel and Vitrogen.
Immunofluorescence protocol	For the immunofluorescence protocol, several modifications were tried for the concentration of Tween-20 and Triton, as well as for the time for the incubation with the antibodies. The optimized version of the protocol is described in the section materials and methods.
Microscope usage	In order to analyze the cells using the microscope, we would normally put the sample between two microscope slides. However, since the samples in our study have a tridimensional structure, using this standard protocol compromises the structure. Therefore, two techniques were tested: <ol style="list-style-type: none"> <li>1. using a rounded microscope slide on top of the structure without applying pressure and then sealing the construction with hot glue.</li> <li>2. visualizing the structures in PBS 1x, without mounting them.</li> </ol> Using a rounded microscope slide gave images with better resolution and kept the sample for longer periods.

### **3.1.4 Immunofluorescence of 3D embedded culture in VitroGel**

Culture media was aspirated, and embedded cultures were rinsed twice with PBS 1x. Cells were fixed in formaldehyde 4% for 20 minutes and permeabilized in PBS-Triton X-100 (0.1%) for 30 minutes. After being rinsed three times (10 minutes each) with PBS-Glycine (0.1%), cells were incubated in blocking solution for 1 hour (3% BSA). Primary antibodies were diluted in blocking solution and cells were incubated with primary antibody on a rocking table for 120 minutes at room temperature or overnight at 4°C (E-cadherin (#3195; Cell Signaling Technology, Danvers, MA),  $\beta$ -catenin (#2677; Cell Signaling Technology), Cx43 (#C219, Sigma-Aldrich), Calponin-1 (#17819, Cell Signaling Technology), Caldesmon-1 (#12503, Cell Signaling Technology)). This step was followed by four washes (five minutes each) with washing solution (0.1% Tween 20). Cells were then incubated with the appropriate secondary antibodies for 60 minutes at room temperature (anti-rabbit IgG Alexa Fluor 488 (#4412s), anti-mouse IgG Alexa Fluor 555 (#4409s) both used at 1/1000 (Cell Signaling), or anti-rabbit IgG DyLight 488 (# 35552) used at 1/200 (ThermoFisher Scientific)). All primary antibodies were used at the concentration recommended by the manufacturer. Cells were washed three times with washing solution and one time with PBS 1x, for 5 minutes each. Nuclei were stained using 4', 6-diamidino-2-phenylindole (DAPI) in PBS 1x (1/1000) for 5 minutes. Two last washing using PBS 1x (five minutes each) were performed. Embedded cultures were mounted with Fluoromount-G (0100-01, SouthernBiotech, Birmingham, AL, USA) and rounded coverslips. The coverslips were then sealed using hot glue for longtime preservation. Immunofluorescence images were obtained with a Nikon A1R+ confocal microscope (Nikon) and analyzed using NIS-elements software (Nikon).

### **3.1.5 Immunofluorescence of 3D embedded culture in Matrigel**

Cell culture media was aspirated, and embedded cultures were rinsed twice with PBS 1x. Cells were fixed in formaldehyde 4% for 20 minutes and permeabilized in PBS-Triton X-100 (0.5%) for 30 minutes. After being rinsed three times (10 minutes each) with PBS-Glycine (0.1%), cells were incubated in blocking solution for 1 hour (2% BSA, 0.1% of Tween 20 and 0.1% of Triton X-100 in PBS 1x). Primary antibodies were diluted in blocking solution and cells were incubated with primary antibody on a rocking table for 120 minutes at room temperature or overnight at 4°C (E-cadherin (#3195; Cell Signaling Technology, Danvers, MA),  $\beta$ -catenin (#2677; Cell Signaling

Technology), Cx43 (#C219, Sigma-Aldrich), Calponin-1 (#17819, Cell Signaling Technology), Caldesmon-1 (#12503, Cell Signaling Technology)). This step was followed by four washes (five minutes each) with washing solution (0.1% Tween 20, 0.1% BSA and 0.5% Triton X-100 in PBS 1x). Cells were incubated with the appropriate secondary antibodies for 60 minutes at room temperature (anti-mouse IgG Alexa Fluor 555 (#4409s) or anti-rabbit IgG Alexa 568 (#A10042; Thermo Fisher) both used at 1/1000 (Cell Signaling), and anti-rabbit IgG DyLight 488 (# 35552) used at 1/200 (ThermoFisher Scientific)). All primary antibodies were used at the concentration recommended by the manufacturer. Cells were then washed three times with washing solution and one time with PBS 1x, for 5 minutes each. Nuclei were stained using 4', 6-diamidino-2-phenylindole (DAPI) in PBS 1x (1/1000) for 5 minutes. Two last washing using PBS 1x for five minutes each were performed. Embedded cultures were mounted with Fluoromount-G (0100-01, SouthernBiotech, Birmingham, AL, USA) and rounded coverslips. Coverslips were sealed later using hot glue. Immunofluorescence images were obtained with a Nikon A1R+ confocal microscope (Nikon) and analyzed using NIS-elements software (Nikon).

### 3.2 Developing a layered co-culture model of the mammary gland

#### 3.2.1 Cell lines

Luminal-like MCF-12A cells (ATCC® CRL-10782™) and myoepithelial-like Myo1089 cells were used for this model. They were maintained in the conditions previously described in section 2.1.1

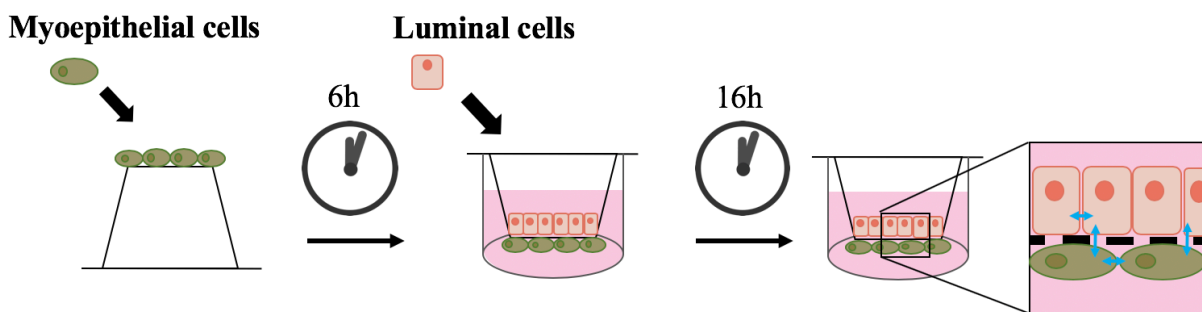


**Figure 13: Bilayered co-culture methodology.**

*Myoepithelial cells were seeded on the abluminal side of the insert, kept in the incubator for adhesion (6h) and the insert was flipped to its original position and luminal cells were seeded on top. The system was then kept for 16h in the incubator to allow interactions to occur between the two layers of cells.*

### 3.2.2 Porous membrane co-culture system

High pore density 3.0 $\mu$ m pore size PET (polyethylene terephthalate) track-etched membrane cell culture inserts (353492/353092, Falcon, Corning) were used in the development of this model. Immunofluorescence analysis were performed using 24-well-plate size inserts, while for other analysis, 6-well-plate (P6) size inserts were preferred. Myo1089 cells were recovered using trypsin, as described before in section 2.1.1, and seeded on an upside-down insert at a cell density of 750,000 cells in 500 $\mu$ l of media for the 6-well plate inserts or 300,000 cells in 200 $\mu$ l of media for the 24-well-plate inserts (Figure 13). The inserts were kept at 37°C and 5% CO<sub>2</sub> for 6 hours to allow cell adhesion. In order to maintain sterility during this time of cell adhesion, the inserts were assembled in an inverted 6 well plate (Figure 14c). The inverted inserts were placed on top of the cover of a 6 well plate and then the bottom of the plate was placed as a cover, keeping the media in place through surface tension and avoiding the cells to dry. After 6 hours, the inserts and the plate were flipped back to the normal position, and MCF-12A cells were seeded at the same cell density as the Myo1089 cells on the upper side of the porous membrane. Media used for MCF-12A was added to fully cover both layers of cells. The system was kept at 37°C and 5%CO<sub>2</sub> for 16h-18h before analyses were performed.

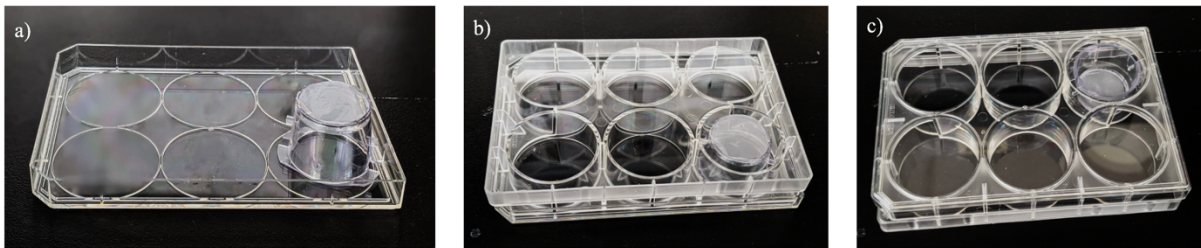


**Figure 14: Bilayered co-culture system.**

*a) The Insert is inverted into a 6 well plate cover, and the myoepithelial cells are seeded on the membrane. b) Media is added, and the bottom of the 6 well plate serves as a cover in order to maintain the cell culture media from leaking. c) After 6 hours, the plate containing inserts is inverted, and luminal cells are seeded on top.*

### 3.2.3 Cell labeling for dye transfer analysis

To analyze the communication between cells in these models, it has been proposed to load cells with fluorescent dyes. By instance, GJIC can be analysed and quantified using Calcein-AM and

DiL (Goldberg *et al.*, 1999). Calcein-AM (1,1'-dioctadecyl-3,3,3',3'-tetramethylindocarbocyanine perchlorate) is a cell-permeant green fluorescent dye that is widely used to study cell viability in eukaryotic cells. In live cells, the nonfluorescent Calcein-AM gets converted into fluorescent Calcein (green). The dye enters the cell through the membrane and then due to the hydrolysis of acetoxymethyl (AM) ester by intracellular esterases it gets trapped inside the cells. After this process the dye can only leave the cell through gap junctions (Mariappan *et al.*, 1999).

DiL (1,1'-dioctadecyl-3,3,3',3' tetramethylindodicarbocyanine perchlorate) is a lipophilic membrane stain which get diffused to stain the cell membrane in its totality. It colours with an orange-red fluorescence after being incorporated into the membrane and it does not get transferred to adjacent cells. It is thus used as a negative control for GJIC assay. It is thus possible to label cells, considered as the donor cells, with Calcein-AM, and co-culture them with receiver cells, labelled with DiL. The number of receiver cells, i.e. cells stained with Calcein and DiL, can then be quantified. Alternatively, the donor cells can be labelled with both Calcein and DiL, the number of receiver cells, i.e. only labelled with Calcein in this case, can be quantified. Therefore, the transfer of calcein from a donor to a receiver cell indicated functional and active GJIC (Warawdekar, 2019).

The assay to analyze GJIC was performed 4 hours after seeding Myo1089 cells on the inserts, MCF-12A cells worked as donor cells and they were labelled with Calcein AM (554217, Corning) and DiLC12(3) (08774502, Corning). To do so, cells were incubated in media containing a mixture of both fluorescence colorants at a concentration of 0.072 $\mu$ M DiL and 5 $\mu$ M Calcein. Cells were kept in the incubator at 37°C and 5%CO<sub>2</sub> for 30 minutes, washed with PBS 1x and then recovered using trypsin. The cells suspension was centrifuged at 125 x g for 7 minutes, the supernatant was discarded, and cells were resuspended in 1x PBS. Washing with PBS was repeated 3 times, and cells were resuspended in media on the last wash. Cells were counted and the appropriate amount was seeded on the top side of the porous membrane. Cells were allowed to interact for 16-18h and analyzed either using flow cytometry or confocal microscopy.

#### **3.2.4 Flow cytometry**

After 16-18h of incubation, inserts containing Calcein-DiL labelled MCF-12A (donor) cells and Myo1089 (receiver) cells on each side of the membrane were washed with PBS 1x. Cells on each side of the membrane were sequentially recovered using trypsin and cell scraper, carefully

separating cells adhered to each side of the membrane. Cells were diluted in culture media, centrifuged at 125 x g for 7 minutes and resuspended in 0.5ml of BD FACS flow™ (10638814, Fisher) and analyzed using a BD LSR Fortessa (BD Bioscience) apparatus. Note that to assure that the dyes were passing through direct interaction between the two layers of cells and not leaking into the media, MCF-12A cells (unlabeled) were also seeded at the bottom of the well and analyzed by flow cytometry. For the analysis of results, cell controls were used for every experiment performed. MCF-12A cells labelled with Calcein-DiL were used as positive control while MCF-12A and Myo1089 without dyes were used as negative control. Receiver cells were positive in presence of Calcein, while donor cells were expected to remain double positive.

### **3.2.5 Cryosection of transwell membranes**

After 16-18h of keeping the system in the incubator, the porous membranes containing MCF-12A (labelled or not with Calcein and DiL) and Myo1089 cells on each side, were cut with a disposable scalpel and placed into cryomatrix FSC 22 frozen section media (3801481, Leica, Wetzlar, Germany) on a metallic container cooled down using dry ice. The set up was kept at -80°C for at least 48h to allow complete solidification. 10µm sections were made using a Microm HM 525 cryostat set at -20°C. The cryosections were kept at -80°C until further use.

### **3.2.6 Immunofluorescence of cryosections**

Cryosections were fixed in a solution of 80% methanol and 20% acetone for 10 minutes and then washed twice with PBS 1x. Blocking was performed with a solution of 2% BSA, 0.1% Triton X-100 diluted in PBS 1x for 60 minutes at room temperature. Primary antibodies were incubated in blocking solution and sections were incubated for 2 hours at room temperature ( $\beta$ -catenin (#2677; Cell Signaling Technology), Cx43 (#C219, Sigma-Aldrich). Immunolabeling was followed by three washes with PBS 1x for 5 minutes each. Cryosections were incubated with the secondary antibody used at 1/1000 dilution for 1 hour at room temperature (anti-mouse IgG Alexa 555 (#4409s; Cell SignalingTechnology) and anti-rabbit IgG Alexa 568 (#A10042; Thermo Fisher). The cryosections were then washed three times for five minutes each with PBS 1x and nuclei were stained with DAPI (1/1000) for 5 minutes. Cryosections were mounted with Fluoromount-G (SouthernBiotech, 0100-01) and placed horizontally at 4°C for 8 hours in the dark.

Immunofluorescence images were obtained with a Nikon A1R+ confocal microscope (Nikon) and analyzed using NIS-elements software (Nikon).

### **3.2.7 Confocal imaging of whole membranes**

Immunofluorescence analysis were also performed on the whole membrane. Cells were co-cultured using the layered system, as described in section 3.2.2. After 16h, cell culture media was removed, and the membranes were washed with PBS 1x. Cells were fixed by using 4% formaldehyde and washed again with PBS 1x twice. Blocking and incubation of antibodies was performed as described in section 2.2.2. Second antibody was washed three times for five minutes each and nuclei were stained with DAPI (1/1000) for 5 minutes at room temperature and finally washed with PBS 1x. After the procedure, the membrane required to be cutted with a clean scalpel to be mounted using Fluoromount-G (SouthernBiotech) onto two microscope cover glass and placed overnight at 4°C. All the process requires the membrane to be completely submerged into the solutions. Therefore, a transwell for 24 well plate was preferred, in order to reduce the volume of antibodies. Nevertheless, this protocol allows to take bigger area pictures than cryosections and observe the two layers of cells with accurate resolution. Whole membranes were also used to take pictures of the DiL and Calcein loading protocol. Cells were loaded and seeded as explained in section 2.2.3 and then fixed just as described above. Membranes were recovered with a scalpel and mounted following the same methodology as previously described.

## 4 Results

---

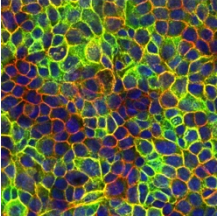
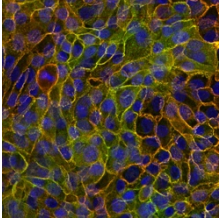
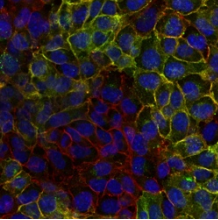
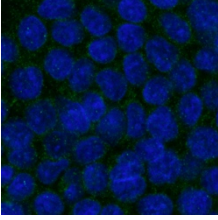
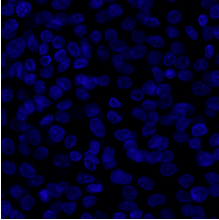
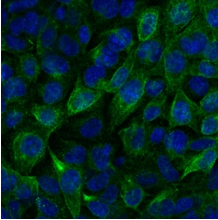
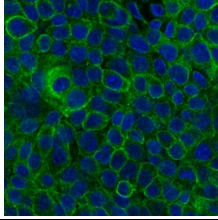
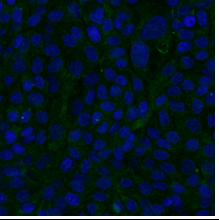
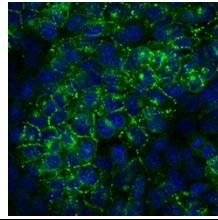
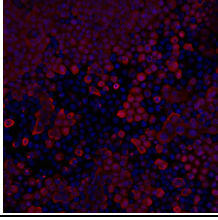
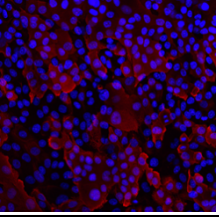
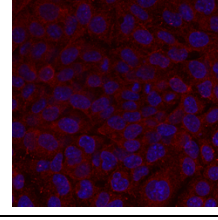
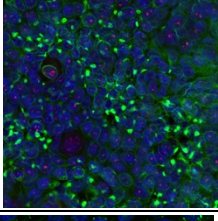
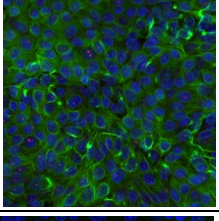
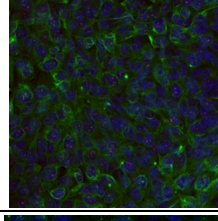
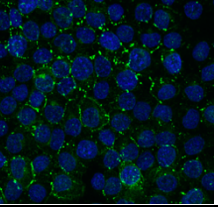
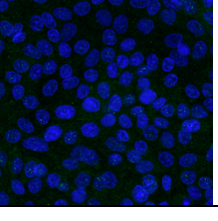
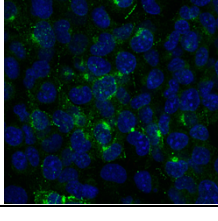
### 4.1 Cell characterization

For the development of the *in vitro* models, the cells lines proposed were characterized in order to confirm the expression of proper cell type specific markers and of junctional proteins. Luminal MCF-12A and MCF-10A cells were tested for markers generally expressed in human luminal mammary gland cells, while Myo1089 cells were tested for the markers generally expressed in human myoepithelial mammary gland cells. Some proteins from gap and adherens junctions were also analyzed in order to further assess cell-cell interactions. Cell characterization was performed by immunofluorescence and western blot (Table3 and Figure 15).

Results have shown that MCF-12A and MCF-10A cells express most of the luminal markers tested (PR a, PR b and k18 for both cell lines, and ER  $\alpha$  for MCF-12A), but only a few markers of myoepithelial cells (k5, k14 for both cell lines and Caldesmon 1 for MCF-12A) (Table 3 and Figure 15). In opposite, Myo1089 cells express most of the myoepithelial markers tested (Caldesmon 1, Calponin 1 and k14), and only one luminal marker (ER  $\alpha$ ). In addition, the three cell lines express E-cadherin,  $\beta$ -catenin, Cx43, Cx32. Together, these results suggest that these cell lines have the expected phenotype and express crucial junctional proteins and are thus appropriate for our studies.



**Table 3: Characterization of luminal MCF-12A, MCF-10A and myoepithelial Myo1089 cells by immunofluorescence.**

	MCF-12A	MCF-10A	Myo1089
<p><math>\beta</math>-catenin is labelled in red. E-cadherin is labelled in green. Nuclei are labelled with DAPI.</p>			
<p>Calponin 1 is labelled in green. Nuclei are labelled with DAPI.</p>			
<p>Caldesmon 1 is labelled in green. Nuclei are labelled with DAPI.</p>			
<p>k14 is labelled in red. Nuclei are labelled with DAPI.</p>			
<p>k18 is labelled in green. Nuclei are labelled with DAPI.</p>			
<p>Cx43 is labelled in green. Nuclei are labelled with DAPI.</p>			

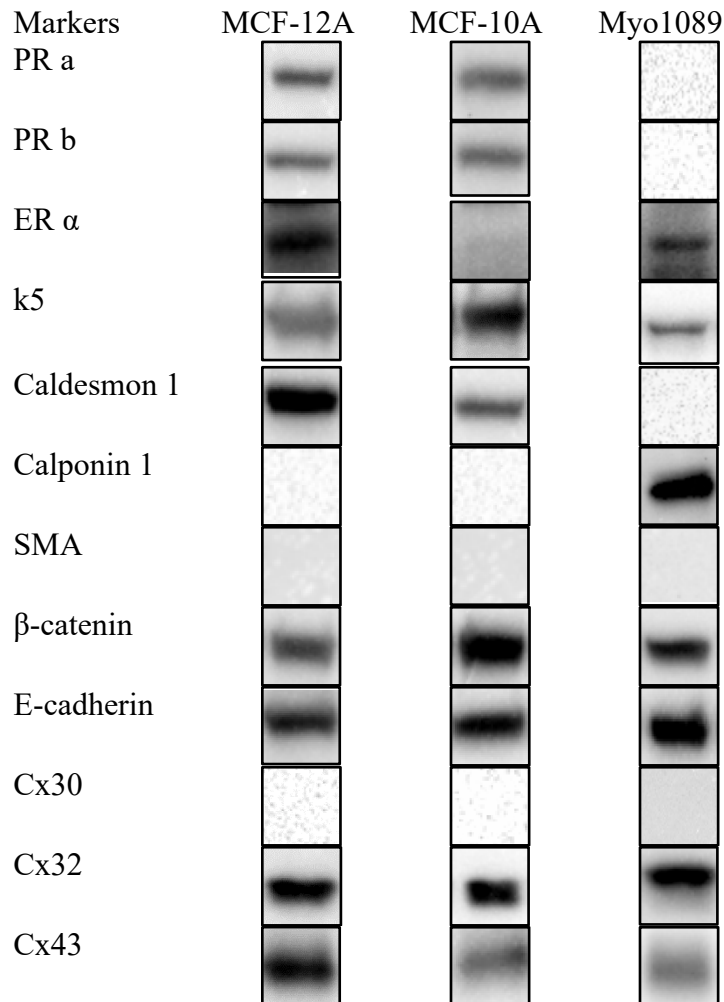


Figure 15: Characterization of luminal MCF-12A, MCF-10A and Myoepithelial Myo1089 cells through Western Blot.

## 4.2 3D bi-layered acinus model

### 4.2.1 Luminal MCF-12A and MCF-10A cells form acini in Matrigel, but not in VitroGel

We first wanted to assess the behavior of luminal and myoepithelial cells in 3D separately. To do so, MCF-12A, MCF-10A and Myo1089 were first cultured in Matrigel 95% and kept in the incubator for 10-12 days. The cells were then stained with E-cadherin and keratin 14 (K14) and imaged by confocal microscopy. While luminal MCF-12A and MCF-10A cells formed acinus-like

structures when seeded in Matrigel (Figure 16 a and b), Myo1089 formed clumps of cells without any specific structure (Figure 16c). Interestingly, for all cell types, E-cadherin staining was

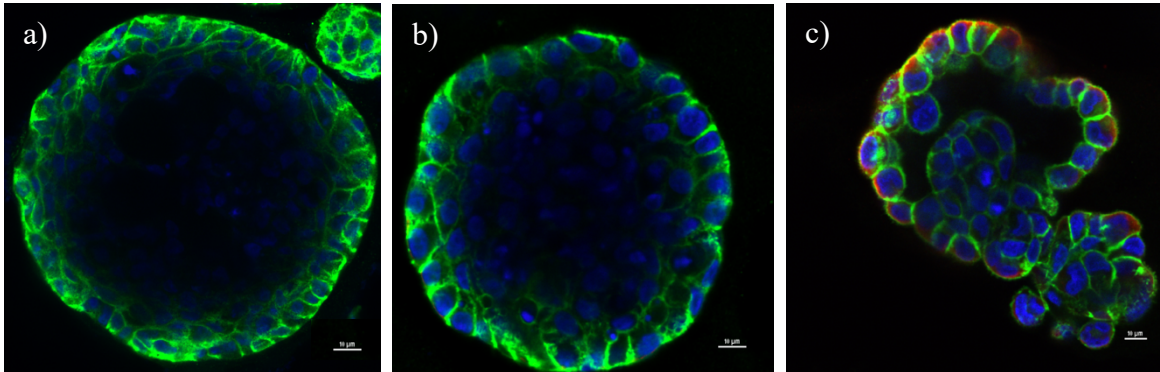


**Figure 16: Cells seeded in monoculture in Matrigel.**

*Cells were marked by immunofluorescence using E-cad (green), K14 (red) and nuclei with DAPI (blue). a) MCF-12A cells in Matrigel and b) MCF-10A cells in Matrigel form acini-like structures. c) Myo1089 cells in Matrigel form clumps of cells without any specific structure.*

localized at cell membranes, likely forming adherens junction between adjacent cells (Figure 16). In Myo1089 cells, K14 staining could be observed, although not forming a typical cytoskeleton staining, but rather a punctate staining (Figure 16c). Nevertheless, these results confirmed that MCF-12A and MCF-10A cells, but not Myo1089 cells, are able to form acini-like structures in Matrigel.

Luminal MCF-12A, MCF-10A and myoepithelial Myo1089 cells were then seeded in monoculture in VitroGel and kept in the incubator for 12-14 days. The cells were cultured with their respective cell culture media. The cultures were then stained with  $\beta$ -Catenin ( $\beta$ -Cat) and Calponin 1 and imaged by confocal microscopy. In VitroGel, luminal MCF-12A and MCF-10A cells formed spherical structures with no more than ten cells at a time (figure 17a and 17b).

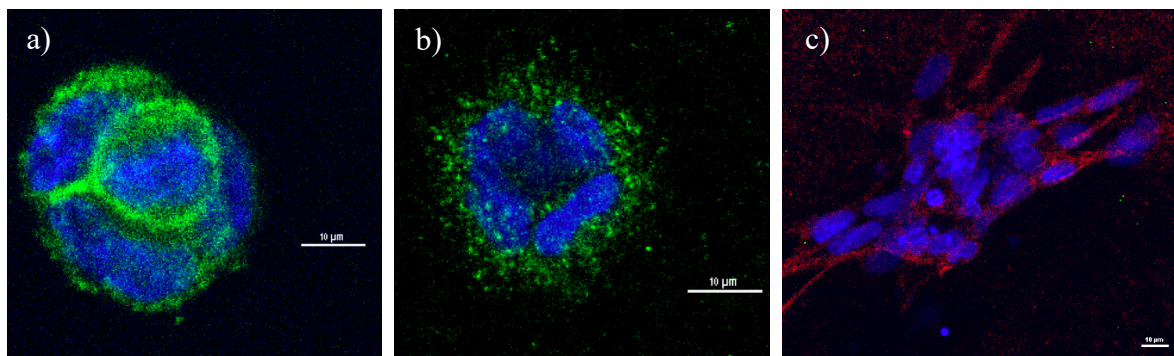


**Figure 17: Cells seeded in monoculture in VitroGel.**

*Cells were marked by immunofluorescence with  $\beta$ -Cat (green), Calponin 1 (red) and nuclei with DAPI (blue). a) MCF-12A cells when cultivated in VitroGel form clumps of cells with spherical shape. b) MCF-10A cells when cultivated in VitroGel form clumps of cells with spherical shape. c) Myo1089 cells when cultivated in VitroGel form mesh-like structures in one dimension of depth.*

Myo1089 cells formed a mesh-like structure in one dimension of depth (Figure 17c). These results suggest that none of the cell lines tested is able to form acini when cultured in Vitrogl.

#### 4.2.2 Luminal MCF-12A cells form bilayered acini when co-cultured with Myo1089 cells in Matrigel

In a second series of experiments, luminal and myoepithelial cells were co-cultured in order to determine if they could form bilayered acini. First, MCF-10A cells were seeded in mixture with Myo1089 cells in Matrigel. After 12-14 days in culture, MCF-10A cells formed acini-like structures, while Myo1089 cells formed clumps of cells without a specific structure, as previously demonstrated (figure 16). However, luminal and myoepithelial cells remained separated in different depth plane and did not interact, suggesting that MCF-10A and Myo1089 are not forming double layered acini when co-cultured in Matrigel (figure 18).

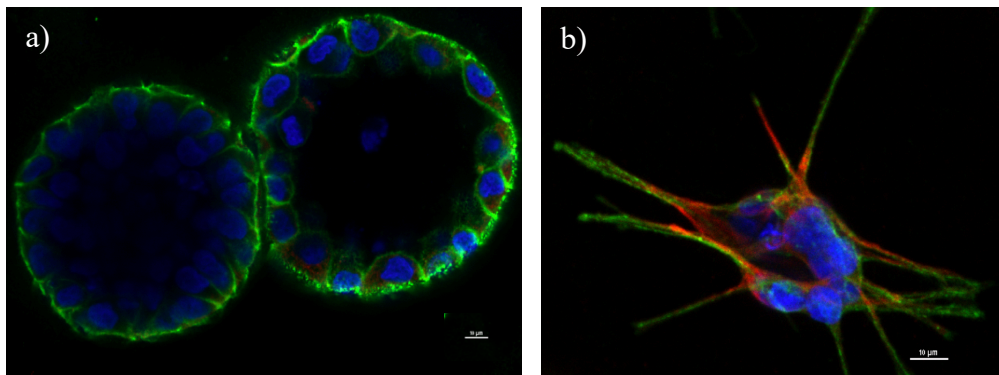


**Figure 18: MCF-10A and Myo1089 cells seeded in mixture in Matrigel and co-cultured for 12-14 days.**

*Cells were marked by immunofluorescence using  $\beta$ -Cat (green), k14 (red) and nuclei with DAPI (blue). a) MCF-10A cells form acini-like structures when seeded in mixture with Myo1089 cells just as they formed when seeded alone. b) Myo1089 cells form clumps of cells without specific structure when seeded in mixture with MCF-10A cells.*

In a second series of experiments, luminal MCF-12A and myoepithelial Myo1089 cells were co-cultured in Matrigel in a ratio of 1:4. In this case, structures similar to the bilayered acini from the mammary gland were observed. The luminal cells form a polarized acinus with the myoepithelial cells surrounding them in a mesh-like manner (Figure 19a), characterized by the presence of lumen (figure 19b and c).

We successfully got a ratio of 50% bilayered acinus structure when cultured in these conditions, while the remaining structures corresponded either to clumps of myoepithelial cells together or luminal cells forming acini-like structures.



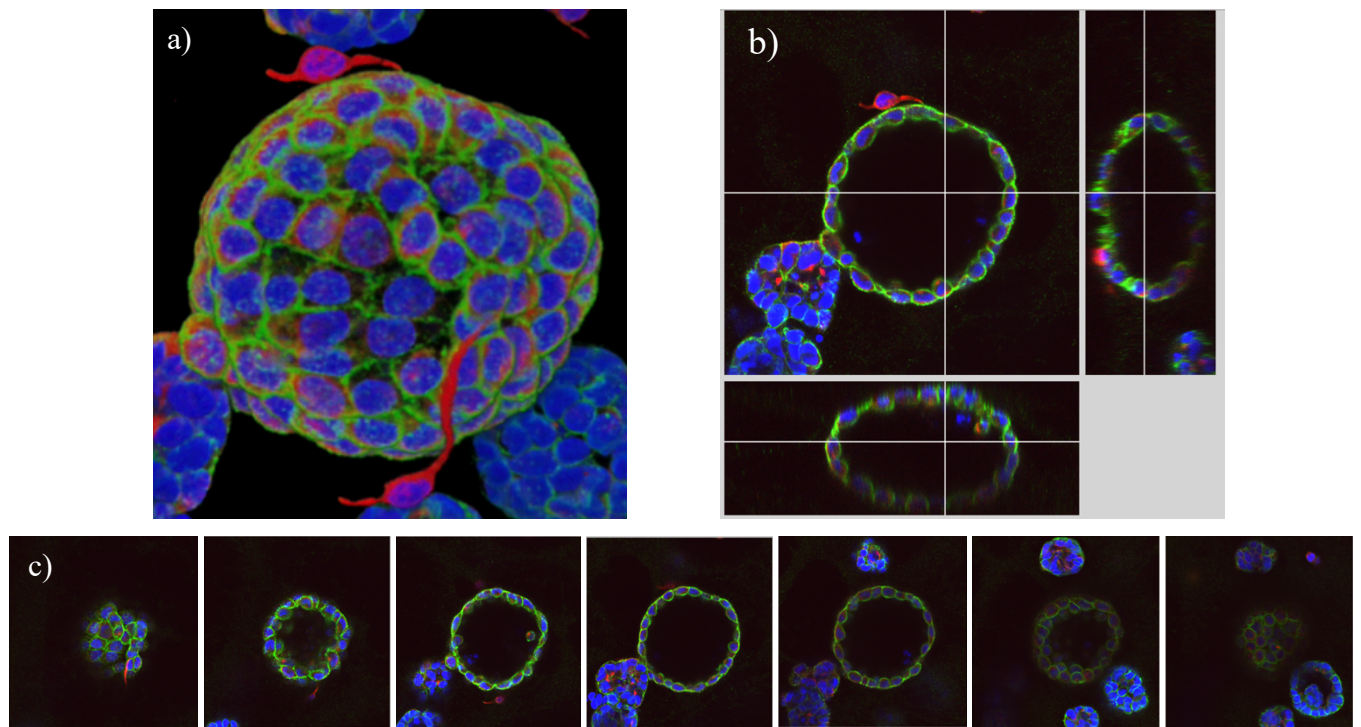


**Figure 19: MCF-12A and Myo1089 cells when co-cultured in Matrigel form structures that represent the bilayered acini of the mammary gland.**

*Cells were marked by immunofluorescence using  $\beta$ -Cat (green), calponin 1 (red) and nuclei with DAPI (blue). a) Luminal MCF-12A and myo1089 cells form bilayered acini, 3D image. b) z-stack of the lumen present when the bilayered acinus is formed. c) Vertical planes from the 3D structure of the bilayered acinus, obtained using confocal microscopy.*

Finally, luminal MCF-12A or MCF-10A cells were co-cultured with Myo1089 cells in VitroGel. Even though many conditions were tested, no acini-like structures could be observed in these co-cultures (figure 20). Interestingly, however, the structures formed by luminal cells show an important difference when they were co-cultured with myoepithelial cells in VitroGel. Indeed, although the two cells types did not directly interact, luminal showed more organized structures than when they were cultured alone (figure 18), suggesting that the indirect interaction is enough to promote a better conformation of structures in the luminal cells of the mammary gland. The structures formed under these conditions were composed of a higher number of cells (more than 5 nuclei were identified) and they formed well rounded spheres.

Together, results demonstrated that MCF-12A and Myo1089 cells can form bilayered acini when co-cultured in Matrigel, but not in VitroGel. These bilayered acini are polarized and closely resemble the structure of the mammary gland epithelium *in vivo*.

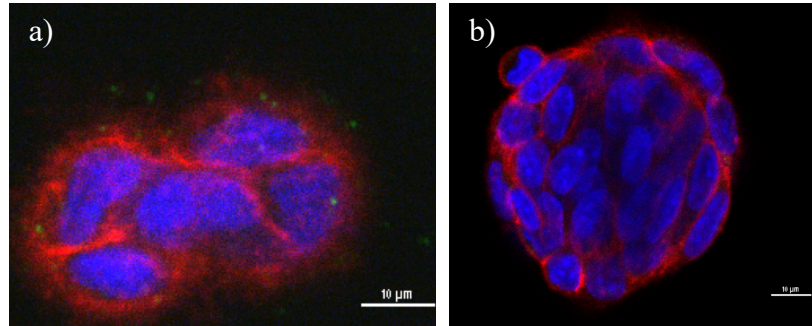


**Figure 20: MCF-12A and Myo1089 cells seeded in co-culture in VitroGel.**

Cells were marked by immunofluorescence with  $\beta$ -Cat (red) and DAPI nuclei with DAPI (blue). a) Neither MCF-12A and Myo1089 cells nor b) MCF-10A and Myo1089 cells when co-cultivated in VitroGel do not form bilayered acini structures.

### 4.3 Layered co-culture model

#### 4.3.1 Luminal MCF-12A and Myo1089 cells can be co-cultured in a layered culture system

Now that we had demonstrated that luminal MCF-12A and myoepithelial Myo1089 cells could form bilayered acini *in vitro*, we next aimed to develop a complementary model in order to be able to evaluate the role of the bidirectional crosstalk between luminal and myoepithelial cells in the formation of the mammary gland epithelium. To do so, luminal MCF-12A cells and myoepithelial Myo1089 cells were co-cultured on each side of a 3  $\mu$ m porous membrane on a cell culture insert. This pore size was chosen to allow direct interaction between the two sides of the porous membrane but avoiding migration of cells. We first confirm that both layers of cells were correctly attached to the membrane (Figure 20). Using immunofluorescence staining, we also demonstrated that  $\beta$ -catenin was localized at the cell membrane in luminal and myoepithelial cells, suggesting that cells in both layers were forming adherens junctions (figure 21).

Interestingly,  $\beta$ -catenin staining was also observed within the pores of the membrane, suggesting the presence of cell projections that reached into the pores of the membrane and of interactions between the two layers of cells (figures 21-22). Similarly, when cells were stained with the gap junctional protein Cx43 by immunofluorescence, a punctate signal typical of Cx43

could be observed in both luminal MCF-12A and myoepithelial Myo1089 cells (figure 22b), but also inside the pores of the membrane, suggesting that this co-culture system was allowing not only the interaction of cells through the membrane but also allowing communication (Figure 22).

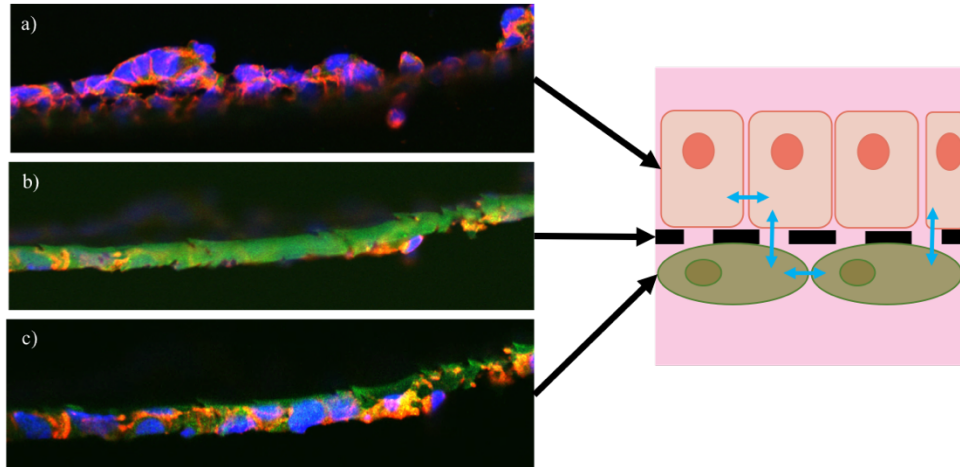


**Figure 21: Immunofluorescence of the layered co-culture system cryosections.**

*Cells were marked with  $\beta$ -cat (red) and nuclei was colored with DAPI (blue). a) Top layer of luminal MCF-12A cells. b) Porous membrane which showed autofluorescence in green. c) Bottom layer of myoepithelial cells.*

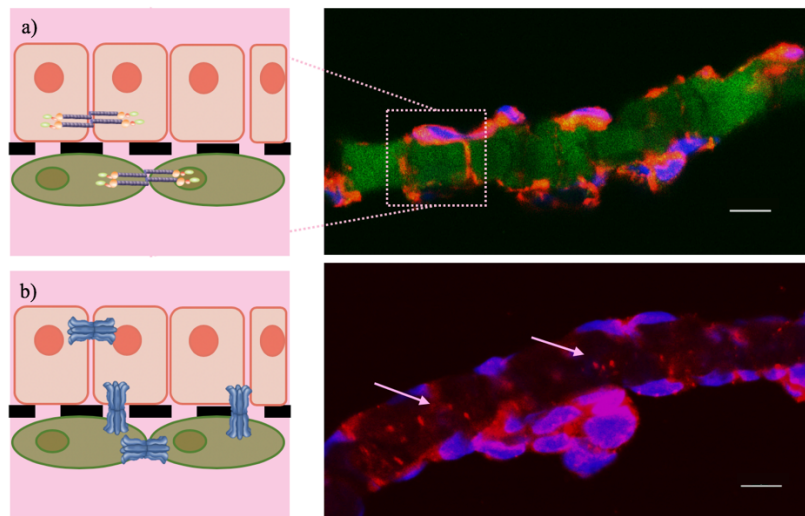


**Figure 22: Junctions were formed between luminal MCF-12A and myoepithelial Myo1089 cells in the layered co-culture system.**

*Luminal and myoepithelial cells expressed adherens junctions when co-culture in the layered culture system. Cells were immunolabeled with  $\beta$ -cat (red) and nuclei with DAPI (blue), the membrane showed autofluorescence (green). b) Luminal and*

myoepithelial cells showed expression of Cx43 located inside of the pores of the membrane. Cells were immunolabeled with Cx43 (red) and nuclei with DAPI (blue), scale bars at 10  $\mu\text{m}$ .

#### 4.3.2 Luminal MCF-12A and Myo1089 cells communicate by gap junction in a layered culture system

As the presence of staining of  $\beta$ -catenin and Cx43 within pores suggested that luminal and myoepithelial cells were interacting, we then wanted to determine if cells were communicating through gap junctions using a DiI and Calcein based dye transfer assay. To do so, MCF-12A luminal cells were preloaded with DiI and Calcein (figure 23a) and then seeded on the insert on which Myo1089 cells were already attached on the other side of the membrane. The presence of Calcein and DiI could be observed through the pores of the membrane shortly after seeding the MCF-12A cells (figure 23b), but not on the lower side of the membrane (figure 24). After 12h of interaction, transferring the Calcein, but no DiI, from luminal cells to myoepithelial cells could be observed (Figure 24), confirming GJIC between the two cell types.

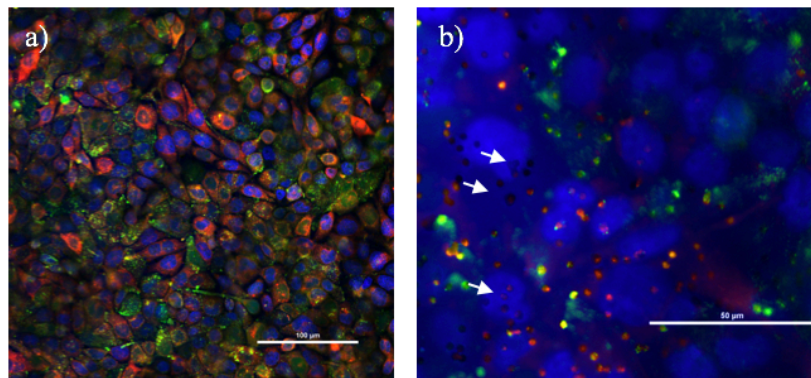


**Figure 23: MCF-12A cells do not migrate to the other side of the membrane.**

Luminal MCF-12A cells were colored with 1.4 $\mu\text{M}$  DiI and 15 $\mu\text{M}$  Cal, cultured on a porous membrane insert and observed under the Nikon AIR+ confocal microscope, just after treatment to dyes. b) The dyes within the upper layer of the insert could be observed through the 3 $\mu\text{m}$  pores when imaged from the lower side of the membrane.



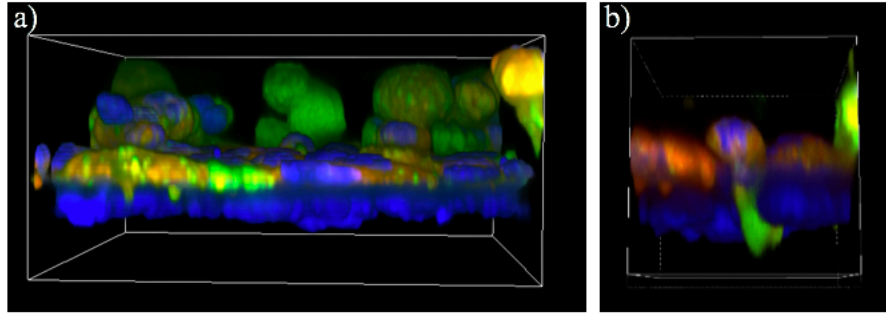


**Figure 24: MCF-12A cells co-cultivated with Myo1089 cells, separated by a porous membrane.**

*a) Just after seeding the cells together ( $t=15$  minutes), MCF-12A cells (top) are previously colored with both Calcein and DiI dye, while Myo1089 cells (bottom) remained non-colored. b) After 12 hours of co-culture, luminal cells start interacting with myoepithelial cells in the bottom and transferring the Calcein dye.*

To further confirm and quantify GJIC, cells from each side of the membrane were harvested separately after 16h of coculture and the number of fluorescence cells was measured using flow cytometry. For this assay, a layer of luminal MCF-12A cells was also seeded in the bottom of the well to ensure that Calcein was being transferred through direct interactions rather than being uptaken through the media (figure 25).

First, we confirmed that luminal MCF-12A cells from the upper side of the membrane were efficiently colored as 70% and 97% showed positive staining for DiI and Calcein, respectively (figure 25a). After interacting, MCF-12A cells successfully transferred Calcein, but not DiI, to Myo1089 cell on the other side of the membrane, as 16% of myoepithelial cells were colored with Calcein, while only 2% were colored with DiI (figure 25b). Only a negligible number of the luminal cells seeded at the bottom of the well were stained Calcein and DiI ( $\leq 0.01\%$  of cells), confirming that Calcein was indeed passing from luminal to myoepithelial cells through GJIC (figure 25). Together, our results confirm that luminal and myoepithelial cells interact and communicate through gap junction when co-cultured in a layered culture system.

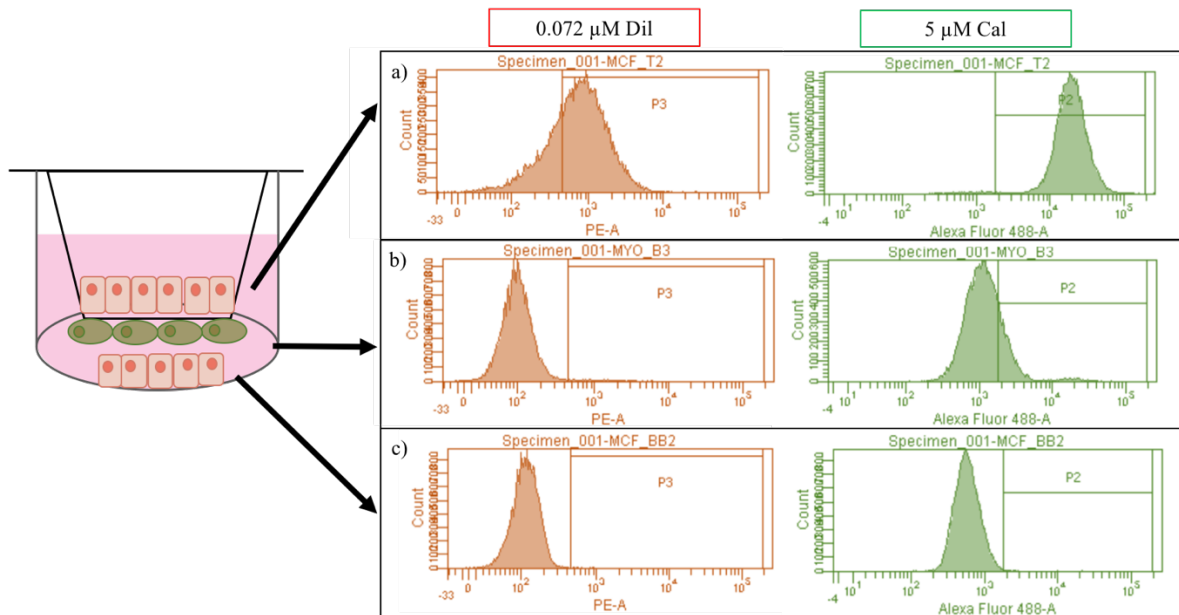


**Figure 25: Luminal and myoepithelial cells communicate through gap junctions.**

Luminal MCF-12A and myoepithelial Myo1089 cells were co-cultured using a porous membrane insert with a control of luminal MCF-12A cells in the bottom of the well. a) After treatment with DiI 0.072  $\mu\text{M}$  and Calcein 5  $\mu\text{M}$ , 70% of luminal MCF-12A cells were successfully colored with DiI and 97% with Calcein. b) After 16h of interaction between colored luminal and myoepithelial cells, 2% of myoepithelial cells were colored with DiI, while 16% of myoepithelial cells were colored Calcein. c) 0.01% of the luminal cells seeded in the bottom of the well were positive for Calcein and DiI.



## 5 Discussion

---

### 5.1 MCF-12A, MCF-10A and Myo1089 are appropriate cell lines for the development of more complex *in vitro* models

The usage of cell lines was of great relevance in the construction of our models. We face a crucial decision in whether to use primary cell culture or cell lines. Primary cells most closely represent the tissue of origin, since they are derived from tissue and not modified, they typically exhibit closer physiology to an *in vivo* state. However, they have a limited lifespan, are hard to genetically modify and will present senescence after a certain number of cell divisions, thus limiting the extent of an experiment. They also present important variability from each source/donor affecting the reproducibility of the assays (Ramos *et al.*, 2014). On opposite, cell lines have acquired the ability to proliferate indefinitely either through random mutation or spontaneous immortalization, such as MCF-12A and MCF-10A cells, or by deliberate modification, such as Myo1089 cells. Cell lines are generally easier to maintain in culture than primary cells but may present altered physiological properties and not represent accurately the *in vivo* state; moreover their characteristics can change over time with extensive passaging (Geraghty *et al.*, 2014). This is the main reason why we performed characterization and kept early passages of the cells in culture. Nevertheless, cell lines were preferred over primary culture in order to generate a standardized version of both models. The aim was indeed to get representative cell culture models that could be genetically modified, while reducing the variation that using primary cell culture would carry. Indeed, so far, most of the *in vitro* models developed by other researchers were either made of luminal cells only, thus not representative of the bilayered mammary epithelium (Froehlich *et al.*, 2016), or were bilayered acini made from primary cells isolated from tissues, thus less reproducible and harder to manipulate genetically (Sokol *et al.*, 2016).

Luminal MCF-12A, MCF-10A and myoepithelial Myo1089 cells were characterized either using western blot or immunofluorescence techniques. This process allowed to verify if the cells were appropriate candidates for the models. After the characterization, the luminal cell lines MCF-12A and MCF-10A were determined to express most of luminal-like markers (figure 15). We also showed that they could form polarized acini when culture in Matrigel. These characteristics confirm that they are representative cells of the luminal layer of the mammary gland. The same

conditions applied for the myoepithelial cells, therefore Myo1089 cells were chosen as representative of the myoepithelial cells of the mammary gland (Table 5). Of note, luminal cells also expressed a few myoepithelial markers, and vice-versa. This is not that surprising as it is well-known that cell in culture can express some proteins that they do not typically express *in vivo*, and can also dedifferentiate (Geraghty *et al.*, 2014). Nevertheless, the chosen cell lines were phenotypically close enough to the cells-of-origin to be considered as good candidates.

**Table 4: Comparison between primary cell culture and cell lines.**

Characteristics	Primary cell culture	Cell lines
Biological representation of <i>in vivo</i> state	High	Low
Proliferation and lifespan	Limited	Unlimited
Variation	High	Low
Phenotype	Maintains <i>in vivo</i> phenotype	Subject to drift over the time
Cell growth	Requires optimizing cell culture conditions	Well established protocols and conditions
Cost	High	Low

**Table 5: Luminal MCF-12A, MCF-10A and myoepithelial Myo1089 cells. Either performed by immunofluorescence or Western blot.**

	MCF12A	MCF10A		Myo1089
PR a	✓	✓	Caldesmon 1	✓
PR b	✓	✓	Calponin 1	✓
ER $\alpha$	✓	✗	SMA	✗
k18	✓	✓	k14	✓

	MCF12A	MCF10A	Myo1089
Cx43	✓	✓	✓
Cx30	✗	✗	✗
Cx32	✓	✓	✓
$\beta$ -catenin	✓	✓	✓
E-cadherin	✓	✓	✓

Every time we referred in the text to an acinus structure, we refer to a structure with a lumen, been confirmed by confocal microscopy. All of the pictures presented are indeed part of a z-stack in which we confirmed the presence of lumen. In order to determine whether the results confirmed the presence of lumen instead of the lack of signal from DAPI, the methodology for immunofluorescence included a permeabilization process in order to get the DAPI and antibodies into the structures formed. Nevertheless, structures were analyzed with the microscope with a high exposure to lasers in order to confirm any possible signal for cell nuclei.

## **5.2 MCF-12A and Myo1089 cells form bilayered acini in Matrigel, but not in VitroGel**

Our results demonstrate that MCF-12A and Myo1089 cells can form bilayered acini in Matrigel, but not in VitroGel. Even though several parameters were adjusted, and constant interactions were maintained with the supplier through all the development steps of this model, we were not able to produce acini or bilayered acini using VitroGel. In VitroGel, structures were smaller and without an acinus-like shape. This notorious difference between the cell cultures with Matrigel in comparison to the cell cultures using VitroGel, reinforced the theory of the laminin-rich environments to be required for the formation of 3D cell culture models. The implication of laminin in the differentiation and polarization of epithelial structures was firstly proposed in 1980 (Ekblom *et al.*, 1980). Since then, further studies *in vivo* have consistently supported the hypothesis that laminin facilitates epithelial polarization by being a spatial cue to cells (Yu *et al.*, 2005).

Previous work in our laboratory showed that when MCF-12A cells and Hs578Bst cells are cultured in Matrigel, 50% of spheres formed were a correct representation of a bilayered acinus (Weber-Ouellette *et al.*, 2018). In the aim of continuing the development of this model, we chose to test parameters in order to improve the ratio of bilayered acini formed in Matrigel. Two approaches were tested: 1) to increase the number of myoepithelial cells within the mixture, and 2) try another ECM. Therefore, in the development of our project, we kept the laminin-rich ECM (Matrigel), but also tried an animal origin free ECM (VitroGel).

One of the main setbacks for the model published by Anne Weber-Ouellette was the growth of Hs578Bst cells, this myoepithelial cell line posed great difficulty, as their doubling time is extremely long (about 36-45 hours), even slowing down with passages, and they can be passaged only a limited number of times. Although several conditions were tested in order to improve the growth rate, including transfection of the cells with the SV40 large T antigen and changing their

cell media composition with higher FBS concentration for a better growth, we could not improve that parameter. It was thus very difficult to obtain a good number of cells to use for 3D models, and we were not able to increase the number of myoepithelial cells within the mixture to improve the ratio of bilayered/monolayered acini. Since the growth of this cell line was complicating the advance of the model, we decided to contact Dr. Louise Jones from Barts Cancer Institute in London, who provided us with the Myo1089 cells. We showed that, similar to Hs578Bst cells, Myo1089 cells can form bilayered acini with MCF-12A cells. Since Myo1089 cells are easier to maintain and grow faster, we can now try to increase the number of myoepithelial cells. To our knowledge these two cell lines are the only human myoepithelial cells from the mammary gland available.

In the search to force luminal cells establish a better relationship with myoepithelial cells and therefore form a greater rate of bilayered acini, we also used Vitrogel. Luminal MCF-12A and MCF-10A cells showed to form acini-like structures when seeded alone in Matrigel, showing that the laminin present in the ECM was sufficient for them to form polarized structures. Therefore, our hypothesis relied on the lack of laminin in Vitrogel being a promoter for myoepithelial cells to secrete laminin and collagen IV, and therefore “obliging” luminal cells to adhere to myoepithelial cells in order to form polarized structures. After several conditions were modified, Matrigel continued providing the best results. Matrigel provides the establishment of epithelial polarity without further modifications and the functionally differentiated state last several weeks in culture (Krause *et al.*, 2008), but it possesses some disadvantages including cost, difficulty for its isolation, poor definition and batch-to-batch variation, tumor origin and poor mechanical properties (Nerger & Nelson, 2019). Therefore, further experiments will be pursued with the animal-free ECM Vitrogel-RGD. The best conditions to be used with Vitrogel-RGD remain to be determined. Cell density, volume of ECM, volume of media and ratio of cells still require modifications until the best set of conditions is found. Furthermore, since our last experiments with Vitrogel, the company has developed a new Vitrogel with RGD peptide highly concentrated and a dilution solution with sucrose in order to maintain osmolality, offering more suitable conditions for cells. They also recently synthesize Vitrogel including peptide mimicking ECM components, including laminin. Further tests will thus be performed with these new compositions since it aims to improve the cell attachment and therefore structure formation. Whether or not these new formulations would improve the rate of bilayered acini remain to be determined.

### 5.3 Beating the gravity: the complex establishment of the layered co-culture model

The main obstacle faced during the development of the layered culture system, was the technical obstacle of seeding cells against gravity on the abluminal surface of the porous membrane. Previous protocols seeded cells in a drop of media on top of an inverted insert (Gaillard *et al.*, 2001; Li *et al.*, 2010). However, after 10 minutes the media leaks through the pores of the membrane, requiring constant monitoring of the inserts and the periodically media addition on top of the cells; this resulted in frequent opening of the incubator (causing fluctuations in temperature, pH and humidity), increased risk for contamination and causing uneven cell seeding due to the media leakage (Gaillard *et al.*, 2001; Li *et al.*, 2010). In order to address the mentioned limitations, another method was proposed, using tubing to create a well on the abluminal side on the insert while having it turn upside down (Figure 26) (Niego & Medcalf, 2013). This well allows to add higher volumes of media in order to counteract the media leaking through the pores and it also includes a silicon plug to be added on the bottom of the upside-down insert to hold the media (Figure 26). This method allows to get undisturbed adherence of cells onto the abluminal membrane surface in an equilibrated incubator, for an extended period of time. As a result, a uniform seeding of cells is achieved (Niego & Medcalf, 2013). Nevertheless, it still presents some limitations: the construction of the system and its deinstallation requires extra manipulation that could increase the risk of contamination and the size of the tubing requires to be precise to avoid the media to leak, as well as it requires to be a material proper for sterilization.



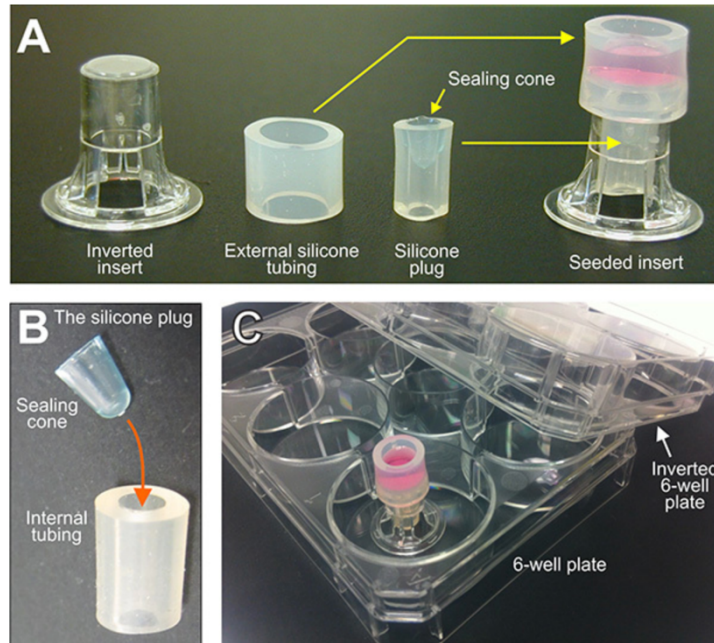


**Figure 26: Cell co-culture model of the brain blood barrier.**

*A) The insert is inverted, a short piece of silicone tubing (external tubing) is assembled around its perimeter and a B) silicone plug is added into the luminal cavity. This assembly creates a well on top of the abluminal surface and prevents media from leaking through the pores. C) Once seeded, the assembled inserts are transported in between two 6-well plates (one plate inverted over the other) to minimize the risk of contamination. (Niego & Medcalf, 2013)*

While we were able to use this method with the 24-well plate size insert, it was more difficult to use of the bigger inserts (figure 27). It required invasive manipulation in order to assemble and disassemble, creating a risk for contamination. We therefore developed a new technique, using a P6 inverted plate (described in materials and methods section 2.2.2). The new method is not only simple, but also reduce the number of manipulations required, therefore the risk of contamination, can easily be adapted to all size of inserts and can easily be reproduce by other labs worldwide. More importantly, this experimental development now allows us to propose a suitable model to evaluate the bidirectional crosstalk between luminal and myoepithelial cells.

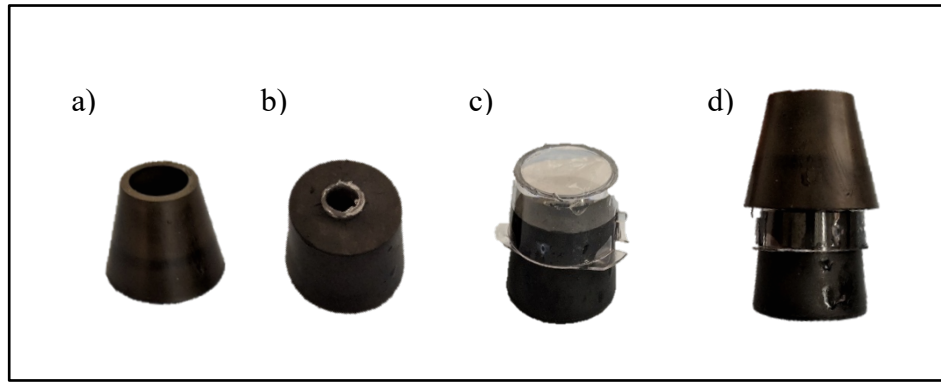


**Figure 27: First adaptation of Niego and Medcalf model Medcalf model for co-culture of cells on inserts.**

*a) Top cover which serve as a chamber to maintain the media on top of the cells. b) Bottom plug which serve to avoid media to leak through. c) Construction with bottom plug and inserts for P6. d) Final construction using the bottom and top plugs, creating a cell culture media chamber to maintain the cells alive and growing while adhering to the abluminal side of the insert.*

#### **5.4 Luminal and myoepithelial cells are communicating through gap junctions**

To establish a model allowing the study of the bidirectional crosstalk between luminal and myoepithelial cells, we based our research on a model developed by Goldberg's team (Goldberg et al., 2002). Using a similar model, they first demonstrated that different molecules can pass through gap junctional channels depending of the connexins composing the channels, and second that donor cells and receiver cells can form contact through projections and communicate by GJIC (Goldberg et al., 2002). We thus adapted this protocol using the two main types of cells of the mammary gland epithelium, namely the luminal and the myoepithelial cells. We showed that Calcein, but not DiI, was passed between the cells, thus confirming the expression of GJIC.

In the murine mammary gland, Cx26, Cx30 and Cx32 are expressed only in the luminal cells and Cx43 is expressed in myoepithelial cells (Mroue *et al.*, 2015), but also between luminal cells and at the junction between luminal and myoepithelial cells (Dianati *et al.*, 2016). The expression of all Cxs have shown to have a stage-dependent expression during the mammary gland development, which supports the theory of them having essential roles in the secretory activity of the gland (Dianati *et al.*, 2016; Mroue *et al.*, 2015). The presence of Cx43 has also been reported between myoepithelial cells on human mammary gland samples obtained from reduction mammoplasties (El-Sabban *et al.*, 2003). One of the goals of our model was to demonstrate whether or not we could demonstrate a functional GJIC between luminal and myoepithelial cells. It has been previously reported that mammary gland epithelial cells could form heterotypic channels Cx26/Cx43, nevertheless this channels did not allow dye transfer (Tomasetto *et al.*,

1993). Nevertheless, we have not been able to assess the expression of Cx26 on the cell lines used, therefore, we might require to further characterize the GJIC that are taking place between the two layers of cells. Perhaps, the 16% transfer rate of dye relies on a higher number of heterotypic GJIC than homotypic GJIC capable of transferring the dye. In addition, Cx43 has been showed to be expressed non-homogenously throughout the bilayered acinus of the mammary gland and at low levels (Dianati *et al.*, 2016), which could potentially explain the low number of myoepithelial cells that received the calcein. In preliminary data (not showed), we performed some time-dependent assays, in order to understand if the dye transferred was happening in a time-dependent manner. These first results confirm that after 16h, 40h and 88h, the dye transferred did not showed any significant difference. Therefore, in order to better understand the reasons behind a 16% ratio of myoepithelial cells receiving the dye, we must continue with the characterization of the GJIC formed.

In the analysis using DiL and Calcein, there was also 2% of the myoepithelial cells that were positive for DiL after 16h interaction with luminal cells. DiL was used as a control to ensure that colored luminal cells were not migrating to the other side of the membrane. In previous studies, cells were loaded with DiD, a dye from the same family of lipophilic fluorescent stains for labeling membranes and other hydrophobic structures (Yumoto *et al.*, 2014). In these studies, a similar percentage of receiver cells were positive for DiD after being co-cultured with donor cells, and that was considered as negligible (Yumoto *et al.*, 2014). As DiL is incorporated within the membrane of the cells, one can postulate that small portions of membrane are exchange between luminal and myoepithelial cells, either through exosomes or gap junctions' connexosomes (Laird, 2006). Indeed, it has been shown previously that when gap junctions are internalized, they form a double-membrane structure that is internalized into one of the two opposing cells (Ivanov *et al.*, 2004). Moreover, it was reported that exosomes could be labeled by DiL and uptaken by human umbilical vein endothelial cells (HUVECs) *in vitro* (Liang *et al.*, 2016), providing another possible explanation for the DiL positive signal in myoepithelial cells.

## 6 Perspectives

---

The models developed through this thesis allowed us to construct a base for more representative cell culture models of the mammary gland *in vitro*. The following long-term steps to be taken therefore should run into two different scopes in parallel. First, our *in vitro* models as to be compared to the current *in vitro* and *in vivo* models available as well as to human response if possible, to assess its accurateness. Comparing a typical model of *in vitro* cell culture in monolayer, our new 3D and layered co-culture models and an animal *in vivo* model to a human mammary gland would be ideal. This comparison should be made using a compound with well-known measurable effects. Although is it impossible to do this in a short period of time, the more we used our alternative models, the more they will be characterized and used to replace animal models.

Second, ideally, we want to develop even more complex model by incorporating other cells of the mammary gland, such as fibroblasts and adipocytes present in the stroma. While the mammary gland acinus might be a representative functional unit of the mammary gland, this organ is also defined by an extensive stroma. It has been shown previously that when luminal and myoepithelial mammary cells are being cultured in an ECM, the addition of adipocytes is directly related to the formation of polarized acinus structures (Nash *et al.*, 2015). This complex multicellular model could give a most accurate representation of the human mammary gland. It is well known that the interactions between the mammary gland epithelium the surrounding stroma is crucial for its proper development. Thus, an ideal model should include all these components. In shorter terms, we will explore other avenues to further improve the models developed in this thesis.

### 6.1 3D bilayered model: characterization and bioprinting

Although we successfully achieve the formation of bilayered acini *in vitro*, both acini and bilayered acini were present in each well. To be able to use this model for drug, toxicological or mechanistic studies, we need to increase the ratio of bilayered acini. As short time perspective, the increase of number of myoepithelial cells in the cell seeding process might improve the ratio or bilayered acini formed, as well as changing from VitroGel-RGD to its new and highly concentrated version. For the long-term perspectives, we can assess the limitations that manually seeding cells brings into

this model. Manually mixing and seeding the cells in the development of 3D models explain, in part, the lack of complete efficiency in our method. It has been shown that for 3D models, the cellular self-assembly process takes days and may require complex spatial and temporal environmental cues, which is the main reason biomanufacturing processes such as 3D bioprinting are being developed (Swaminathan *et al.*, 2019). This technique enables the precise positioning of cells in an automated and high throughput manner. It has previously been shown that bioprinting systems could provide solutions for the random nature of manually seeded 3D structures. Bioprinting could therefore decrease the variations due to the random localization and proximity of cells embedded in the ECM, which cause differences in the development of structures (Reid *et al.*, 2018). The development of representative cell culture models *in vitro* is a ground breaking field of research. These alternative models are being developed in order to get a cost-efficient and time-wise alternative for toxicology and pharmacology screening, among other usages. For that purpose, the ECM used requires to have previous studies, in order to confirm that the ECM itself do not alter the results of any experiments by interacting with the compounds to be tested. In our case, we are proceeding to the characterization of the bilayered acinus model, even if we got a 50% ratio of bilayered acinus. This characterization will allow us to assess its advantages and limitations for its use in the toxicology studies already in development in our laboratory.

## **6.2 The layered co-culture model: unravelling the role of the bidirectional crosstalk on signaling in each cell type**

Our results showed that luminal and myoepithelial cells communicate through GJIC. The next logical step with this model is to analyze how this interaction impact cell signaling within each cell type. The next experiments to be performed for this model, should thus be the characterization of cells before and after interaction. To do so, we can use the protocol developed to recover the cells to analyze GJIC by cytometry, and extract protein or RNA from each cell type. After establishment, this model would allow to unravel the mechanisms activated when different cell populations are co-cultured together. This interaction can later be compared to the different mechanisms triggered by co-cultured healthy mammary gland cells with cancerous cells. Luminal MCF-12A and Myo1089 cells can also be modified through CRISPR-Cas system in order to test different constructions of connexins and analyze the effects of them on the communication between layered monoculture and layered co-culture of cells. Toxicological and pharmaceutical

screenings could be performed in this model, giving specific information regarding the cell type due to the ease to separate cells after being co-cultured.

## 7 Conclusion

---

Two models were developed on this project; the 3D bilayered acinus model and the layered co-culture system, both of them allowing us to have alternative models for the study of the mammary gland structure. The first is a more representative cell culture model than the standard monolayer of cells *in vitro*, thanks to the presence of a 3D structure and of the main two types of cell composing the mammary gland epithelium. The second model gave important information on the communication between luminal and myoepithelial cells. This layered culture system is the first model, to the best of our knowledge, to show *in vitro* functional GJIC between luminal-like and myoepithelial-like human mammary gland cells. The mechanism behind this communication and whether it reflects the *in vivo* process remain to be studied.

The construction of these models included several steps of optimization and validation in a continuous cycle. In this work, we only presented the positive outcomes after several rounds of optimization; nevertheless, countless experiments were performed in order to modify and validate every parameter involved in the construction of both models. Developing complex cell culture *in vitro* models is fastidious, but lessons learned from these experiments can be applied to several fields of research and is a step forward in a quest for a gold-standard model. In terms, such models could be used in screening platforms, providing a more cost-effective and precise preclinical setting for drug discovery or toxicology screens (Simian & Bissell, 2017). In the future, we will use these two models in parallel, as they can give complementary information. The layered culture model using transwell porous membranes remain useful mainly for the ease in which two cell populations can be combined and later separated for analysis; while the intimate relationship of luminal and myoepithelial cells in the 3D co-culture model, provide information on the important implications for mammary gland structure and function. The mammary gland is a unique organ that adapts dramatically throughout development, undergoing significant stage specific changes in differentiation and tissue morphology. Innovative models developed during this project will be used to enhance our understanding of disease processes, toxicology and pharmaceutical effects.

## 8 Bibliography

---

- Adriance MC, Inman JL, Petersen OW, Bissell MJ (2005) Myoepithelial cells: good fences make good neighbors. *Breast Cancer Research* 7(5):190-197.
- Ahima RS & Flier JS (2000) Adipose tissue as an endocrine organ. *Trends in Endocrinology and Metabolism* 11(8):327-332.
- Alexander DB, Ichikawa H, Bechberger JF, Valiunas V, Ohki M, Naus CC, Kunimoto T, Tsuda H, Miller WT, Goldberg GS (2004) Normal cells control the growth of neighboring transformed cells independent of gap junctional communication and SRC activity. *Cancer Research* 64(4):1347-1358.
- Alhaque S, Themis M, Rashidi H (2018) Three-dimensional cell culture: from evolution to revolution. *Philosophical Transactions of the Royal Society of London. Series B: Biological Sciences* 373(1750).
- Anderson SM, Rudolph MC, McManaman JL, Neville MC (2007) Key stages in mammary gland development. Secretory activation in the mammary gland: it's not just about milk protein synthesis! *Breast Cancer Research* 9(1):204.
- Antoni D, Burckel H, Josset E, Noel G (2015) Three-dimensional cell culture: a breakthrough in vivo. *International Journal of Molecular Sciences* 16(3):5517-5527.
- Barcellos-Hoff MH, Aggeler J, Ram TG, Bissell MJ (1989) Functional differentiation and alveolar morphogenesis of primary mammary cultures on reconstituted basement membrane. *Development* 105(2):223-235.
- Borowsky AD (2003) Genetically engineering a mouse. *Comparative Medicine* 53(3):249-250.
- Borowsky AD (2011) Choosing a mouse model: experimental biology in context--the utility and limitations of mouse models of breast cancer. *Cold Spring Harbor Perspectives in Biology* 3(9):a009670.
- Brennan K, Offiah G, McSherry EA, Hopkins AM (2010) Tight junctions: a barrier to the initiation and progression of breast cancer? *Journal of Biomedicine and Biotechnology* 2010:460607.
- Breslin S & O'Driscoll L (2013) Three-dimensional cell culture: the missing link in drug discovery. *Drug Discovery Today* 18(5-6):240-249.
- Brunelle M, Nordell Markovits A, Rodrigue S, Lupien M, Jacques PE, Gevry N (2015) The histone variant H2A.Z is an important regulator of enhancer activity. *Nucleic Acids Res* 43(20):9742-9756.
- Bruno RD, Reid J, Sachs PC (2019) The revolution will be open-source: how 3D bioprinting can change 3D cell culture. *Oncotarget* 10(46):4724-4726.
- Cagnet S, Glukhova MA, Raymond K (2017) Contractility Assay for Established Myoepithelial Cell Lines. *Mammary Gland Development: Methods and Protocols*, Martin F, Stein

- T,Howlin J (Édit.) Springer New York, New York, NY10.1007/978-1-4939-6475-8\_8. p 189-198.
- Campbell HK, Maiers JL,DeMali KA (2017) Interplay between tight junctions & adherens junctions. *Experimental Cell Research* 358(1):39-44.
- Chandler EM, Berglund CM, Lee JS, Polacheck WJ, Gleghorn JP, Kirby BJ,Fischbach C (2011) Stiffness of photocrosslinked RGD-alginate gels regulates adipose progenitor cell behavior. *Biotechnology and Bioengineering* 108(7):1683-1692.
- Charbe N, McCarron PA,Tambuwalla MM (2017) Three-dimensional bio-printing: A new frontier in oncology research. *World Journal of Clinical Oncology* 8(1):21-36.
- Clevers H (2016) Modeling Development and Disease with Organoids. *Cell* 165(7):1586-1597.
- Coisne C, Dehouck L, Faveeuw C, Delplace Y, Miller F, Landry C, Morissette C, Fenart L, Cecchelli R, Tremblay P,Dehouck B (2005) Mouse syngenic in vitro blood-brain barrier model: a new tool to examine inflammatory events in cerebral endothelium. *Laboratory Investigation* 85(6):734-746.
- Daniel CW, Berger JJ, Strickland P,Garcia R (1984) Similar growth pattern of mouse mammary epithelium cultivated in collagen matrix in vivo and in vitro. *Developmental Biology* 104(1):57-64.
- Darcy KM, Black JD, Hahm HA,Ip MM (1991) Mammary organoids from immature virgin rats undergo ductal and alveolar morphogenesis when grown within a reconstituted basement membrane. *Experimental Cell Research* 196(1):49-65.
- Deli MA, Abraham CS, Kataoka Y,Niwa M (2005) Permeability studies on in vitro blood-brain barrier models: physiology, pathology, and pharmacology. *Cellular and Molecular Neurobiology* 25(1):59-127.
- Deugnier MA, Teulière J, Faraldo MM, Thierry JP,Glukhova MA (2002) The importance of being a myoepithelial cell. *Breast Cancer Research* 4(6):224-230.
- Dianati E, Poiraud J, Weber-Ouellette A,Plante I (2016) Connexins, E-cadherin, Claudin-7 and beta-catenin transiently form junctional nexuses during the post-natal mammary gland development. *Developmental Biology* 416(1):52-68.
- Djomehri SI, Burman B, Gonzalez ME, Takayama S,Kleer CG (2019) A reproducible scaffold-free 3D organoid model to study neoplastic progression in breast cancer. *J Cell Commun Signal* 13(1):129-143.
- Dontu G, Al-Hajj M, Abdallah WM, Clarke MF,Wicha MS (2003) Stem cells in normal breast development and breast cancer. *Cell Proliferation* 36 Suppl 1:59-72.
- Edmondson R, Broglie JJ, Adcock AF,Yang L (2014) Three-dimensional cell culture systems and their applications in drug discovery and cell-based biosensors. *Assay and Drug Development Technologies* 12(4):207-218.
- Eklblom P, Alitalo K, Vaheri A, Timpl R,Saxen L (1980) Induction of a basement membrane glycoprotein in embryonic kidney: possible role of laminin in morphogenesis. *Proceedings of the National Academy of Sciences of the United States of America* 77(1):485-489.



- Ekblom P, Lonai P, Talts JF (2003) Expression and biological role of laminin-1. *Matrix Biology* 22(1):35-47.
- El-Sabban ME, Abi-Mosleh LF, Talhouk RS (2003) Developmental regulation of gap junctions and their role in mammary epithelial cell differentiation. *Journal of Mammary Gland Biology and Neoplasia* 8(4):463-473.
- Fata JE, Mori H, Ewald AJ, Zhang H, Yao E, Werb Z, Bissell MJ (2007) The MAPK(ERK-1,2) pathway integrates distinct and antagonistic signals from TGF $\alpha$  and FGF7 in morphogenesis of mouse mammary epithelium. *Developmental Biology* 306(1):193-207.
- Fatehullah A, Tan SH, Barker N (2016) Organoids as an in vitro model of human development and disease. *Nature Cell Biology* 18:246.
- Flecknell P (2002) Replacement, reduction and refinement. *ALTEX* 19(2):73-78.
- Florian S, Iwamoto Y, Coughlin M, Weissleder R, Mitchison TJ (2019) A human organoid system that self-organizes to recapitulate growth and differentiation of a benign mammary tumor. *Proceedings of the National Academy of Sciences of the United States of America* 116(23):11444-11453.
- Froehlich K, Haeger JD, Heger J, Pastuschek J, Photini SM, Yan Y, Lupp A, Pfarrer C, Mrowka R, Schleussner E, Markert UR, Schmidt A (2016) Generation of Multicellular Breast Cancer Tumor Spheroids: Comparison of Different Protocols. *Journal of Mammary Gland Biology and Neoplasia* 21(3-4):89-98.
- Gaillard PJ, Voorwinden LH, Nielsen JL, Ivanov A, Atsumi R, Engman H, Ringbom C, de Boer AG, Breimer DD (2001) Establishment and functional characterization of an in vitro model of the blood-brain barrier, comprising a co-culture of brain capillary endothelial cells and astrocytes. *European Journal of Pharmaceutical Sciences* 12(3):215-222.
- Geraghty RJ, Capes-Davis A, Davis JM, Downward J, Freshney RI, Knezevic I, Lovell-Badge R, Masters JR, Meredith J, Stacey GN, Thraves P, Vias M (2014) Guidelines for the use of cell lines in biomedical research. *British Journal of Cancer* 111(6):1021-1046.
- Goldberg GS, Lampe PD, Nicholson BJ (1999) Selective transfer of endogenous metabolites through gap junctions composed of different connexins. *Nature Cell Biology* 1(7):457-459.
- Goldberg GS, Moreno AP, Lampe PD (2002) Gap junctions between cells expressing connexin 43 or 32 show inverse permselectivity to adenosine and ATP. *Journal of Biological Chemistry* 277(39):36725-36730.
- Goldberg GS, Valiunas V, Brink PR (2004) Selective permeability of gap junction channels. *Biochimica et Biophysica Acta (BBA) - Bioenergetics* 1662(1-2):96-101.
- Goodenough DA, Goliger JA, Paul DL (1996) Connexins, connexons, and intercellular communication. *Annual Review of Biochemistry* 65:475-502.
- Goodenough DA & Paul DL (2009) Gap junctions. *Cold Spring Harbor Perspectives in Biology* 1(1):a002576.
- Gudapati H, Dey M, Ozbolat I (2016) A comprehensive review on droplet-based bioprinting: Past, present and future. *Biomaterials* 102:20-42.

- Gudjonsson T, Adriance MC, Sternlicht MD, Petersen OW, Bissell MJ (2005) Myoepithelial cells: their origin and function in breast morphogenesis and neoplasia. *Journal of Mammary Gland Biology and Neoplasia* 10(3):261-272.
- Gudjonsson T, Ronnov-Jessen L, Villadsen R, Rank F, Bissell MJ, Petersen OW (2002) Normal and tumor-derived myoepithelial cells differ in their ability to interact with luminal breast epithelial cells for polarity and basement membrane deposition. *Journal of Cell Science* 115(Pt 1):39-50.
- Hait WN (2010) Anticancer drug development: the grand challenges. *Nature Reviews Drug Discovery* 9(4):253-254.
- Harbell JW, Bowman PD, Shannon JM, Daniel CW (1977) Long-term organ culture of mouse mammary gland. *In Vitro* 13(8):490-496.
- Harrison H, Farnie G, Howell SJ, Rock RE, Stylianou S, Brennan KR, Bundred NJ, Clarke RB (2010) Regulation of breast cancer stem cell activity by signaling through the Notch4 receptor. *Cancer Research* 70(2):709-718.
- Harrison RG, Greenman MJ, Mall FP, Jackson CM (1907) Observations of the living developing nerve fiber. *The Anatomical Record* 1(5):116-128.
- Haslam SZ & Woodward TL (2003) Host microenvironment in breast cancer development: epithelial-cell-stromal-cell interactions and steroid hormone action in normal and cancerous mammary gland. *Breast Cancer Research* 5(4):208-215.
- Hassiotou F & Geddes D (2012) Anatomy of the human mammary gland: Current status of knowledge. *Clinical Anatomy* 26(1):29-48.
- Henderson VC, Demko N, Hakala A, MacKinnon N, Federico CA, Fergusson D, Kimmelman J (2015) A meta-analysis of threats to valid clinical inference in preclinical research of sunitinib. *Elife* 4:e08351.
- Hennighausen L & Robinson GW (2005) Information networks in the mammary gland. *Nature Reviews: Molecular Cell Biology* 6(9):715-725.
- Hirschi KK, Xu CE, Tsukamoto T, Sager R (1996) Gap junction genes Cx26 and Cx43 individually suppress the cancer phenotype of human mammary carcinoma cells and restore differentiation potential. *Cell Growth and Differentiation* 7(7):861-870.
- Holen I, Speirs V, Morrissey B, Blyth K (2017) In vivo models in breast cancer research: progress, challenges and future directions. *Disease Models & Mechanisms* 10(4):359-371.
- Honegger P (2001) Overview of cell and tissue culture techniques. *Current Protocols in Pharmacology Chapter 12:Unit 12* 11.
- Hopkins AL (2008) Network pharmacology: the next paradigm in drug discovery. *Nature Chemical Biology* 4(11):682-690.
- Ichinose RR & Nandi S (1964) Lobuloalveolar Differentiation in Mouse Mammary Tissues in vitro. *Science* 145(3631):496-497.
- Inman JL, Robertson C, Mott JD, Bissell MJ (2015) Mammary gland development: cell fate specification, stem cells and the microenvironment. *Development* 142(6):1028-1042.

- Itoh M & Bissell MJ (2003) The organization of tight junctions in epithelia: implications for mammary gland biology and breast tumorigenesis. *Journal of Mammary Gland Biology and Neoplasia* 8(4):449-462.
- Ivanov AI, Nusrat A, Parkos CA (2004) Endocytosis of epithelial apical junctional proteins by a clathrin-mediated pathway into a unique storage compartment. *Molecular Biology of the Cell* 15(1):176-188.
- Ivascu A & Kubbies M (2006) Rapid generation of single-tumor spheroids for high-throughput cell function and toxicity analysis. *Journal of Biomolecular Screening* 11(8):922-932.
- Iyengar P, Combs TP, Shah SJ, Gouon-Evans V, Pollard JW, Albanese C, Flanagan L, Tenniswood MP, Guha C, Lisanti MP, Pestell RG, Scherer PE (2003) Adipocyte-secreted factors synergistically promote mammary tumorigenesis through induction of anti-apoptotic transcriptional programs and proto-oncogene stabilization. *Oncogene* 22(41):6408-6423.
- Jackson SJ & Thomas GJ (2017) Human tissue models in cancer research: looking beyond the mouse. *Disease Models & Mechanisms* 10(8):939-942.
- Jamieson PR, Dekkers JF, Rios AC, Fu NY, Lindeman GJ, Visvader JE (2017) Derivation of a robust mouse mammary organoid system for studying tissue dynamics. *Development* 144(6):1065-1071.
- Kaemmerer E, Melchels FP, Holzapfel BM, Meckel T, Huttmacher DW, Loessner D (2014) Gelatine methacrylamide-based hydrogels: an alternative three-dimensional cancer cell culture system. *Acta Biomaterialia* 10(6):2551-2562.
- Kelm JM, Timmins NE, Brown CJ, Fussenegger M, Nielsen LK (2003) Method for generation of homogeneous multicellular tumor spheroids applicable to a wide variety of cell types. *Biotechnology and Bioengineering* 83(2):173-180.
- Klebe RJ (1988) Cytoscribing: a method for micropositioning cells and the construction of two- and three-dimensional synthetic tissues. *Experimental Cell Research* 179(2):362-373.
- Knight E & Przyborski S (2015) Advances in 3D cell culture technologies enabling tissue-like structures to be created in vitro. *Journal of Anatomy* 227(6):746-756.
- Knudsen KA & Wheelock MJ (2005) Cadherins and the mammary gland. *Journal of Cellular Biochemistry* 95(3):488-496.
- Kobayashi K, Oyama S, Numata A, Rahman MM, Kumura H (2013) Lipopolysaccharide disrupts the milk-blood barrier by modulating claudins in mammary alveolar tight junctions. *PLoS One* 8(4):e62187.
- Koch L, Gruene M, Unger C, Chichkov B (2013) Laser assisted cell printing. *Current Pharmaceutical Biotechnology* 14(1):91-97.
- Kodama J, Shinyo Y, Hasengaowa, Kusumoto T, Seki N, Nakamura K, Hongo A, Hiramatsu Y (2005) Loss of basement membrane heparan sulfate expression is associated with pelvic lymph node metastasis in invasive cervical cancer. *Oncology Reports* 14(1):89-92.
- Kola I (2008) The state of innovation in drug development. *Clinical Pharmacology and Therapeutics* 83(2):227-230.

- Koukoulis GK, Virtanen I, Korhonen M, Laitinen L, Quaranta V, Gould VE (1991) Immunohistochemical localization of integrins in the normal, hyperplastic, and neoplastic breast. Correlations with their functions as receptors and cell adhesion molecules. *American Journal of Pathology* 139(4):787-799.
- Krause S, Maffini MV, Soto AM, Sonnenschein C (2008) A novel 3D in vitro culture model to study stromal-epithelial interactions in the mammary gland. *Tissue Eng Part C Methods* 14(3):261-271.
- Kurosawa H (2007) Methods for inducing embryoid body formation: in vitro differentiation system of embryonic stem cells. *Journal of Bioscience and Bioengineering* 103(5):389-398.
- Laird DW (2006) Life cycle of connexins in health and disease. *Biochemical Journal* 394(Pt 3):527-543.
- Lancaster MA & Knoblich JA (2014) Organogenesis in a dish: Modeling development and disease using organoid technologies. *Science* 345(6194):1247125.
- Leberfinger AN, Dinda S, Wu Y, Koduru SV, Ozbolat V, Ravnic DJ, Ozbolat IT (2019) Bioprinting functional tissues. *Acta Biomaterialia* 95:32-49.
- Lee SW, Reimer CL, Oh P, Campbell DB, Schnitzer JE (1998) Tumor cell growth inhibition by caveolin re-expression in human breast cancer cells. *Oncogene* 16(11):1391-1397.
- Li G, Simon MJ, Cancel LM, Shi ZD, Ji X, Tarbell JM, Morrison B, 3rd, Fu BM (2010) Permeability of endothelial and astrocyte cocultures: in vitro blood-brain barrier models for drug delivery studies. *Annals of Biomedical Engineering* 38(8):2499-2511.
- Liang X, Zhang L, Wang S, Han Q, Zhao RC (2016) Exosomes secreted by mesenchymal stem cells promote endothelial cell angiogenesis by transferring miR-125a. *Journal of Cell Science* 129(11):2182-2189.
- Liu J, Tan Y, Zhang H, Zhang Y, Xu P, Chen J, Poh YC, Tang K, Wang N, Huang B (2012) Soft fibrin gels promote selection and growth of tumorigenic cells. *Nat Mater* 11(8):734-741.
- Macias H & Hinck L (2012) Mammary gland development. *Wiley Interdiscip Rev Dev Biol* 1(4):533-557.
- Mariappan MR, Williams JG, Prager MD, Eberhart RC (1999) "Engineering" the wound-healing process. *IEEE Engineering in Medicine and Biology Magazine* 18(6):22-26.
- Markov AG, Aschenbach JR, Amasheh S (2017) The epithelial barrier and beyond: Claudins as amplifiers of physiological organ functions. *IUBMB Life* 69(5):290-296.
- Meng W & Takeichi M (2009) Adherens junction: molecular architecture and regulation. *Cold Spring Harbor Perspectives in Biology* 1(6):a002899.
- Mestas J & Hughes CC (2004) Of mice and not men: differences between mouse and human immunology. *Journal of Immunology* 172(5):2731-2738.
- Morizane A, Doi D, Kikuchi T, Nishimura K, Takahashi J (2011) Small-molecule inhibitors of bone morphogenic protein and activin/nodal signals promote highly efficient neural induction from human pluripotent stem cells. *Journal of Neuroscience Research* 89(2):117-126.

- Mroue R & Bissell MJ (2013) Three-dimensional cultures of mouse mammary epithelial cells. *Methods in Molecular Biology* 945:221-250.
- Mroue R, Inman J, Mott J, Budunova I, Bissell MJ (2015) Asymmetric expression of connexins between luminal epithelial- and myoepithelial- cells is essential for contractile function of the mammary gland. *Developmental Biology* 399(1):15-26.
- Naba A, Pearce OMT, Del Rosario A, Ma D, Ding H, Rajeeve V, Cutillas PR, Balkwill FR, Hynes RO (2017) Characterization of the Extracellular Matrix of Normal and Diseased Tissues Using Proteomics. *Journal of Proteome Research* 16(8):3083-3091.
- Nakanishi H & Takai Y (2004) Roles of nectins in cell adhesion, migration and polarization. *Biological Chemistry* 385(10):885-892.
- Nash CE, Mavria G, Baxter EW, Holliday DL, Tomlinson DC, Treanor D, Novitskaya V, Berditchevski F, Hanby AM, Speirs V (2015) Development and characterisation of a 3D multi-cellular in vitro model of normal human breast: a tool for cancer initiation studies. *Oncotarget* 6(15):13731-13741.
- Nerger BA & Nelson CM (2019) 3D culture models for studying branching morphogenesis in the mammary gland and mammalian lung. *Biomaterials* 198:135-145.
- Nguyen-Ngoc KV, Shamir ER, Huebner RJ, Beck JN, Cheung KJ, Ewald AJ (2015) 3D culture assays of murine mammary branching morphogenesis and epithelial invasion. *Methods in Molecular Biology* 1189:135-162.
- Niego B & Medcalf RL (2013) Improved method for the preparation of a human cell-based, contact model of the blood-brain barrier. *J Vis Exp* 10.3791/50934(81):e50934.
- Oda Y, Yoshimura Y, Ohnishi H, Tadokoro M, Katsube Y, Sasao M, Kubo Y, Hattori K, Saito S, Horimoto K, Yuba S, Ohgushi H (2010) Induction of pluripotent stem cells from human third molar mesenchymal stromal cells. *Journal of Biological Chemistry* 285(38):29270-29278.
- Okamoto-Inoue M, Kamada S, Kimura G, Taniguchi S (1999) The induction of smooth muscle alpha actin in a transformed rat cell line suppresses malignant properties in vitro and in vivo. *Cancer Letters* 142(2):173-178.
- Osborne MP, HJ, Lippman ME, Morrow M, Osborne CK (2000) Breast Anatomy and Development. *Diseases of the breast*, Lippincott Williams & Wilkins. p 1-14.
- Overduin M, Harvey T, Bagby S, Tong K, Yau P, Takeichi M, Ikura M (1995) Solution structure of the epithelial cadherin domain responsible for selective cell adhesion. *Science* 267(5196):386-389.
- Ozbolat IT & Hospodiuk M (2016) Current advances and future perspectives in extrusion-based bioprinting. *Biomaterials* 76:321-343.
- Paine IS & Lewis MT (2017) The Terminal End Bud: the Little Engine that Could. *Journal of Mammary Gland Biology and Neoplasia* 22(2):93-108.
- Pedron S & Harley BA (2013) Impact of the biophysical features of a 3D gelatin microenvironment on glioblastoma malignancy. *Journal of Biomedical Materials Research, Part A* 101(12):3404-3415.

- Petersen OW, Ronnov-Jessen L, Howlett AR, Bissell MJ (1992) Interaction with basement membrane serves to rapidly distinguish growth and differentiation pattern of normal and malignant human breast epithelial cells. *Proceedings of the National Academy of Sciences of the United States of America* 89(19):9064-9068.
- Plante I, Stewart MK, Barr K, Allan AL, Laird DW (2011) Cx43 suppresses mammary tumor metastasis to the lung in a Cx43 mutant mouse model of human disease. *Oncogene* 30(14):1681-1692.
- Poltavets V, Kochetkova M, Pitson SM, Samuel MS (2018) The Role of the Extracellular Matrix and Its Molecular and Cellular Regulators in Cancer Cell Plasticity. *Frontiers in Oncology* 8:431.
- Ponti D, Costa A, Zaffaroni N, Pratesi G, Petrangolini G, Coradini D, Pilotti S, Pierotti MA, Daidone MG (2005) Isolation and in vitro propagation of tumorigenic breast cancer cells with stem/progenitor cell properties. *Cancer Research* 65(13):5506-5511.
- Pound P & Ritskes-Hoitinga M (2018) Is it possible to overcome issues of external validity in preclinical animal research? Why most animal models are bound to fail. *Journal of Translational Medicine* 16(1):304.
- Preuss TM (2006) Who's afraid of Homo sapiens? *J Biomed Discov Collab* 1:17.
- Raeber GP, Lutolf MP, Hubbell JA (2005) Molecularly engineered PEG hydrogels: a novel model system for proteolytically mediated cell migration. *Biophysical Journal* 89(2):1374-1388.
- Ramos TV, Mathew AJ, Thompson ML, Ehrhardt RO (2014) Standardized cryopreservation of human primary cells. *Current Protocols in Cell Biology* 64:A 3I 1-8.
- Reid JA, Mollica PA, Bruno RD, Sachs PC (2018) Consistent and reproducible cultures of large-scale 3D mammary epithelial structures using an accessible bioprinting platform. *Breast Cancer Research* 20(1):122.
- Reynolds BA & Weiss S (1992) Generation of neurons and astrocytes from isolated cells of the adult mammalian central nervous system. *Science* 255(5052):1707-1710.
- Rodriguez-Boulan E & Macara IG (2014) Organization and execution of the epithelial polarity programme. *Nature Reviews: Molecular Cell Biology* 15(4):225-242.
- Ronnov-Jessen L, Petersen OW, Bissell MJ (1996) Cellular changes involved in conversion of normal to malignant breast: importance of the stromal reaction. *Physiological Reviews* 76(1):69-125.
- Sager R, Anisowicz A, Neveu M, Liang P, Sotiropoulou G (1993) Identification by differential display of alpha 6 integrin as a candidate tumor suppressor gene. *FASEB Journal* 7(10):964-970.
- Sakakura T, Nishizuka Y, Dawe CJ (1976) Mesenchyme-dependent morphogenesis and epithelium-specific cytodifferentiation in mouse mammary gland. *Science* 194(4272):1439-1441.
- Scheele CLGJ, Hannezo E, Muraro MJ, Zomer A, Langedijk NSM, van Oudenaarden A, Simons BD, van Rheenen J (2017) Identity and dynamics of mammary stem cells during branching morphogenesis. *Nature* 542:313.

- Shamir ER & Ewald AJ (2014) Three-dimensional organotypic culture: experimental models of mammalian biology and disease. *Nature Reviews: Molecular Cell Biology* 15(10):647-664.
- Silberstein GB (2001) Tumour-stromal interactions. Role of the stroma in mammary development. *Breast Cancer Research* 3(4):218-223.
- Simian M & Bissell MJ (2017) Organoids: A historical perspective of thinking in three dimensions. *Journal of Cell Biology* 216(1):31-40.
- Simian M, Hirai Y, Navre M, Werb Z, Lochter A, Bissell MJ (2001) The interplay of matrix metalloproteinases, morphogens and growth factors is necessary for branching of mammary epithelial cells. *Development* 128(16):3117-3131.
- Smart CE, Morrison BJ, Saunus JM, Vargas AC, Keith P, Reid L, Wockner L, Askarian-Amiri M, Sarkar D, Simpson PT, Clarke C, Schmidt CW, Reynolds BA, Lakhani SR, Lopez JA (2013) In vitro analysis of breast cancer cell line tumourspheres and primary human breast epithelia mammospheres demonstrates inter- and intrasphere heterogeneity. *PloS One* 8(6):e64388.
- Sogaard PP, Ito N, Sato N, Fujita Y, Matter K, Itoh Y (2019) Epithelial polarization in 3D matrix requires DDR1 signaling to regulate actomyosin contractility. *Life Sci Alliance* 2(1).
- Sohl G, Maxeiner S, Willecke K (2005) Expression and functions of neuronal gap junctions. *Nature Reviews: Neuroscience* 6(3):191-200.
- Sokol ES, Miller DH, Breggia A, Spencer KC, Arendt LM, Gupta PB (2016) Growth of human breast tissues from patient cells in 3D hydrogel scaffolds. *Breast Cancer Research* 18(1):19.
- Sopel M (2010) The myoepithelial cell: its role in normal mammary glands and breast cancer. *Folia Morphologica* 69(1):1-14.
- Steele VE & Lubet RA (2010) The use of animal models for cancer chemoprevention drug development. *Seminars in Oncology* 37(4):327-338.
- Stelwagen K & Singh K (2013) The role of tight junctions in mammary gland function. *Journal of Mammary Gland Biology and Neoplasia* 19(1):131-138.
- Streuli CH, Bailey N, Bissell MJ (1991) Control of mammary epithelial differentiation: basement membrane induces tissue-specific gene expression in the absence of cell-cell interaction and morphological polarity. *Journal of Cell Biology* 115(5):1383-1395.
- Sun W, Kang K-S, Morita I, Trosko JE, Chang C-C (1999) High Susceptibility of a Human Breast Epithelial Cell Type with Stem Cell Characteristics to Telomerase Activation and Immortalization. *Cancer Research* 59(24):6118-6123.
- Swaminathan S, Hamid Q, Sun W, Clyne AM (2019) Bioprinting of 3D breast epithelial spheroids for human cancer models. *Biofabrication* 11(2):025003.
- Takahashi K, Nakanishi H, Miyahara M, Mandai K, Satoh K, Satoh A, Nishioka H, Aoki J, Nomoto A, Mizoguchi A, Takai Y (1999) Nectin/PRR: an immunoglobulin-like cell adhesion molecule recruited to cadherin-based adherens junctions through interaction with Afadin, a PDZ domain-containing protein. *Journal of Cell Biology* 145(3):539-549.

- Takai Y, Irie K, Shimizu K, Sakisaka T, Ikeda W (2003) Nectins and nectin-like molecules: roles in cell adhesion, migration, and polarization. *Cancer Science* 94(8):655-667.
- Takekuni K, Ikeda W, Fujito T, Morimoto K, Takeuchi M, Monden M, Takai Y (2003) Direct binding of cell polarity protein PAR-3 to cell-cell adhesion molecule nectin at neuroepithelial cells of developing mouse. *Journal of Biological Chemistry* 278(8):5497-5500.
- Tomasetto C, Neveu MJ, Daley J, Horan PK, Sager R (1993) Specificity of gap junction communication among human mammary cells and connexin transfectants in culture. *Journal of Cell Biology* 122(1):157-167.
- Tung YC, Hsiao AY, Allen SG, Torisawa YS, Ho M, Takayama S (2011) High-throughput 3D spheroid culture and drug testing using a 384 hanging drop array. *Analyst* 136(3):473-478.
- Ustyugov A, Chicheva M, Lysikova E, Vikhareva E (2018) Development of 3D cell culture on Ultra-High Molecular Weight Polyethylene (UHMWPE) as the basis of cellular matrix. *Biomedical Chemistry: Research and methods*.
- Vafaizadeh V, Klemmt P, Brendel C, Weber K, Doebele C, Britt K, Grez M, Fehse B, Desrivières S, Groner B (2010) Mammary Epithelial Reconstitution with Gene-Modified Stem Cells Assigns Roles to Stat5 in Luminal Alveolar Cell Fate Decisions, Differentiation, Involution, and Mammary Tumor Formation. *Stem Cells* 28(5):928-938.
- Warawdekar UM (2019) An Assay to Assess Gap Junction Communication in Cell Lines. *Journal of Biomolecular Techniques* 30(1):1-6.
- Watson CJ (2006) Involution: apoptosis and tissue remodelling that convert the mammary gland from milk factory to a quiescent organ. *Breast Cancer Research* 8(2):203.
- Weaver VM, Lelièvre S, Lakins JN, Chrenek MA, Jones JC, Giancotti F, Werb Z, Bissell MJ (2002) beta4 integrin-dependent formation of polarized three-dimensional architecture confers resistance to apoptosis in normal and malignant mammary epithelium. *Cancer Cell* 2(3):205-216.
- Weber-Ouellette A, Busby M, Plante I (2018) Luminal MCF-12A & myoepithelial-like Hs 578Bst cells form bilayered acini similar to human breast. *Future Sci OA* 4(7):FSO315.
- Xu T, Jin J, Gregory C, Hickman JJ, Boland T (2005) Inkjet printing of viable mammalian cells. *Biomaterials* 26(1):93-99.
- Yu W, Datta A, Leroy P, O'Brien LE, Mak G, Jou TS, Matlin KS, Mostov KE, Zegers MM (2005) Beta1-integrin orients epithelial polarity via Rac1 and laminin. *Molecular Biology of the Cell* 16(2):433-445.
- Yumoto K, Berry JE, Taichman RS, Shiozawa Y (2014) A novel method for monitoring tumor proliferation in vivo using fluorescent dye DiD. *Cytometry A* 85(6):548-555.
- Zajchowski DA, Band V, Trask DK, Kling D, Connolly JL, Sager R (1990) Suppression of tumor-forming ability and related traits in MCF-7 human breast cancer cells by fusion with immortal mammary epithelial cells. *Proceedings of the National Academy of Sciences of the United States of America* 87(6):2314-2318.



Zhang L, Adileh M, Martin ML, Klingler S, White J, Ma X, Howe LR, Brown AM, Kolesnick R (2017) Establishing estrogen-responsive mouse mammary organoids from single Lgr5(+) cells. *Cellular Signalling* 29:41-51.

Zhao Y, Yao R, Ouyang L, Ding H, Zhang T, Zhang K, Cheng S, Sun W (2014) Three-dimensional printing of HeLa cells for cervical tumor model in vitro. *Biofabrication* 6(3):035001.

